Selection and development of algorithms based on surface fluorescence compounds of fish for non-destructively monitoring freshness during storage

OMWANGE KEN ABAMBA

2022

Selection and development of algorithms based on surface fluorescence compounds of fish for non-destructively monitoring freshness during storage

[貯蔵段階における魚体表の蛍光物質を用いた非侵襲的な鮮度評価のためのアルゴリズムの選定と開発]

By

Omwange Ken Abamba

Laboratory of Bio-Sensing Engineering

Division of Environmental Science and Technology

Graduate school of Agriculture

Kyoto University, Japan.

A Dissertation

Submitted to Graduate School of Agriculture, Kyoto University, Japan in Partial Fulfillment of the Requirements for the Doctor of Agricultural Science Degree

2022

Thesis Committee

Naoshi KONDO

Professor, Laboratory of Bio-Sensing Engineering

Division of Environmental Science and Technology

Graduate School of Agriculture, Kyoto University, Japan.

Michihisa IIDA

Professor, Laboratory of Field Robotics

Division of Environmental Science and Technology

Graduate School of Agriculture, Kyoto University, Japan**.**

Yuichi OGAWA

Associate Professor, Laboratory of Bio-Sensing Engineering

Division of Environmental Science and Technology

Graduate School of Agriculture, Kyoto University, Japan.

Table of Contents

Table of Figures

IV

List of Tables

CHAPTER I: INTRODUCTION

1.1 Research overview

The demand for fish and its related products in the human diet has been increasing significantly in the recent past, as reported by Dale (1994). This is because it has proved to be an alternative sources of proteins and low-fat food contents providing a range nutritional benefits upon consumption like brain boosting through omega-3 fatty acids and reduced risks for heart diseases (Lavie et al., 2009). This has boosted the total fish consumption, as well as the number of consumers has been sharply increasing compared to other meats. However, fish is a highly perishable food, which can easily get spoiled and losing its freshness quickly. However, the shelf-life of fish is limited because of high perishability through biological and chemical spoilage (Hassoun and Karoui, 2015); and therefore there is need to have proper monitoring methods and techniques to track quality changes during storage.

Various parameters influence the quality of fish products; they include the nutritional value, freshness level, safety, availability, consumption patterns (sushi/sashimi or cooked) and the physical attributes (color, mucus, scale firmness, injuries, stiffness, eyes shape, smell among others). The level of fish freshness forms an important concept which directly affects the quality of fish, and it can be described by various properties of fish like good appearance, low ATP degradation, and low microbial counts as indicated in Fig. 1.1 (Dowlati et al., 2012).
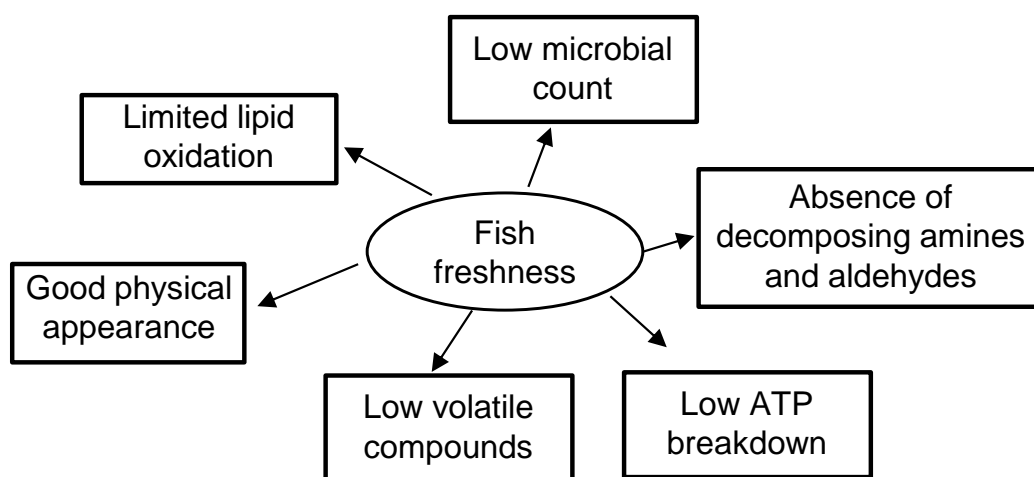
Fig. 1.1: Impression of fish freshness

The quality of fish and its products has continuously remained a significant concern globally in the fish industry (Gram and Huss, 1996). In the recent past, conventional methods such

1

as sensory technique, biochemical (ATP breakdown and its metabolites) and bacteriological analysis have been relied on for fish freshness estimation during storage and relating the results with the predetermined standards like freshness index (K-value) set with specific limits for consumption. However, even with these methods, fish freshness cannot be adequately estimated because the techniques have their limitations; costly, cumbersome and taking time to yield positive results (Dowlati et al., 2012; Karoui et al., 2017; Shumilina et al., 2015). Also, the methods involve one-time measurement (at an interval) and therefore cannot be used for online monitoring of freshness changes. This has led to many losses and wastage of resources by many fish getting spoiled.

Fish spoilage mechanism

Spoilage of fish also known as "Putrefaction" is a process which causes decline in fish quality, thus, contaminating the fish, producing undesirable changes in color, flavor, texture, appearance, smell, and many others. Fish spoilage is caused enzymatic degradation, bacterial activities, chemical breakdown, and mechanical damage. Spoiled fish can be characterized by just observing the extent of color changes, skin and scales sliminess, fishy smell, flesh firmness and backbone discoloration (Castillo-Yánez et al., 2014; Ghaly et al., 2010). The common causes of fish spoilage are spoilage micro-organisms, enzymatic activities, and oxidative nature of nutritive elements in fish. The major factors responsible for spoilage include but not limited to, improper handling, high moisture content of fish, weak nature of fish's muscle tissues and ambient temperature for storage. When fish spoilage occurs, it takes different forms, depending on the freshness stage. This takes different forms covering from rigor mortis, autolysis, bacterial spoilage and chemical spoilage (Hong et al., 2017; Masniyom, 2011).

i. *Rigor mortis*

Rigor mortis explains the physical effect on the fish's muscle tissues produced by chemical changes after death. For live fishes, the movements are regulated by chemical indicators which facilitate relaxation and stiffing of muscles responsible for swimming actions (Hong et al., 2017). Usually, the normal circulatory system stops and leakage of chemical signals into the muscles makes them stiffen with time. That means that the glycogen present in the muscles of a live fish is converted to carbon dioxide (CO_2) and water after body cells are supplied with oxygen. Blood circulation stops immediately after the fish dies, thus blocking the respiration process (supply of

2

oxygen). The enzymes in the muscles start converting glycogen molecules into lactic acid, resulting in a decline of pH for the fish muscle. Lactic acid continues accumulating until the glycogen supply is completely exhausted.

The duration a fish takes to pass through rigor mortis depends on various factors such as fish species, the physical condition during catch, degree of exhaustion just before death, fish size, and storage temperature (FAO 2001). Different fish species takes different times to go into and pass through the rigor mortis stage because they possess different chemical compositions. For instance, whiting fish go into rigor so fast and may be completely stiff within one hour after death, whereas redfish subjected to the same condition may take over 20 hours to attain full rigor. Well-fed fishes during capture takes longer time to go into and pass through the rigor mortis stage as compared to malnourished ones. This is because underfed/malnourished fishes have little reserve energy in muscles to keep it flexible. Similarly, fish that struggles for a long-time during catch become exhausted and have less reserved energy, therefore, it will quickly go into rigor. Temperature is the major determinant for dictating the time a fish will take into and pass through the rigor. This is because, temperature can be regulated. Warmer storage makes the fish get into and pass-through rigor stage very fast. For instance, when gutted cod is stored at about 0 °C, it will take around 60 hours to go through rigor mortis, but the same fish will take just 2 hours when stored at 30 °C (FAO 2001).

Rigor mortis takes three forms namely, pre-rigor, rigor, and post rigor. Immediately after death, the muscle tissues are soft and relaxed (see Fig. 1.2 a), however after some hours, the muscles start to harden up and stiffen (Watanabe et al., 1989), but still somehow flexible. At this stage, it marks the onset of rigor mortis stage called pre-rigor as seen from Fig. 12.2 b. During the rigor mortis stage, the muscles appear hardened and the even if the fish is held from one end, it will not bend as seen from Fig. 1.2 c. It has been reported that rigor mortis starts from fish's tail, and spreads gradually towards the head until whole muscles get stiff (Watanabe et al., 1989). This is because at the fish's tail, the surface area to volume ratio of muscles is small when compared to the other body parts. After the rigor mortis stage is completed, stiffness of muscles gradually declines with increasing pH thus making the muscles to become soft as seen from Fig. 1.2 d.
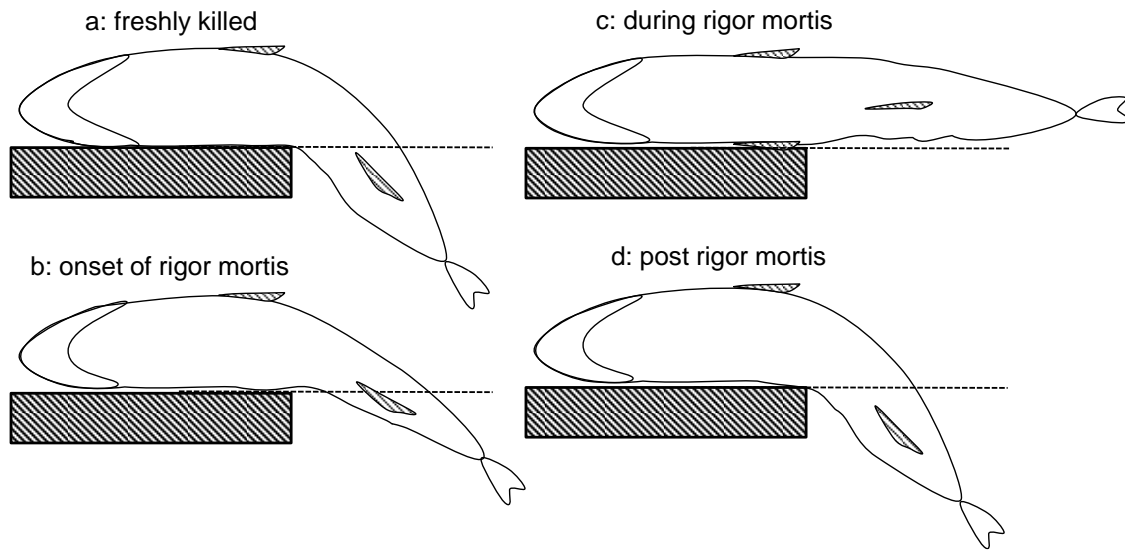
Fig. 1.2: Stages of Rigor mortis spoilage in fish.

ii. Autolysis

Autolysis refers to enzymatic degradation (self-digestion) and it damage the fish cells by releasing autolytic enzymes which destroys the cell components such as proteins and fats (Shumilina et al., 2015), hence changing the flavor of fish. In this stage, anaerobic glycolysis breaks down glycogen (main carbohydrate of fish muscle) into lactic acid. This process involve two enzymes called hydrolytic (maltose pathway) or glycolytic pathway (Shumilina et al., 2015). This process causes a significant drop in the fish muscle's pH (neutral to slightly acidic). Breakdown of nucleotide is a significant enzymatic process because it produces either pleasant flavors at the onset of nucleotide degradation cycle or unpleasant flavors which comes later at nucleotide degradation cycle; thus affecting the fish's taste (Fereidoon and Zhong, 2010). Oxidation of lipids and free fatty acids in fish by enzymatic generates peroxides and hydroperoxides which produce rancid flavors and rotten smell that is common with fish spoiled fish. Some enzymatic activities oxidizes fats, which return affects the of fish color hence affecting their quality (Haard, 1992).

iii. Chemical spoilage

Unlike autolysis where enzymes play a vital role in fish quality degradation, chemical spoilage is caused by auto-oxidation process where lipids are oxidized by non-enzymatic processes. Large amounts of polyunsaturated fatty acids in lipids make it vulnerable to oxidation (Gram and Huss, 1996). The auto-oxidation of lipids on unsaturated fatty acids happens due to the

4

catalysis of hematic compounds such as myoglobin, hemoglobin, and cytochromes forming hydroperoxides. From Hsieh and Kinsella, (1989), decomposition of hydroperoxides produce sour flavors and fall-odors in the fish muscles and fading away of skin color (fading of carotenoid pigments). As a result, some technologies that measure auto-oxidation products in fish like peroxides, free fatty acids, alcohols and carbonyls have been suggested for fish freshness evaluation through chemical analysis (Ryder, 1985). During chemical spoilage proteolytic micro-organisms breaks down proteins into amino acids, ammonia, amines, and hydrogen sulphide as seen from Eqn. 1.1. Fermentative microorganisms split carbohydrates into alcohols, acids (see Eqn. 1.2), and gases as lipolytic microorganisms converts fats into glycerol and fatty acids as seen in Eqn. 1.3).

❑ **Protein degradation**

$$\text{Protein} \xrightarrow{\text{Proteolytic micro-organisms}} \text{Amino Acids} + \text{Ammonia} + \text{Amines} + \text{Hydrogen sulphide} \qquad \dots \text{Eqn 1.1}$$
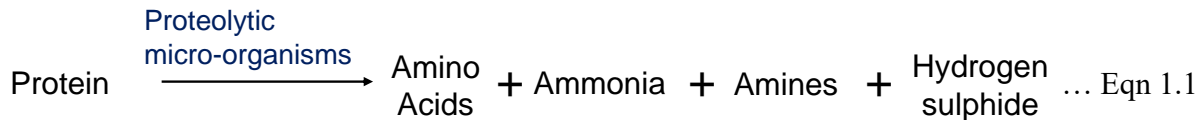
❑ **Carbohydrate degradation**

$$\text{Carbohydrate} \xrightarrow{\text{Fermentative micro-organisms}} \text{Alcohols} + \text{Acids} + \text{Gases} \qquad \dots \text{Eqn 1.2}$$

❑ **Fat degradation**

$$\text{Fat} \xrightarrow{\text{Lipolytic micro-organisms}} \text{Fatty acids} + \text{Glycerol} \qquad \dots \text{Eqn 1.3}$$

iv. *Bacteriological spoilage*

This process is associated with microbial activities in fish which build up after the fish dies. A fish acquire bacterial load from the gills and body surface, and therefore, bacterial spoilage will begin from surface slime, skin and gills (Gram and Huss, 1996) and spread throughout the fish's body as storage time progresses. Different bacteria families attack the fish differently at different storage temperatures optimum for their survival. Bacteria cause fish spoilage in different ways: (i) spoilage bacteria reduce the odorless Trimethylamine oxide (TMAO) to foul smelling Trimethylamine (TMA). They degrade amino acids to primary amines such as Histidine to Histamine and Glutamic acid to Arginine. These are very dangerous because they can easily cause

food poisoning. Bacterial also breaks down urea to ammonia which also produce a bad smell. Most putrid compounds have been used as freshness indicators of several species of fish.

Existing fish freshness evaluation techniques

The freshness of fish is important for both the consumer and seller. The sellers need to know which fish should be sold fast and avoid food wastage and economic losses, but for the consumers, they are more concerned about the safety/quality of the product before consumption to prevent food poisoning. Fish freshness can be evaluated using: (i) sensory technique, (ii) physical assessment, (iii) microbiological analysis and (iv) biochemical analysis which monitors the adenosine-triphosphate (ATP) breakdown (Abbas and Alshikh Khalil, 2016; Elmasry et al., 2015).

i. Sensory technique

Sensory techniques relies on specially trained personnel in estimating the fish freshness by use of human senses: sight, taste, smell, touch, and hearing (Rahman et al., 2016). Fish's body parts such as eyes, meat, scales, and gills have regularly been used in the assessment process freshness. Mostly, the physical color changes of fisheye act as freshness indicator for both consumers and sellers (Dowlati et al., 2013). The fish surface loss moisture and become dry during storage and the eyes become softer due to increased membrane permeability which allows water and eye compounds to be lost, hence lowering transparency. Also, the eye tissues rapture, thereby accumulating materials increasing the concentration of liquid substances, consequently changing their compositions (Yapar and Yetim, 1998). The muscle can also reveal freshness deterioration in fish because through autolysis and microbial activities on proteins, fats and connective tissues affects tenderization, pH and structure found in the muscles (Gram and Huss, 1996; Samaranayaka and Li-Chan, 2008).

This technique has led to the development of artificial equipment whish imitate the human senses such as e-tongue and e-nose which can detect the smell change and taste variation. Fish freshness assessment using sensory methods can give objective and reliable results if it is properly carried out under controlled environments. The technique relies on experts with specialized skills and expertise in obtaining accurate and reliable results.

Table 1.1: EU Scheme for white fish.

Part	Freshness category			
	Extra	**A (Good quality)**	**B (Satisfactory quality)**	**Rejected (Not admitted)**
Eyes	Convex (bulging cornea Black, and right pupil, Transparent cornea	Convex & slightly sunken. Black, dull pupil, Slightly opalescent cornea	Flat opalescent cornea Opaque pupil	Concave in the center Grey pupil Milky cornea
Smell of gills & abdominal cavity	Fresh fishy smell (Sea weedy)	No smell of seaweed, Neutral smell	Fermented, slightly sour	Sour/spoilt
Flesh	Firm & elastic, smooth surface	Less elastic	Slightly soft (flaccid), less elastic, waxy (velvety) & dull surface	Soft (flaccid), Scales easily detached from skin, Surface rather wrinkled
Skin	Bright, iridescent pigment (save for redfish) or opalescent no discoloration	Pigmentation bright but not lustrous	Pigmentation in the process of becoming discolored & dull	Dull pigmentation
Skin mucus	Aqueous, transparent	Slightly cloudy	Milky	Yellowish, grey, opaque mucus
Gills	Bright color, No mucus	Less colored, Transparent mucus	Brown /green Becoming discolored, thick, Opaque mucus	Yellowish, milky mucus
Peritoneum on gutted fish	Smooth, bright, difficult to detach from flesh	Slightly dull, can be detached from flesh easily	Speckled, comes away easily from flesh	Dark and easily rapture.

ii. *Physical techniques*

This technique uses a designed tools which can give quality indices by Quality Index Method (QIM). The features depend on significant raw fish parameters where the score system ranges as 0-1, 0-2, 0-3, 0-4 and even more (Hyldig et al., 2010). The fact that different fish species possess various flavors, appearance, and varying smell, this method can evaluate textural changes in evaluating fish's quality deterioration (Ocaño-Higuera et al., 2011). Fish is accurately cut and then compressed to record the stress-strain graph which calculates deformability modulus. Physical technique is a direct extension of sensory assessment 'figure press test'. Unfortunately, the high training requirements of personnel for proper and accurate results makes it exceptionally expensive because every fish species have different spoilage patterns.

iii. *Bacteriological analysis*

Bacterial metabolites fastens the fish spoilage rate which in return results in the emission of rotten smell and bad flavors (Gram and Huss, 1996). Bacterial growth and metabolism processes produce sulfides, amines, alcohols, ketones, aldehydes, and organic acids characterized by foul odors and flavors. For objective quality indicator of fish, the number of specific spoilage organisms (SSOs) and their metabolite concentration is usually used to determine fish's shelf life. Bacteria are always classified depending on the temperature conditions: psychrotrophic, mesophilic and thermophilic. Usually, low temperatures such as ≤10 °C impair bacterial growth; medium temperatures (between 10 °C and 35 °C) are optimal for most bacterial activities with high reproducibility as high temperatures (≥35 °C) are known for denaturing many bacterial activities (Gram and Dalgaard, 2002).

Microbiological analyses purely focus on testing for the absence or presence of specific strain and determining the number of colony-forming units (CFU) called "total viable counts (TVC)" or "aerobic plate count (APC)," or number of CFU of indicator organisms such as Coliforms, Enterobacteriaceae, or Enterococci (Corry et al., 2007). Microbial growth models help to determine the effects of various exposure time and temperature combinations on the fish's shelf life in the whole production and distribution chain. There exists already established mathematical models for determining the growth of spoilage bacteria like *Photobacterium phosphoreum*, *Shewanella putrefaciens* (Dalgaard, 1995), *Brochothrix thermosphacta*, *Listeria monocytogenes* (Carrasco et al., 2007), and *Clostridium perfringens* (Juneja et al., 2006), shown to compare with the remaining shelf-life of the product and also associated better than classical TVC measurements.

iv. Biochemical analysis

This method trails the chemical breakdown of nucleotides, production of biogenic amines, hydrolysis and oxidation of lipids for freshness estimation. Changes in fish during storage due to some processes like microbial activity, autolytic enzymes, chemical reactions are useful indicators of fish quality or spoilage. For K value index: adenosine triphosphate (ATP) degrades through dephosphorylation and deamination and breakdown into its metabolites. The metabolites include adenosine diphosphate (ADP), adenosine monophosphate (AMP), inosine monophosphate (IMP), inosine (HxR) and hypoxanthine (Hx) as seen in Fig. 1.3 below. Hx is characterized by bitter taste which accompanies the off flavor in decayed fish. In 1959, Japanese researchers suggested the K value index, as an objective index of fish freshness (Saito et al., 1959). Biochemical technique follows set standards with tolerance levels of spoilage indicators (Hassoun and Karoui, 2015). The use of chemical approach to estimate fish quality by focusing on total volatile basic amines (TVBA), trimethylamine (TMA), dimethylamine (DMA) from autolytic enzymes and ammonia (NH_3) from spoilage bacteria and lipid oxidation. The concentration levels of these compounds in the fish tissues are determined by steam distillation method. Some other chemical methods may focus Peroxide Value (Pv), Iodine value (Iv), Thiobarbituric Acid (TBA) which greatly constitute to formation of sour flavors in fish and fish products (Hassoun and Karoui, 2015).

$$K \text{ value} = \frac{H_xR + H_x}{ATP + ADP + AMP + IMP + H_xR + H_x} \times 100 \quad \dots \quad (Eqn.1.4)$$
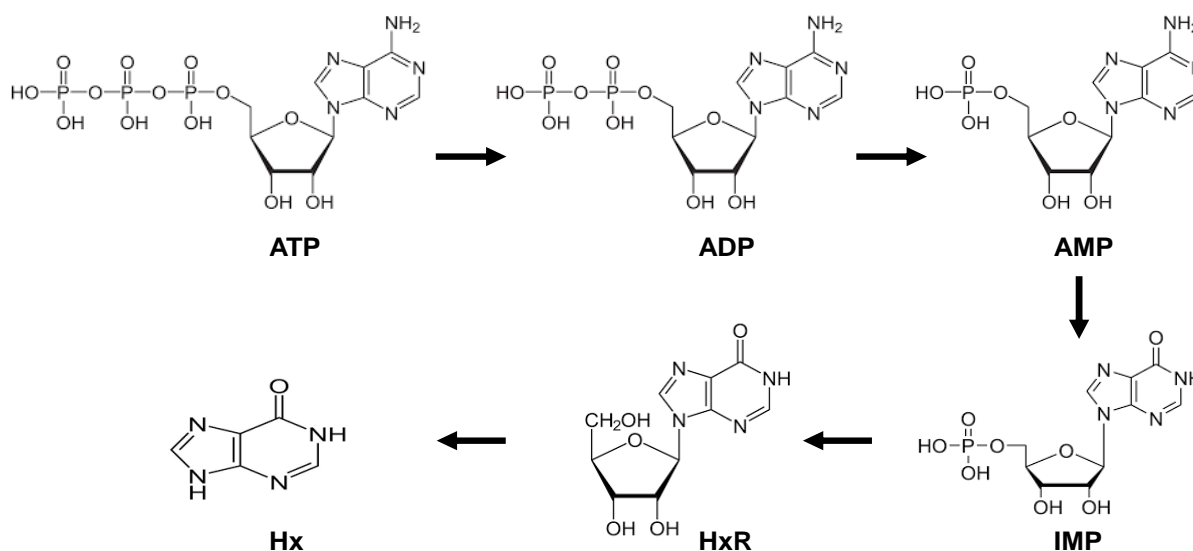
Fig. 1.3: Chemical structure of freshness pathway.

The concentration levels of nucleotides in the fish muscles associated with the feeding behavior and physiological activities when the fish is alive (Lowe et al., 1993). After death, the phosphate levels in ATP drops gradually due to a series of catalyzing enzymes (Rahman et al., 2016). The different metabolites have different chemical compounds as shown below. The rate of decomposition and degradation for these compounds dependent on various factors like; the fish species, type of muscles (dark or white), antemortem condition, level of stress during capture, handling methods, season of capture, feeding habits and storage conditions (Cheng et al., 2015).

The initial *K* value of living fish (immediately after capture) is less than 10%; but this value gradually increases during storage due to biochemical activities. At some point in time (inflection point) of storage, *K* value shows a rapid increase, and this is attributed to presence of bacteria which fastens the rate of spoilage (Lowe et al., 1993). Various freshness indices are used to define freshness levels; *K* value less than 40% is the ideal freshness limit thus the fish can be consumed. Any value above 40% will imply the fish has exceeded the fresh limits and therefore it is regarded as spoiled (rejection point) (Itoh et al., 2013). In this research, they defined different *K* index levels; where, between 0 and 10% is for living fish, less 20% the fish is fresh, and it can be consumed raw (sashimi/sushi), more than 20% but less than 40% means the fish is fresh but can only be consumed after cooking. Between 40% and 60% can only be consumed by processing the meat. *K* index above 60% or more implies the fish is not fit for consumption at all. Therefore, *K* index can show a predictive function during storage and show an objective indicator of monitoring changes during storage. However, these methods are complex, laboratory based (requires skilled personnel), time consuming.

Emerging Technologies

Other techniques include electronic methods such as electronic nose and electronic tongue), electrical measurements, optical measurements (spectroscopy and imaging techniques) (Hong et al., 2014)

Electronic nose and electronic tongue technique

This electronic equipment are designed to imitate the human senses of smelling and tasting in estimating the fish's freshness level (Han et al., 2020) as seen from Fig. 1.4 a and b. Electronic nose also known as e-nose is technique detect and quantify the concentration and accumulation of volatile compounds in fish which are emitted during spoilage. Fall odor develop due to microbial

growth and oxidation of biological compounds and subsequent degradation of tissues. Short chain alcohols, esters and carbonyls, trimethylamine, methylmercaptan, hydrogen sulfide, dimethyl-disulfide and dimethyl-trisulfide are among the volatile compounds formed due to tissue degradation processes and the concentration is high in the headspace. The e-nose can detect some of these volatile degradation compounds at the onset of fish spoilage, hence acting as an indicator for freshness deterioration (Han et al., 2020). However, calibration is necessary for e-nose of various compounds in different samples to build a reference database for better results. The electronic tongue (e-tongue) often imitates the operation of the human tongue detect dissolved organic and inorganic compounds.
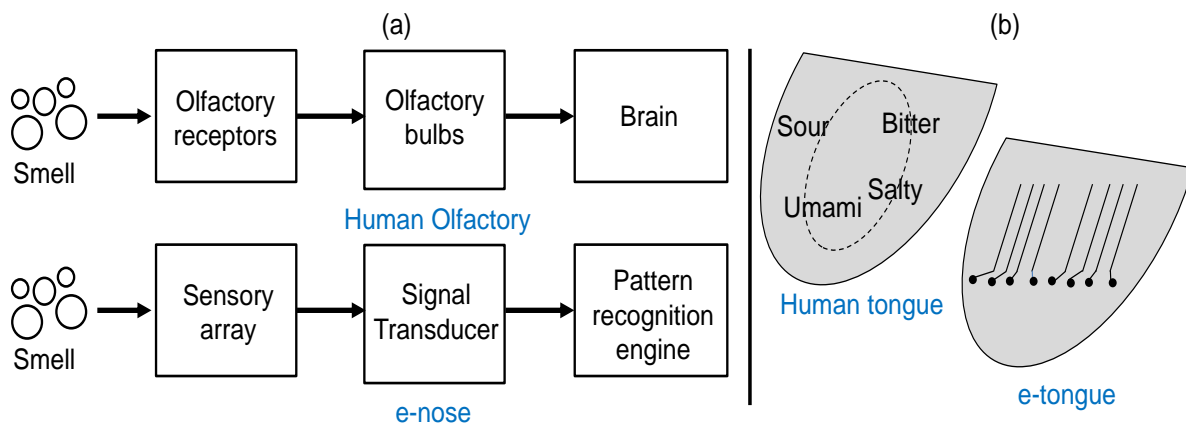
Fig. 1.4: (a) Basic smell recognition system for a human olfactory and e-nose (b) basic tasting pattern for human tongue and e-tongue

Electrical technique

Electrical properties of fish muscles can potentially act as freshness indicators. Microbial activity and breakdown of compounds in fish changes the electrical properties of fish muscles which are pertinent indicators of freshness deterioration in fish. After the fish has dies, the changes are caused by rigor mortis, autolysis, bacterial growth chemical spoilage breaks down the cell membranes thereby affecting the electrical properties such as capacitance, impedance, and conductance of the muscles (Jason and Richards, 1975). This method shows similar tendency with the sensory scores for fish freshness. This technique relies on three different instruments: Torrymeter (UK), Intelectron Fischtester VI fish-tester (Germany) and RT freshness grader (Iceland). The method is limited to the existence of the skin hence it will only work for whole fish and fillets with skin.

VIS *spectroscopy (optical measurement)*

The fish muscles absorb various light components differently, and this is depending on the composition and condition of the muscle such as existence of different organic substances and its extent of hydration and thickening, hence can tell difference in light absorptions (see Fig. 1.5). Therefore, the spectra change will depend on the muscles' degree of spoilage during storage. This forms the origin of a technique established by Fiskeriforskning in Norway (Heia et al., 2003; Nilsen et al., 2002). Nilsen et al., (2002) demonstrated that estimating freshness of tiny fish like cod gives more accurate results when using the visible wavelengths only. This technique was later expounded by Heia et al. (2003) with the help of the transmission spectra which was measured using a portable spectrometer. The technique is more precise when estimating the quality of fillets, where it is difficult to adopt sensory analysis especially in the absence of the head. Optical technique has been utilized in frozen and thawed cod fish research to estimate the water-holding capacity (Bechmann and Jørgensen, 1998). Also, with the appropriate chemometric tools, front-face fluorescence spectroscopy technique has shown the potential to evaluate fish freshness during storage (Dufour et al., 2003). Therefore, optical technique is suitable for assessing the quality of fish fillets, thus reducing the challenge of relying on sensory technique in the absence of the head; thereby adding value to fish fillets processing industries (Olafsdottir et al., 2004).
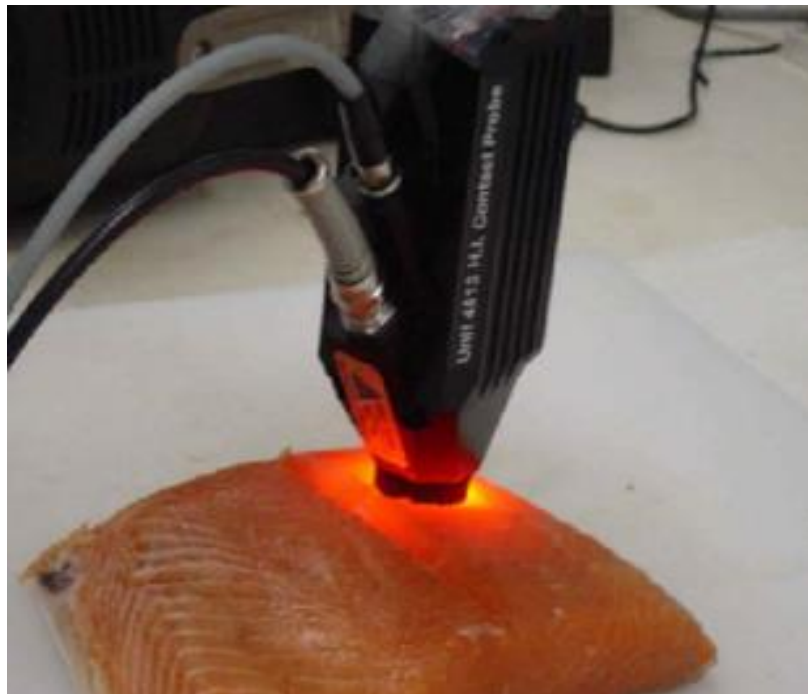
Fig. 1.5: The optical/VIS spectroscopic measurement technique.

Imaging technique

Imaging can quantify the color changes of fish surface by measuring the appearance of intact fish (fisheyes, skin) and surface of fish fillets. The images can be acquired using different cameras such as CCD or DSLR cameras and the analysis done to compute the spatial coherence between micro-patterns around the image, color, mucus turbidity on the skin and the muscle fiber coarseness for fillet surfaces (Kohler et al., 2002). Previous researches have reported the adoption of imaging technique in evaluation of fish quality for whole fish imaging (Dowlati et al., 2012; Hu et al., 2012; White et al., 2006); fillet imaging (Dowlati et al., 2012; Mery et al., 2011; Misimi et al., 2007), fish eye and skin color imaging (Dowlati et al., 2013; Wang et al., 2020). Other researchers have demonstrated the potential of hyperspectral imaging as a powerful tool in monitoring fish freshness during storage and processing (Cheng et al., 2015; Zhu et al., 2013).
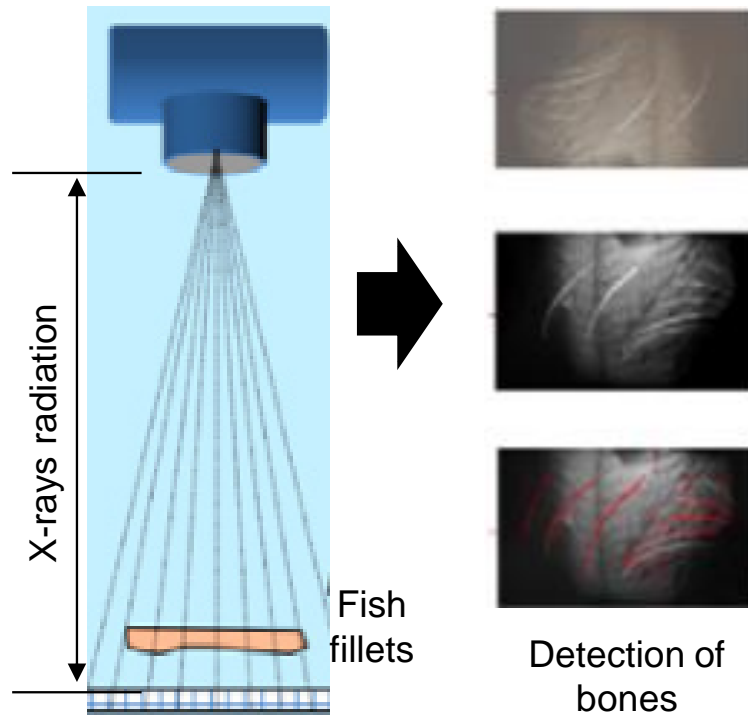
Fig. 1.6: Fish fillet imaging using X-rays for detection of bones.

Spectroscopic analysis

Fish and fish products contains protein, fat, moisture, and other compositions which absorb different light components. Therefore, spectroscopic methods could potentially detect pathogen growth, structure changes of protein, oxidation of fats and production of secondary products associated with quality changes in fish during storage. For instance, the visible spectroscopy (380-

780 nm) corresponds with sensory evaluation, thus suitable for assessment of color, texture change during storage (Nilsen and Esaiassen, 2005). Near infrared (NIR) spectroscopy covers 780-2526 nm, and it is another useful technique which can track fish freshness especially by detecting activities of microorganisms, predict the moisture content and glycogen concentrations on fish fillets (Sone et al., 2011). Besides, some other popular spectroscopic techniques such as *Raman* spectroscopy (Leelapongwattana et al., 2008), nuclear magnetic resonance spectroscopy (Sánchez-Alonso et al., 2012) mid-infrared spectroscopy (Rodriguez-Casado et al., 2007).

Additionally, there exists fluorescence spectroscopy which has demonstrated some great potential for assessing fish freshness. Amongst all these spectroscopic techniques, fluorescence spectroscopy proves to be more powerful due to high sensitivity and specificity for its analytical ability. This has made it to be widely adopted in assessing food quality in the recent past (Valeur and Bochon, 2001). Fluorescence spectroscopy can be utilized for non-destructive measurement of samples to reveal information of various fluorescent compounds and their environment for different biological samples. It is reported to be very sensitive (100-1000 times more sensitive) than other spectrophotometric methods (Strasburg and Ludescher, 1995), thus making it to attract many researches on food quality assessment. The principle operation of theory of fluorescence spectroscopy is explained as shown follows.

Fundamental principles of Fluorescence spectroscopy

Definition of Fluorescence
Fluorescence is a luminescence created by electromagnetic excitation, and it is short-lived. The principles of fluorescence can simply be illustrated by a Jablonski diagram (see Fig. 1.7). When a molecule is excited by external photon (hv_{ex}), (where h - Plank's constant and *v* - frequency) the electron moves from the ground singlet states (S_0) to an excited singlet state (S_1'). The excited electron then undergoes some conformational changes during interaction with molecular environment to convert from a higher electronically excited state (S_1') to a lesser one (S_1). At this level, emission occurs, which is estimated to take like 10^{-8} seconds after excitation and emit some photon (hv_{em}) at a longer wavelength as the electron returns to a more stable ground state (S_0) (Christensen et al., 2006). Fluorescence is often showed by molecules with firm molecular skeletons such as heterocycles and polyaromatic hydrocarbons. The molecules exhibiting less

vibrational and motional freedom usually have greater difference in energy levels between the ground electronic and excited singlet states thus resulting in fluorescence (Karoui and Blecker, 2010).
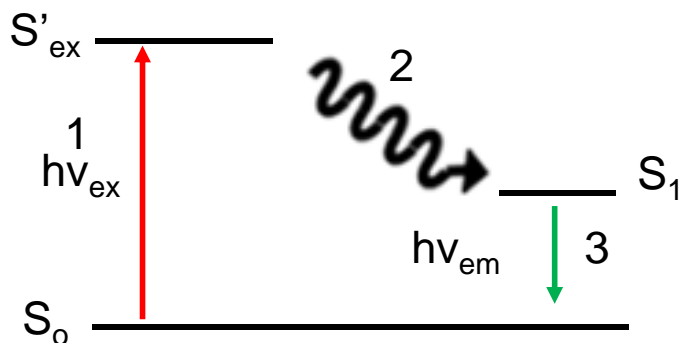
Fig. 1.7: Jablonski diagram explaining the basic principles of fluorescence spectroscopy.

Quantum Yield (ϕ)

This is the most significant characteristic of fluorophore molecules. It describes the ratio of the number of photons emitted to those absorbed as seen in Eqn. 1.5 (Brandt, 2010). The molecules with the largest quantum yield like rhodamines and chlorophyll exhibits brightest emissions. Non-fluorescent molecules such as carotenoids are known to contain possess zero or very low quantum yields, thus their fluorescence cannot be measured because the absorbed energy is quickly lost through collision deactivation

$$\text{Quantum yield } (\emptyset) = \frac{\text{number of quanta emitted}}{\text{number of quanta absorbed}} \qquad \dots \qquad \text{Eq.1.5}$$

Excitation and Emission Spectra

Fluorescent phenomenon has two spectra characteristic: excitation spectrum and emission spectrum. They are commonly referred to as the molecule's fingerprint or fluorescence signature. That means, it is not possible to have two molecules sharing the same fluorescence signature, making fluorometry a more highly specific analytical tool. Shape of excitation spectrum ought to be identical with the molecule's absorption spectrum and independent of the wavelengths for measuring fluorescence. The emission spectrum emanates from the absorbed molecule radiations. The emission spectrum defines the relative radiation intensity emitted at different wavelengths. Theoretically, emission spectrum shape and quantum efficiency are independent of excitation radiation wavelength.

Stokes Shift

Stokes shift represents the difference in band maxima of absorption and emission spectra in the same electronic transition. From the Jablonski diagram (Fig. 1.7), the emission energy is lower than that of excitation. This means that emission takes place at longer wavelengths than the excitation. Behlke, et al., (2005) defined Stokes shift as the gap between excitation and emission wavelengths as seen from Fig. 1.8. Stoke shift is important when determining the sensitivity of fluorescence measurements. Eqn. 1.6 below illustrates how Stokes shift is calculated (Karoui and Blecker, 2010).

$$\text{Stokes shift (cm}^{-1}) = 10^7 \left(\frac{1}{\lambda_{ex}} - \frac{1}{\lambda_{em}} \right) \qquad \ldots \qquad \text{Eqn.1. 6}$$

where λ_{ex} and λ_{em} are the maximum excitation and emission wavelengths (nm), respectively.
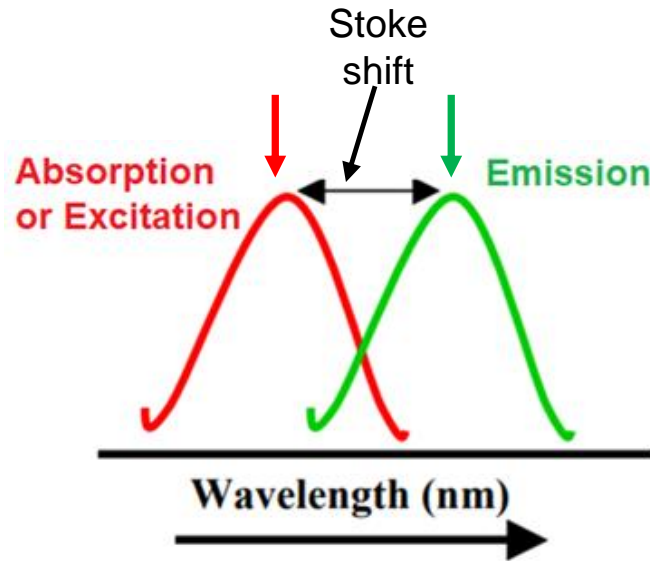
Fig. 1.8: Excitation spectrum and emission spectrum showing the Stoke shift.

Fluorescence intensity

Fluorescence intensity is a significant parameter that measures the concentration of a target (fluorophores). The changes in fluorescence intensity of a sample can be calculated using the Beer-Lambert law, which can explain the relationship of fluorescence intensity to its concentration as seen from Eqn. 1.7 below. The fluorescence intensity specific fluorescence compounds show a linear relationship with its concentration when subjected to similar measurement environment. Generally, the fluorescence intensity of given a sample(s) is expressed as amount of the fluorescence contribution from every inherent fluorophore in the sample.

$$I_f = 2.3\phi I_0 \varepsilon l c \qquad \dots \qquad \text{Eqn.1.7}$$

where I_f represents fluorescence intensity, ϕ denotes quantum yield, I_0 is the incident light intensity, ε is the molar absorptivity, l represents sample's optical depth, and c the molar concentration of fluorophores.

Factors affecting fluorescence intensity

The fluorescence intensity of compounds is affected by several factors such as quenching effect, concentration of samples, structure of macromolecules, local environment (polarity of the solvent), Scattering and reflection of incident light, and pH. Fluorescence quenching covers any procedure that can decrease fluorescence intensity of a sample. It relates to deactivating of excited molecule through either inter- or intramolecular connections. Concentration influences the fluorescence intensity of substances. Concentrated samples cause decline in intensity due to inner filter effects that apparently decreases the emission quantum yield and even distorts the band shapes due to re-absorption of emitted radiations, or absorption of incident radiations by other substances other than the fluorophore (Christensen et al., 2006). Macromolecule structure and the fluorophore locations can potentially affect emission intensity and quantum yields of compounds. The polarity of solvent influences the emission of polar fluorophores. More polar environments cause excited fluorophores relax to lower vibrational energy state before emission, causing a shift to lower energy (longer wavelengths). The pH value cause protonation and dissociation in changing the nature of the non-radiative processes which compete, thereby changing the quantum yields of fluorophores. Scattering and reflection of incident light have substantive effects on fluorescence intensity, especially the solid opaque and turbid samples.

Application of fluorescence techniques in evaluating food quality assessment

Fluorescence spectroscopy has been widely adopted in evaluation of food quality in the recent past. It offers sensitive, rapid, and simple sample approach for the characterization of food substances. This is because, food contains several auto-fluorescent compounds important for evaluating the nutritive, composition, and technological quality of foods. This has made researchers to generate a web-based food fluorescence library (Database) as seen from Table 1.2 and Fig. 1.9. This comprises of naturally occurring fluorophores in food stuffs to be generated (Christensen et al., 2006). Due to abundance of fluorophore compounds in agricultural products,

fluorescence spectroscopy method has demonstrated ability to assess food quality such as olive oil and wine origin and ageing condition (Airado-Rodríguez et al., 2011; Al Riza et al., 2021), cheese classification (Rouissi et al., 2008) and authentication of botanical and geographical origin honey (Ruoff et al., 2006).

Fish are rich in auto-fluorescent substances such as proteins, amino acids, vitamins, collagen, and lipid oxidation products. This makes fluorescence spectroscopic techniques quite useful for assessing fish quality/freshness. Previously, fluorescence spectroscopy has demonstrated that it can rapidly discriminate fresh from frozen-thawed sea bass fillets (Karoui et al., 2017), non-invasive estimation of freshness changes of frozen horse mackerel fillets (Elmasry et al., 2015). Right angle fluorescence spectroscopy (RAFS) was used by Liao et al., (2018) to investigate the fluorescence properties and tendencies of fisheye fluid. From their findings, they confirmed that fisheye fluid contains fluorescence compounds whose intensity vary during storage. They demonstrated that uric acids which is present in the fisheye accumulate gradually as the freshness of the fish continues to deteriorate. Despite thus method proving to be sensitive and more specific, its destructive sampling nature (abstracting the fisheye fluid with a syringe and needle) form the eye for measurement made it cumbersome, time consuming and unsuitable for online monitoring systems. Therefore, there is need for a quick, non-destructive, and near application technique. Since front-face fluorescence spectroscopy (FFFS) can help overcome the challenged posed by RAFS, this informs the reason for adopting in the current study to evaluate fish freshness during storage.

Table 1.2: Naturally occurring fluorophores and their properties

No.	Fluorophore	Excitation λ_{max} (nm)	Emission λ_{max} (nm)
1.	Phenylalanine	258	284
2.	Tyrosine	276	302
3.	Tryptophan	280	357
4.	Vitamin A (retinol)	346	480
5.	Vitamin B_2 (riboflavin)	270 (382,448)	518
6.	Vitamin B_6 (pyridoxin)	328	393
7.	Vitamin E (α-tocopherol)	298	326
8.	NADH	344	465
9.	ATP	292	388
10.	Chlorophyll α	428	663
11.	Hematoporphyrin	396	614
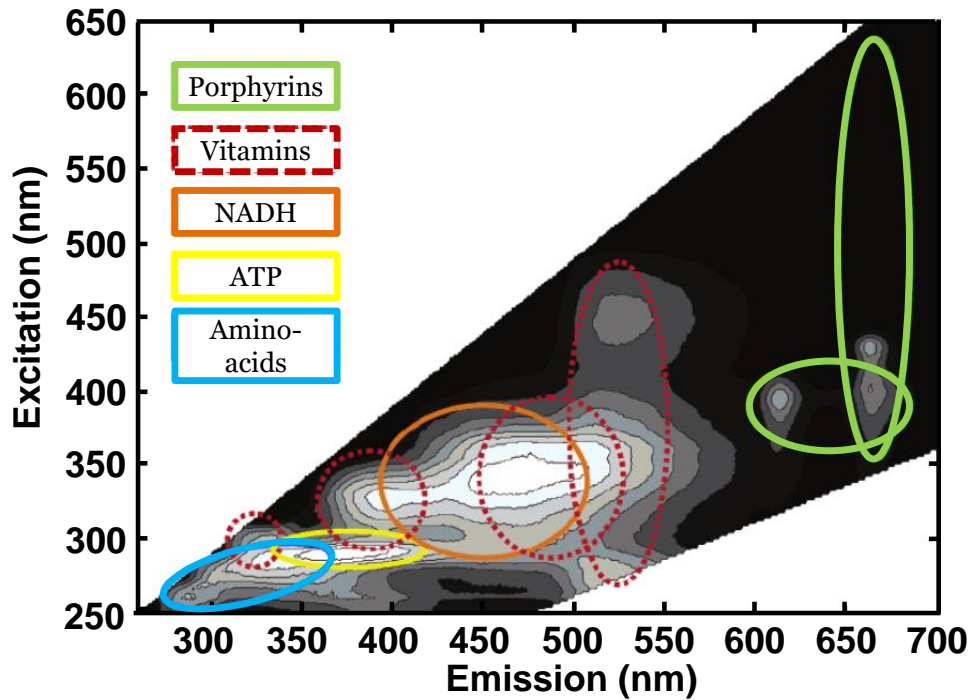
Fig. 1.9: Contour plot of normalized fluorescence landscape of common fluorophores

1.2 Research objectives

Various methods have been suggested for the evaluation of fish freshness, however, most of them could be limited to industrial application owing to their complexity, laboratory based, time

consuming, or difficulty of interpreting results. Since fish are highly perishable and its freshness deteriorates very fast, there is need for a simple but rapid freshness monitoring devices that can guarantee quality for fish consumers. The final goal of this study is to establish an accurate, quick, and simple intact fish freshness assessment technique using machine vision systems. To achieve this, pre-liminary experiment was carried out using FFFS on the eyeball and surface scales to determine the optimum excitation wavelengths for imaging. Mature fishes come in different sizes and shapes. Unlike big fishes (usually >1000 g) that require to be cut and sold in small sizes, small fishes (<300 g) are sold while the whole body is in intact state. Therefore, establishing a quality monitoring mechanism during storage for a fish whose body parts are intact will be more realistic compared to fish fillets and steaks. Japanese dace (*Tribolodon hakonensis*) fish is used for this experimental because it is a common freshwater fish in Japan. The external parts of the fish (eyeball, surface containing scales, and belly) would be used because since they lie on the surface of the fish, they will be suitable for non-destructive freshness evaluation of intact fishes. Additionally, these parts are not consumable, hence, there is less damage to the edible parts. Since these experimenting parts lies on the surface of the fish, development of non-destructive online monitoring techniques such as non-contact sensor or machine vision could potentially resolve the challenge of quality assessment.

To realize this goal, three studies were carried out as outlined below:

a) Investigating the fluorescence characteristics of Japanese dace fish's eyeballs and scales to find optimum wavelengths related with freshness deterioration for monitoring quality during storage.

b) Investigated the source of fluorescence for eyeball (whether is surface or inside the eyeball). With the optimal selected wavelengths, we developed a computer vision system for monitoring fluorescence color changes (using 365 nm UV LED) of fisheyes with freshness deterioration during storage using.

Investigating the fluorescence properties of other external parts (scales and belly parts) and combine them with eyeball to develop a multiwavelength imaging system (280 nm, 365 nm, 395 nm and white light LEDs) for tracking fish freshness changes by color. 280, 365 nm and white LEDs are commercially available in the market. 280 nm LED can monitor fluorescence changes associated with proteins and amino acids compounds; 365 nm LED can monitor the third peak

20

with excitation at 350 nm. 395 nm LED was used to complement 365 nm LED because the spectral range for the target peak extends from 345-390 nm.

1.3 Outline of the thesis

The dissertation is made up of six main chapters.

Chapter 1: Provides the research background and general introductions, states the problem statement, objectives.

Chapter 2: Introduces the main experimental materials and methodology.

Chapter 3: Discusses the findings on sensitive wavelength regions for freshness evaluation using EEM data for eyeball, scales, and muscle parts. Here, we propose the appropriate excitation wavelengths useful for monitoring fish freshness during storage.

Chapter 4: Investigates the fluorescence properties of fisheye to reveal the source of the fluorescence features on the eyeball (whether it is from inside the eye or outside the eye surface. A simple UV-induced fluorescence imaging on the eye was established based on one of the important selected excitations of fish eyeball (350 nm) from chapter III above. The paper discusses the findings of UV-fluorescence imaging on the fisheye imaging results.

Chapter 5: Presents the use of UV-induced fluorescence imaging (365 and 395 nm), deep UV imaging (280 nm) and white light images. This chapter discusses the imaging results for fish eyeball, scales, and belly parts for all the important wavelength bands (280 and 350 nm).

Chapter 6: Summarizes the story by giving overall conclusions and highlights the challenges and limitations of this technique. This chapter proposes some ideas for improving the reported findings and possible future research

REFERENCES

Abbas, B., Alshikh Khalil, M., 2016. An experimental method for determination of the refractive index of liquid samples using michelson interferometer. Acta Phys. Pol. A 129, 59–63. https://doi.org/10.12693/APhysPolA.129.59

Airado-Rodríguez, D., Durán-Merás, I., Galeano-Díaz, T., Wold, J.P., 2011. Front-face fluorescence spectroscopy: A new tool for control in the wine industry. J. Food Compos. Anal. 24, 257–264. https://doi.org/10.1016/j.jfca.2010.10.005

Al Riza, D.F., Kondo, N., Rotich, V.K., Perone, C., Giametta, F., 2021. Cultivar and geographical origin authentication of Italian extra virgin olive oil using front-face fluorescence spectroscopy and chemometrics. Food Control 121, 107604. https://doi.org/10.1016/j.foodcont.2020.107604

Bechmann, I.E., Jørgensen, B.M., 1998. Rapid assessment of quality parameters for frozen cod using near infrared spectroscopy. LWT - Food Sci. Technol. 31, 648–652. https://doi.org/10.1006/fstl.1998.0418

Behlke, M.A., Huang, L., Bogh, L., Rose, S., Devor, E.J., 2005. Fluorescence and Fluorescence Applications 1–13.

Brandt, M., 2010. Fluorescence Spectroscopy 20–26.

Carrasco, E., Valero, A., Pérez-Rodríguez, F., García-Gimeno, R.M., Zurera, G., 2007. Management of microbiological safety of ready-to-eat meat products by mathematical modelling: Listeria monocytogenes as an example. Int. J. Food Microbiol. 114, 221–226. https://doi.org/10.1016/j.ijfoodmicro.2006.09.013

Castillo-Yánez, F.J., Jiménez-Ruíz, E.I., Canizales-Rodríguez, D.F., Márquez-Ríos, E., Montoya-Camacho, N., Ruíz-Cruz, S., Ocaño-Higuera, V.M., 2014. Postmortem biochemical changes and evaluation of the freshness in the muscle of tilapia (Oreochromis niloticus) during the storage in ice. J. Fish. Aquat. Sci. 9, 435–445. https://doi.org/10.3923/jfas.2014.435.445

Cheng, J.H., Sun, D.W., 2014. Hyperspectral imaging as an effective tool for quality analysis and control of fish and other seafoods: Current research and potential applications. Trends Food Sci. Technol. 37, 78–91. https://doi.org/10.1016/j.tifs.2014.03.006

Cheng, J.H., Sun, D.W., Pu, H., Zhu, Z., 2015. Development of hyperspectral imaging coupled with chemometric analysis to monitor K value for evaluation of chemical spoilage in fish fillets. Food Chem. 185, 245–253. https://doi.org/10.1016/j.foodchem.2015.03.111

Christensen, J., Nørgaard, L., Bro, R., Engelsen, S.B., 2006. Multivariate Autofluorescence of Intact Food Systems. Am. Chem. Soc. 106. https://doi.org/10.1021/cr050019q

Corry, J.E.L., Jarvis, B., Passmore, S., Hedges, A., 2007. A critical review of measurement uncertainty in the enumeration of food micro-organisms. Food Microbiol. 24, 230–253. https://doi.org/10.1016/j.fm.2006.05.003

Dale, N., 1994. National research council nutrient requirements of poultry — ninth revised edition (1994), Journal of Applied Poultry Research. https://doi.org/10.1093/japr/3.1.101

Dalgaard, P., 1995. Modelling of microbial activity and prediction of shelf life for packed fresh fish. Int. J. Food Microbiol. 26, 305–317. https://doi.org/10.1016/0168-1605(94)00136-T

Dowlati, M., de la Guardia, M., Dowlati, M., Mohtasebi, S.S., 2012. Application of machine-vision techniques to fish-quality assessment. TrAC - Trends Anal. Chem. 40, 168–179. https://doi.org/10.1016/j.trac.2012.07.011

Dowlati, M., Mohtasebi, S.S., Omid, M., Razavi, S.H., Jamzad, M., De La Guardia, M., 2013. Freshness assessment of gilthead sea bream (Sparus aurata) by machine vision based on gill and eye color changes. J. Food Eng. 119, 277–287. https://doi.org/10.1016/j.jfoodeng.2013.05.023

Dufour, E., J.P. Frencia, A., Kane, E., 2003. Development of a rapid method based on front-face fluorescence spectroscopy for the monitoring of fish freshness. Food Res. Int. 36, 415–423. https://doi.org/10.1016/S0963-9969(02)00174-6

Elmasry, G., Nagai, H., Moria, K., Nakazawa, N., Tsuta, M., Sugiyama, J., Okazaki, E., Nakauchi, S., 2015. Freshness estimation of intact frozen fish using fluorescence spectroscopy and chemometrics of excitation-emission matrix. Talanta 143, 145–156. https://doi.org/10.1016/j.talanta.2015.05.031

Fereidoon, S., Zhong, Y., 2010. RSC_CS_B922183M 4067..4079 _ Enhanced Reader.pdf. Chem.

Soc. Rev. 39, 4067–4079. https://doi.org/0.1039/b922183m

Ghaly, a E., Dave, D., Budge, S., Brooks, M.S., 2010. Fish Spoilage Mechanisms and Preservation Techniques : Review Department of Process Engineering and Applied Science , Dalhousie University Halifax , Nova Scotia , Canada. Am. J. Appl. Sci. 7, 859–877.

Gram, L., Dalgaard, P., 2002. Fish spoilage bacteria - Problems and solutions. Curr. Opin. Biotechnol. 13, 262–266. https://doi.org/10.1016/S0958-1669(02)00309-9

Gram, L., Huss, H.H., 1996. Microbiological spoilage of fish and fish products. Int. J. Food Microbiol. 33, 121–37.

Haard, N.F., 1992. Control of chemical composition and food quality attributes of cultured fish. Food Res. Int. 25, 289–307. https://doi.org/10.1016/0963-9969(92)90126-P

Han, F., Zhang, D., Aheto, J.H., Feng, F., Duan, T., 2020. Integration of a low-cost electronic nose and a voltammetric electronic tongue for red wines identification. Food Sci. Nutr. 8, 4330–4339. https://doi.org/10.1002/fsn3.1730

Hassoun, A., Karoui, R., 2015. Front-face fluorescence spectroscopy coupled with chemometric tools for monitoring fish freshness stored under different refrigerated conditions. Food Control 54, 240–249. https://doi.org/10.1016/j.foodcont.2015.01.042

Heia, K., Esaiassen, M., Nilsen, H., 2003. Measurement of quality of fish using visible light. Netherlands Wageningen Acad. Publ. 201–209.

Hong, H., Regenstein, J.M., Luo, Y., 2017. The importance of ATP-related compounds for the freshness and flavor of post-mortem fish and shellfish muscle: A review, Critical Reviews in Food Science and Nutrition. https://doi.org/10.1080/10408398.2014.1001489

Hong, H., Yang, X., You, Z., Cheng, F., 2014. Visual quality detection of aquatic products using machine vision. Aquac. Eng. 63, 62–71. https://doi.org/10.1016/j.aquaeng.2014.10.003

Hsieh, R.J., Kinsella, J.E., 1989. Oxidation of Polyunsaturated Fatty Acids: Mechanisms, Products, and Inhibition with Emphasis on Fish. Adv. Food Nutr. Res. 33, 233–341. https://doi.org/10.1016/S1043-4526(08)60129-1

Hu, J., Li, D., Duan, Q., Han, Y., Chen, G., Si, X., 2012. Fish species classification by color, texture and multi-class support vector machine using computer vision. Comput. Electron. Agric. 88, 133–140. https://doi.org/10.1016/j.compag.2012.07.008

Hyldig, G., Bremmer, A., Martinsdottir, E., Schelvis, R., 2010. "Quality Index Methods." Handbook of seafood and seafood products. Blackwell Publishing.

Itoh, D., Koyachi, E., Yokokawa, M., Murata, Y., Murata, M., Suzuki, H., 2013. Microdevice for On-Site Fish Freshness Checking Based on K-Value Measurement. Anal. Chem. 85, 10962–10968. https://doi.org/10.1021/ac402483w

Jason, A.C., Richards, J.C.S., 1975. The development of an electronic fish freshness meter. J. Phys. E. 8, 826–830. https://doi.org/10.1088/0022-3735/8/10/011

Juneja, V.K., Huang, L., Thippareddi, H.H., 2006. Predictive model for growth of Clostridium perfringens in cooked cured pork. Int. J. Food Microbiol. 110, 85–92. https://doi.org/10.1016/j.ijfoodmicro.2006.01.038

Kanamori, K., Shirataki, Y., Liao, Q., Ogawa, Y., Suzuki, T., Kondo, N., 2017. Fish freshness estimation using eye image processing under white and UV lightings. Sens. Agric. Food Qual. Saf. IX 10217, 102170E. https://doi.org/10.1117/12.2260622

Karoui, R., Blecker, C., 2010. Fluorescence Spectroscopy Measurement for QualityAssessment of Food Systems—a Review. Food Bioprocess Technol 4, 364–386.

Karoui, R., Hassoun, A., Ethuin, P., 2017. Front face fluorescence spectroscopy enables rapid differentiation of fresh and frozen-thawed sea bass (Dicentrarchus labrax) fillets. J. Food Eng. 202, 89–98. https://doi.org/10.1016/j.jfoodeng.2017.01.018

Kohler, A., Skaga, A., Hjelme, G., Skarpeid, H.J., 2002. Sorting salted cod fillets by computer vision: A pilot study. Comput. Electron. Agric. 36, 3–16. https://doi.org/10.1016/S0168-1699(02)00068-6

Lavie, C.J., Milani, R. V., Mehra, M.R., Ventura, H.O., 2009. Omega-3 Polyunsaturated Fatty Acids and Cardiovascular Diseases. J. Am. Coll. Cardiol. 54, 585–594. https://doi.org/10.1016/j.jacc.2009.02.084

Leelapongwattana, K., Benjakul, S., Visessanguan, W., Howell, N.K., 2008. Raman spectroscopic analysis and rheological measurements on natural actomyosin from haddock (Melanogrammus aeglefinus) during refrigerated (4 °C) and frozen (-10 °C) storage in the presence of trimethylamine-N-oxide demethylase from kidney of lizardfish . Food Chem. 106, 1253–1263. https://doi.org/10.1016/j.foodchem.2007.06.061

Liao, Q., Suzuki, T., Shirataki, Y., Kuramoto, M., Kondo, N., 2018. Freshness related fluorescent compound changes in Japanese dace fish (Tribolodon hakonensis) eye fluid during storage. Eng. Agric. Environ. Food 11, 95–100. https://doi.org/10.1016/j.eaef.2018.01.001

Lowe, T.E., Ryder, J.M., Carragher, J.F., Wells, R.M.G., 1993. Flesh Quality in Snapper, Pagrcrs auratus, Affected by Capture Stress. J. Food Sci. 58, 770–773. https://doi.org/10.1111/j.1365-2621.1993.tb09355.x

Masniyom, P., 2011. Deterioration and shelf-life extension of fish and fishery products by modified atmosphere packaging, Songklanakarin Journal of Science and Technology. Mueang, Pattani. https://doi.org/rdo.psu.ac.th/sjstweb/journal/33-2/0125-3395-33-2-181-192.pdf

Mery, D., Lillo, I., Loebel, H., Riffo, V., Soto, A., Cipriano, A., Aguilera, J.M., 2011. Automated fish bone detection using X-ray imaging. J. Food Eng. 105, 485–492. https://doi.org/10.1016/j.jfoodeng.2011.03.007

Misimi, E., Mathiassen, J.R., Erikson, U., 2007. Computer vision-based sorting of Atlantic salmon (Salmo salar) fillets according to their color level. J. Food Sci. 72, S030–S035. https://doi.org/10.1111/j.1750-3841.2006.00241.x

Nilsen, H., Esaiassen, M., 2005. Predicting sensory score of cod (Gadus morhua) from visible spectroscopy. LWT - Food Sci. Technol. 38, 95–99. https://doi.org/10.1016/j.lwt.2004.05.001

Nilsen, H., Esaiassen, M., Heia, K., Sigernes, F., 2002. Visible/near-infrared spectroscopy: A new tool for the evaluation of fish freshness? J. Food Sci. 67, 1821–1826. https://doi.org/10.1111/j.1365-2621.2002.tb08729.x

Ocaño-Higuera, V.M., Maeda-Martínez, A.N., Marquez-Ríos, E., Canizales-Rodríguez, D.F.,

Castillo-Yáñez, F.J., Ruíz-Bustos, E., Graciano-Verdugo, A.Z., Plascencia-Jatomea, M., 2011. Freshness assessment of ray fish stored in ice by biochemical, chemical and physical methods. Food Chem. 125, 49–54. https://doi.org/10.1016/j.foodchem.2010.08.034

Olafsdottir, G., Nesvadba, P., Di Natale, C., Careche, M., Oehlenschläger, J., Tryggvadóttir, S. V., Schubring, R., Kroeger, M., Heia, K., Esaiassen, M., Macagnano, A., Jørgensen, B.M., 2004. Multisensor for fish quality determination. Trends Food Sci. Technol. 15, 86–93. https://doi.org/10.1016/j.tifs.2003.08.006

Rahman, A., Kondo, N., Ogawa, Y., Suzuki, T., Kanamori, K., 2016. Determination of K value for fish flesh with ultraviolet-visible spectroscopy and interval partial least squares (iPLS) regression method. Biosyst. Eng. 141, 12–18. https://doi.org/10.1016/j.biosystemseng.2015.10.004

Rasmus Bro, and S.B.E.J.C.L.N., 2006. Multivariate Autofluorescence of Intact Food Systems. Am. Chem. Soc. 106, 1979–1994. https://doi.org/10.1021/cr050019q

Rodriguez-Casado, A., Carmona, P., Moreno, P., Sánchez-González, I., Macagnano, A., Natale, C. Di, Careche, M., 2007. Structural changes in sardine (Sardina pilchardus) muscle during iced storage: Investigation by DRIFT spectroscopy. Food Chem. 103, 1024–1030. https://doi.org/10.1016/j.foodchem.2006.09.054

Rouissi, H., Dridi, S., Kammoun, M., De Baerdemaeker, J., Karoui, R., 2008. Front face fluorescence spectroscopy: A rapid tool for determining the effect of replacing soybean meal with scotch bean in the ration on the quality of Sicilo-Sarde ewe's milk during lactation period. Eur. Food Res. Technol. 226, 1021–1030. https://doi.org/10.1007/s00217-007-0627-7

Ruoff, K., Luginbuhl, W., Kunzli, R., Bogdanov, S., Bosset, J.O., Ohe, K. Von Der, Ohe, W. Von Der, Amado, R., 2006. Authentication of the Botanical and Geographical Origin of Honey by Front-Face Fluorescence Spectroscopy. J. Agric. Food Chem. 6858–6866.

Ryder, J.M., 1985. Determination of Adenosine Triphosphate and Its Breakdown Products in Fish Muscle by High-Performance Liquid Chromatography. J. Agric. Food Chem. 33, 678–680. https://doi.org/10.1021/jf00064a027

Saito, T., Arai, K. ichi, Matsuyoshi, M., 1959. A New Method for Estimating the Freshness of Fish. Nippon Suisan Gakkaishi (Japanese Ed. 24, 749–750. https://doi.org/10.2331/suisan.24.749

Samaranayaka, A.G.P., Li-Chan, E.C.Y., 2008. Autolysis-assisted production of fish protein hydrolysates with antioxidant properties from Pacific hake (Merluccius productus). Food Chem. 107, 768–776. https://doi.org/10.1016/j.foodchem.2007.08.076

Sánchez-Alonso, I., Martinez, I., Sánchez-Valencia, J., Careche, M., 2012. Estimation of freezing storage time and quality changes in hake (Merluccius merluccius, L.) by low field NMR. Food Chem. 135, 1626–1634. https://doi.org/10.1016/j.foodchem.2012.06.038

Shumilina, E., Ciampa, A., Capozzi, F., Rustad, T., Dikiy, A., 2015. NMR approach for monitoring post-mortem changes in Atlantic salmon fillets stored at 0 and 4 °c. Food Chem. 184, 12–22. https://doi.org/10.1016/j.foodchem.2015.03.037

Sone, I., Olsen, R.L., Dahl, R., Heia, K., 2011. Visible/near-infrared spectroscopy detects autolytic changes during storage of atlantic salmon (Salmo salar L.). J. Food Sci. 76, 203–209. https://doi.org/10.1111/j.1750-3841.2011.02062.x

Strasburg, G.M., Ludescher, R.D., 1995. Theory and applications of fluorescence spectroscopy in food research. Trends Food Sci. Technol. 6, 69–75. https://doi.org/10.1016/S0924-2244(00)88966-9

Sykes, A. V., Oliveira, A.R., Domingues, P.M., Cardoso, C.M., Andrade, J.P., Nunes, M.L., 2009. Assessment of European cuttlefish (Sepia officinalis, L.) nutritional value and freshness under ice storage using a developed Quality Index Method (QIM) and biochemical methods. LWT - Food Sci. Technol. 42, 424–432. https://doi.org/10.1016/j.lwt.2008.05.010

Valeur, B., Bochon, J.C., 2001. New trends in fluorescence spectroscopy—Applications to chemical and life sciences. Springer.

Wang, L. mei, Luo, M. kun, Yin, H. ran, Zhu, W. bin, Fu, J. jun, Dong, Z. jie, 2020. Effects of background adaptation on the skin color of Malaysian red tilapia. Aquaculture 521, 735061. https://doi.org/10.1016/j.aquaculture.2020.735061

Watanabe, A., Tsuneishi, E., Takimoto, Y., 1989. Analysis of ATP and Its Breakdown Products in Beef by Reversed-Phase HPLC. J. Food Sci. 54, 1169–1172. https://doi.org/10.1111/j.1365-2621.1989.tb05948.x

White, D.J., Svellingen, C., Strachan, N.J.C., 2006. Automated measurement of species and length of fish by computer vision. Fish. Res. 80, 203–210. https://doi.org/10.1016/j.fishres.2006.04.009

Yapar, A., Yetim, H., 1998. Determination of anchovy freshness by refractive index of eye fluid. Food Res. Int. 31, 693–695. https://doi.org/10.1016/S0963-9969(99)00047-2

Zhu, F., Zhang, D., He, Y., Liu, F., Sun, D.W., 2013. Application of Visible and Near Infrared Hyperspectral Imaging to Differentiate Between Fresh and Frozen-Thawed Fish Fillets. Food Bioprocess Technol. 6, 2931–2937. https://doi.org/10.1007/s11947-012-0825-6

CHAPTER II: MATERIALS AND METHODS

2.1 Sample information

In this study, Japanese Dace fish (*Tribolodon hakonensis*) (Fig. 2.1), was used as the experimental fish species; with their scientific classification information presented in Table 2. 1.

The Japanese dace fish were bred between March and April of every year in the 2018, 2019 and 2020 and raised at 20 ºC temperature in fresh water for about ten months, Wakayama Prefecture, Japan. They were purchased in September of 2018 2019 and 2020 from Hamaichi bait manufacturer Co. Ltd., Wakayama prefecture, Japan, with a fork length 160 ± 15 mm.

Table 2.1: Classification of fish samples used in the experiment

Scientific class	Japanese dace	Ayu
Kingdom	Animalia	Animalia
Phylum	Chordata	Chordata
Class	Actinopterygii	Actinopterygii
Order	Cypriniformes	Osmeriformes
Family	Cyprinidae	Plecoglossidae
Genus	Tribolodon	Plecoglossus
Species	T. *hakonensis*	P. *altivelis*

Fig. 2.1: Images of fish used for research.

2.2 Devices

i. *Freshness Evaluation (K-value measurement instrument)*

Fig. 2.2a shows a freshness checker machine (QS 3201, QS solution, Japan) which represents one of the conventional methods for checking freshness of meat products was used to measure the freshness level of fish meat during the experiment; it was machine was developed by Prof. Minoru Sato (Professor, Tohoku University, Japan). The freshness checker tracks down the

breakdown of phosphate compounds during the ATP breakdown to form its metabolites. These metabolites include ATP, ADP, AMP, IMP, H_xR and H_x; where H_xR and Hx represents spoilt components. Freshness is determined by taking the ratio of spoilt components (H_xR and Hx) to the whole nucleotide disintegrated compounds (ATP, ADP, AMP, IMP, H_xR and H_x); defined as K-value or freshness index and expressed as percentage, where low value indicates good quality (high freshness) and vice versa.
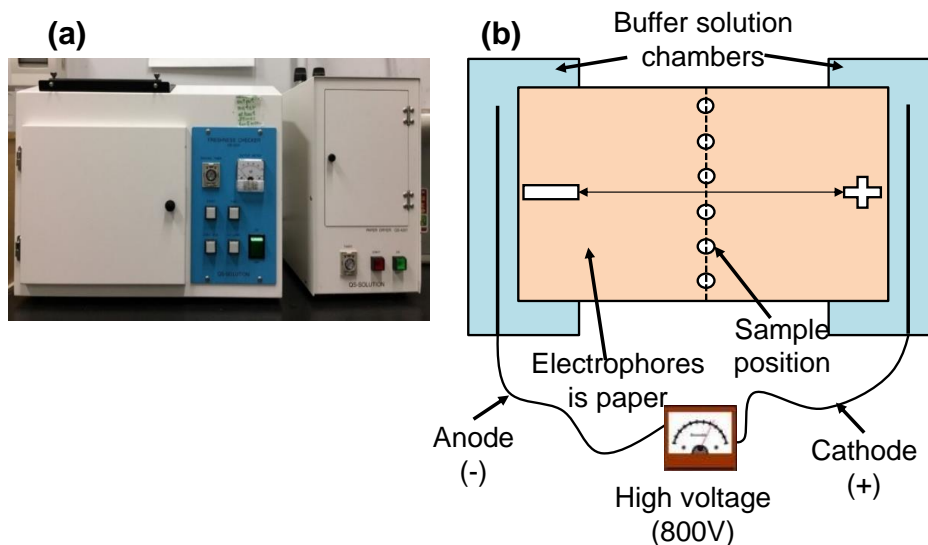
Fig. 2.2: (a) Freshness checker machine (b) The principle of electrophoresis measurement.

a. Principle of Freshness checker

The freshness checker machine utilizes the principle of paper electrophoresis; where a buffer solution is used to moisten a filter paper and the ends of this paper are dipped into buffer reservoir with electrodes. At the center of the paper are marked spots where drops of supernatant sample solutions are spotted. When a high voltage is applied, and the spots migrate according to their individual charges, where the charge carried by molecule depends on the pH of the medium. After the electrophoresis process, the separated components are detected using UV light for spot analysis (Fig. 2.2b).

b. Procedure for freshness checking

A piece of meat was cut from the dorsal part of the fish and chopped into small pieces. About 200 mg of chopped meat was weighed and used for determining the freshness index (K-value). The sampled was crashed in a 600 μL of extraction reagent A (supplied by QS solution, Japan) in plastic lock tubes. About 450 μL 5.61% (v/w) (potassium hydroxide) solution B was used

as a neutralizing agent and later about 150 μL solution C for fine pH adjustment, use the litmus papers. Freshness checker (QS 3201, QS solution, Japan) was used in the paper electrophoresis measurement process to determine the freshness level. During the electrophoresis measurement, the electrophoresis paper was mounted on a special holder and sprayed with an electrophoresis buffer solution (QS solution, Japan) until it was moderately. Three microliters (3 μl) of the supernatant solution were applied to the spots at the centerline of the electrophoresis paper, while the suspending ends of the paper were dipped in a buffer solution in the chamber. Fig. 2.3 illustrates the electrophoresis measurement which was carried out under 800 V for 5 minutes. Thereafter, the paper was dried using forced air convection dryer (Paper dryer QS 4201, Japan) set at 100 ℃ for 5 minutes.
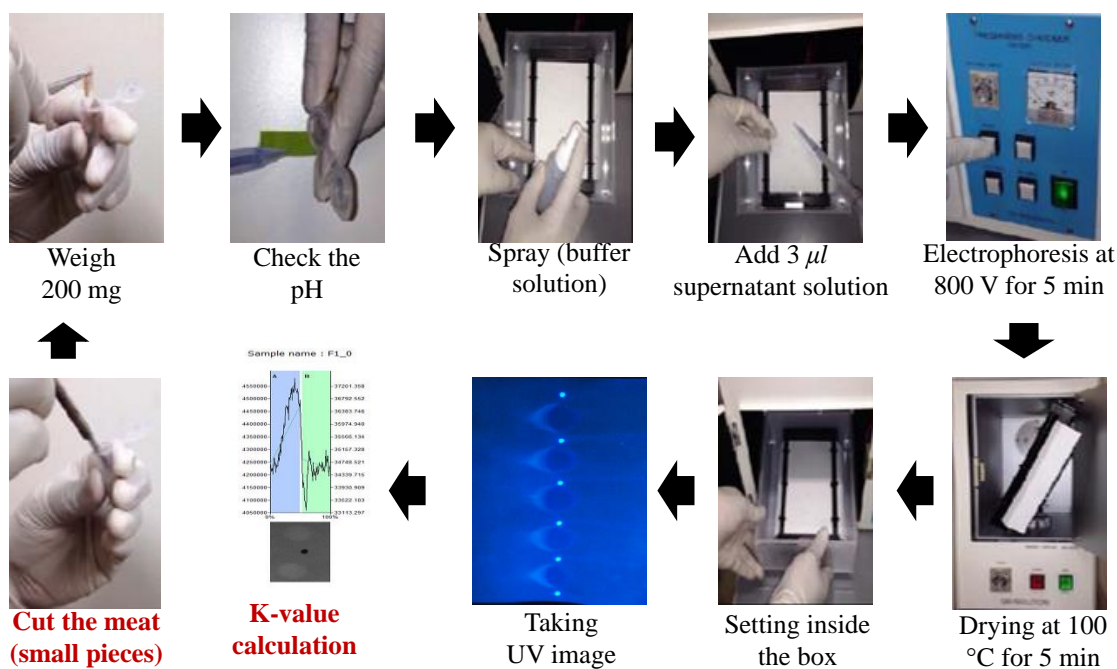
Fig. 2.3: *K*-value measurement using freshness checker.

The dried paper was put back into the freshness checker machine for illumination of the spots using 254 nm UV light box. A digital camera (Canon EOS M3, Tokyo, Japan) was used to record the color intensity of the developed spots by acquiring images. Finally, the freshness index (*K* value) was calculated using the Spot Analyzer (QS Solution, Tokyo, Japan) software expressed as a percentage.

The evaluation of freshness using this method (biochemical examination technique) as reported by Itoh et al. (2013) and Elmasry et al. (2015) is accepted as a conventional technique for

evaluating the quality of meat and fish products. This is because the method can quantitatively track down the disintegration of adenosine triphosphate (ATP) compounds to its metabolites: adenosine di-phosphates (ADP), adenosine monophosphates (AMP), inosine monophosphates (IMP), inosine (H_xR), and hypoxanthine (H_x) and uric acid as a final product (Cheng et al., 2016; Watanabe, Tsuneishi, & Takimoto, 1989). To tell the freshness of the fish, a ratio of non-phosphatic ATP to the total ATP-related compounds including decomposition products expressed as a percentage is widely accepted as a standard freshness indicator for meat products. The resultant value (see Eqn. 2.1) is commonly referred to as K value.

$$K \text{ value} = \frac{H_xR + H_x}{ATP + ADP + AMP + IMP + H_xR + H_x} \times 100 \ldots \quad \text{(Eqn. 2.1)}$$

c. *Spot analysis*

The process of analyzing UV images acquired after illuminating the dry electrophoresis paper with 254 nm UV lamp inside the freshness checker machine (QS 3201, QS solution, Japan). Image analysis is done by spot analyzer software by checking the extent to which ATP has broken down. Results can be shown on the screen, or even printed as hard copy and saved to a database. The analysis was done using the spot analyzer software installed in a hp laptop computer as displayed in Fig. 2.4.
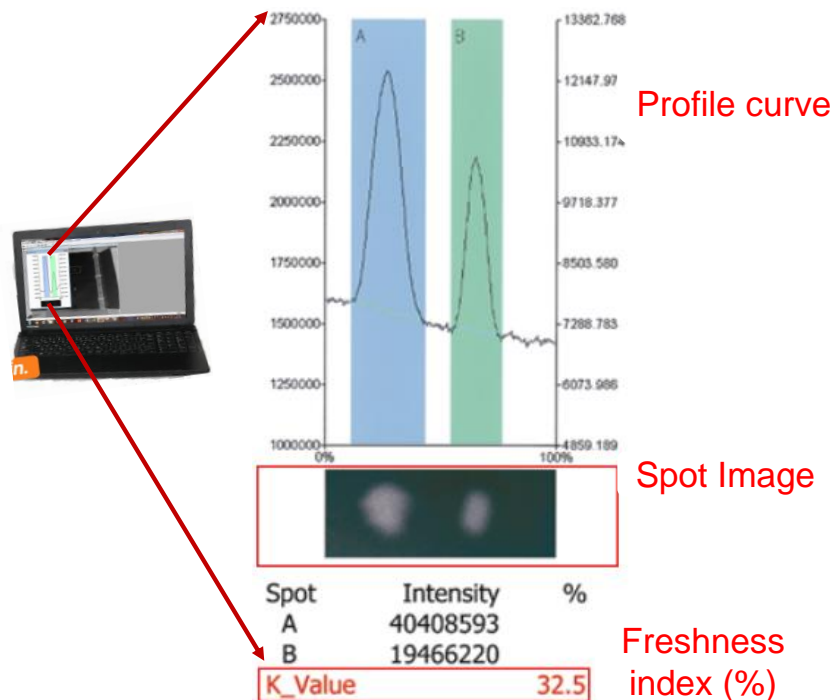
Fig. 2.4: Spot analysis for calculating K-value (freshness level) of fish.

33

ii. Spectrofluorometer

Spectrofluorometer (shown in Fig. 2.5) is known for fluorescence measurement of various samples. The geometry of sampling has a considerable effect on the obtained fluorescence signal, but this depends on the angle of excitation, sample form (liquid or solid) or property (transparent or opaque). There exist two techniques for fluorescence measurement; right-angle (the angle between excitation light and the detector is placed at 90 °) (see Fig. 2.6a) and front-face (the angle between excitation light and the detector is about 30 °) as shown in Fig. 2.6b. Right-angle is commonly known for measuring liquid substances (mostly transparent) with low concentrations; unlike front-face which is common for untreated samples (high concentration) and solid samples which are not transparent. Because front-face fluorescence is used to measure opaque materials like food samples, and this makes it possible to measure turbid substances which the light cannot penetrate. In front face measurement, the incident angle of excitation light was set as 30° to avoid the reflectance effects on fluorescence emission.
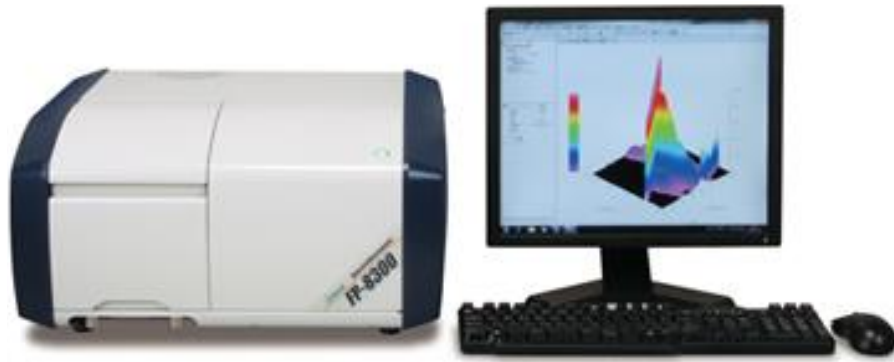
Fig. 2.5: Spectrofluorometer device for measuring EEM.

(a)

(b)
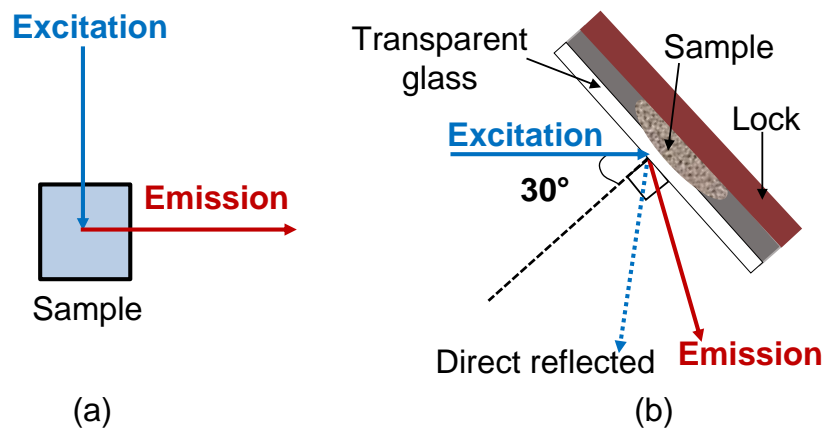
Fig. 2.6: Types of fluorescence techniques; (a) Right-angle and (b) Front-face fluorescence.

Fluorescence spectroscopy utilizes two measurement techniques as seen from Fig. 2.6 above. In this study, fluorescence EEM were measured done using front-face fluorescence technique (see Fig. 2.6b) to obtain the spectra data using spectrofluorometer, JASCO FP-8300 (JASCO Co., Tokyo, Japan). Fig. 2.7 demonstrates how the sample was mounted on the device for measurement. After refrigerating the fish for two hours, the eyeballs were removed for EEM measurement. The eye was then dissected to separate the parts (cornea, lens, eye fluid and gel) for further fluorescence examination of different structures of the fisheye. The measurement principle of the spectrometer machine for front-face fluorescence spectroscopy (FFFS) is as indicated in Fig. 2.8 below; with Table 2.2 giving the full names of the labels used. The spectrometer specifications are as shown in Table 2.3.

Fig. 2.7: Fluorescence measurement of the eye structure.

Fig. 2.8: FFFS measurement principle of the spectrofluorometer machine.

35

Table 2.2: Labels for the spectrofluorometer machine

Label	Description
M_1 - M_8	Mirrors
BS	Beam splitter
Ch	Chopper
F_1, F_2	Filter (FP 8300)
PD	Monitoring detector/photodiode
Hg	Low pressure mercury lamp
G_1, G_2	Concave diffraction grating
S_1, S_2	Spectrograph slit
PMT	Detector (Photomultiplier tube)

Table 2.3: Spectrofluorometer specifications

Characteristics	Description
Spectrofluorometer model	Jasco FP-8300
Photometric system	Monochromatic light to monitor Xe lamp intensity output
Light source	150-watt Xe lamp
Wavelength range	Zero order, 200 - 900 nm
Resolution	1.0 nm
Wavelength accuracy	1.5 nm
Scanning speed	20 to 20000 nm/min
Detector	Excitation: Silicon photodiode; Emission: PMT

a. Spectra processing

The recorded raw EEM was corrected by standardizing the light source and response detector using the calibration spectra protocol as outlined by JASCO Company. The corrected EEM was converted from the arbitrary unit (A.U) to Raman units (R.U) to prevent instrumental effects/biases on the results (Lawaetz and Stedmon, 2009). The collected data was converted from arbitrary units (A.U) to Raman units (R.U) to standardize the results for easy comparison.

iii. Image acquisition

(a)

(b)

Fig. 2.9: Cameras used for capturing images.

Fish images were taken in a dark room using Canon camera, EOS DSLR (kiss x7, Color Inc., Japan) (Fig. 2.9a) for white, 395 nm and 365 nm light emitting diodes (LEDs) and UV-Camera (ARTCAM-407UV- WOM) for deep UV (280 nm LED) (see (Fig. 2.9b). The LEDs were characterized with different images, such as reflectance images from white lighting and fluorescence images excited from 280, 365 and 395 nm. The EOS DSLR camera was fixed at about 250 mm above the sample surface with a focal length of 55 mm and the UV camera was mounted at 300 mm above the sample. All images were taken with same F-number (f/6.3) and ISO (100). In the white lighting to two white bar LEDs (LDL2-80 × 16SW2, CCS Inc. Japan). In the first experiment, color images were taken under the 4 halogen lamps (of color temperature 2700 K) with a shutter speed of 1/10 s, f/6.3 and an ISO of 200. Fluorescence images were acquired using a 365 nm UV-LED excitation source (LDR2-60UV2-365-N, CCS Inc., Japan) with a shutter speed of 4 s, f/6.3 and an ISO of 200. The UV-LED was placed 120 mm above the sample surface. In the second experiment, the sample was illuminated using two white bar LEDs (LDL2-80 × 16SW2, CCS Inc. Japan) with a shutter speed of 1/5 s for normal color images; two 365 nm UV bar LEDs (LDL-71 × 12UV2-365- N, CCS Inc. Japan) with a shutter speed of 2.5 s; two 395 nm ring LEDs (HLV-24VL395-4WNRBTNJ, CCS Inc. Japan) with a shutter speed of 1/ 4 s and a 280 nm ring (LED (LDR2-100UV2-280-W, CCS Inc. Japan) with software filter parameters (brightness: 50, contrast: 0, sharpness: 11, and gamma: 80; global gain 350 and shutter speed 0.1 s). The distance between the sample and the lighting devices was set as; 160 mm (white bar LEDs),

37

180 mm (365 nm bar LEDs); 120 mm (395 nm LED), for the with a Canon camera imaging system, the 280 nm LED was placed 250 mm above the sample with UV camera imaging system. The color camera was equipped with a polarizing filter (PL) to prevent any form of direct reflection from the samples. The layouts of the LEDs and cameras was as seen from Fig. 2.11a, b and c.

(a)

| Real imaging set-up | 3D Layout | Cross-sectional view |

1: Camera   3 – 6: Halogen lamps
2: 365 nm LED   7: Sample

H_{cam} – Height of Camera = 180 mm
H_{UV} – Height of UV LED = 120 mm
H_{hal} – Height og Halogen lamps = 100 mm

(b)

| Real imaging set-up | 3D Layout | Cross-sectional view |

1 – Canon Camera   3 – 365 nm LED   4 – 395 nm LED
2 – White LED   5 – Sample

(c) Real imaging set-up	3D Layout	Cross-sectional view

1 – UV Camera	2 – 280 nm LED	3 – Shield	4 – Sample

Fig. 2.10: Layout of a computer vision system used during experiment.

Image processing

Image processing was carried out using MATLAB 9.5 R2020b (MathWorks, USA). The regions of interest (ROIs) comprised of the eye (pupil and iris), belly (fish bottom side), and dorsal part (characterized with more scales). The eye part was automatically selected using '*imfind circles*' function in MATLAB, whereas the belly and dorsal parts were segmented using grey values for B-channel from images from 365 nm lighting device with a program in MATLAB software. Subsequently, the ROI was masked then overlaid with the corresponding images from different lighting devices (white, 365 nm and 395 nm). Average R, G and B values for RGB color space was extracted for analysis.

2.3 Statistical analysis

i. Univariate analysis

Univariate analysis is the simplest approach of analyzing data. "Uni" represents "one", so in simple terms, the data is made up of one variable. Its main purpose is describing a variable and it does not factor in relationships or causes as compared to regression (Tsumoto and Tsumoto, 2010). Therefore, it simply takes the data, summarizes it and find its patterns.

ii. Multivariate analysis

This is a statistical procedure for analyzing data that involving more than one type of observation or measurement. It involves solving problems where dependent variables are analyzed simultaneously with other variables (Xu et al., 2015). Since it considers many factors of independent variables which effects how dependent variables behave, it helps draw more accurate conclusions which are more realistic and near to real-life situations.

iii. Partial Least Squares (PLS) Regression Analysis

PLS regression is a statistical technique that bears relation to the principal component regressions. It finds linear regression models by projecting predicted and observable variables to a new space. Regression analysis: a set of statistical process for approximating the relationships between dependent variable ('response' or 'outcome') and more than one independent variables ('predictors', 'explanatory variables', 'covariates' or 'features'). Linear regression analysis is the common form of regression in which one tries to find the line that most fits the data as per specific mathematical criterion. In prediction, regression analysis has substantial overlapping with machine learning field. Regression analysis can also be used to infer causal relationships between dependent and independent variables.

iv. Validation and Evaluation of the Model performance

The performance of calibrated and predicted models for K value were evaluated in terms of root mean square error of calibration RMSE (see Eq. 2.1) and coefficient of determination of cross- determination, R^2 (see Eq. 2.2) (Cheng et al., 2016).

v. Root Mean Square Error (RMSE)

The root-mean-square error is used as measure of the differences between sample values predicted by the model or an estimator and the actual values (Nie et al., 2020; Rahman et al., 2015). The RMSE represents a quadratic mean of these differences, and the deviations are called residuals after the calculations have been performed over a data sample used for estimation as seen from Eqn. 2.2; thus, called errors (prediction errors) when computed out-of-sample. The RMSE serves to aggregate the degrees of the errors in predictions for various times into a single measure of predictive power. Therefore, it is a measure of accuracy, to compare forecasting errors of different models for a dataset and not between datasets, because it is scale dependent.

$$RMSE = \sqrt{\frac{\sum_{i=1}^{N}(Predicted_i - Observed_i)^2}{n}} \qquad \ldots \qquad \text{(Eqn 2.2)}$$

Where: n represents the sample number, $Predicted_i$ represents the output values from the model and $Observed_i$ represents the measured values.

vi. Coefficient of determination, R^2

Coefficient of determination or famously known as R-squared (R^2) is a statistical measure representing the proportion of variance for dependent variables explained by independent variables or variables used in a regression model. Its correlation explains the strength of the relationship between independent and dependent variables (Ali et al., 2018). Additionally, R^2 can tell the extent of variance for one variable explains the variance of the second one as seen from Eqn. 2.3. If for instance the R^2 of a model is 0.75, then approximately three-quarter of the observed variation can perfectly be accounted for by the inputs model used. Therefore, it measures on how well the observed outcomes of a regression model are simulated by the model, based on the amount of total variation of outcomes.

$$R^2 = 1 - \frac{\sum_{i=1}^{n}(y_{cal} - y_{act})^2}{\sum_{i=1}^{n} y_{cal} - y_{mean}^2} \qquad \ldots \qquad \text{(Eqn 2.3)}$$

Where, n is the sample number, y_{act} is the measured value, y_{cal} is the calculated value, y_{mean} is the average value and y_{pred} is the predicted value of the corresponding parameters.

REFERENCES

Ali, H., Saleem, M., Anser, M.R., Khan, S., Ullah, R., Bilal, M., 2018. Validation of Fluorescence Spectroscopy to Detect Adulteration of Edible Oil in Extra Virgin Olive Oil (EVOO) by Applying Chemometrics. Appl. Spectrosc. 72, 1371–1379. https://doi.org/10.1177/0003702818768485

Cheng, J.H., Sun, D.W., Qu, J.H., Pu, H. Bin, Zhang, X.C., Song, Z., Chen, X., Zhang, H., 2016. Developing a multispectral imaging for simultaneous prediction of freshness indicators during chemical spoilage of grass carp fish fillet. J. Food Eng. 182, 9–17. https://doi.org/10.1016/j.jfoodeng.2016.02.004

Lawaetz, A.J., Stedmon, C.A., 2009. Fluorescence intensity calibration using the Raman scatter peak of water. Appl. Spectrosc. 63, 936–940. https://doi.org/10.1366/000370209788964548

Nie, S., Al Riza, D.F., Ogawa, Y., Suzuki, T., Kuramoto, M., Miyata, N., Kondo, N., 2020. Potential of a double lighting imaging system for characterization of "Hayward" kiwifruit harvest indices. Postharvest Biol. Technol. 162, 111113. https://doi.org/10.1016/j.postharvbio.2019.111113

Rahman, A., Kondo, N., Ogawa, Y., Suzuki, T., Shirataki, Y., Wakita, Y., 2015. Prediction of K value for fish flesh based on ultraviolet-visible spectroscopy of fish eye fluid using partial least squares regression. Comput. Electron. Agric. 117, 149–153. https://doi.org/10.1016/j.compag.2015.07.018

Tsumoto, Y., Tsumoto, S., 2010. Exploratory Univariate Analysis on the Characterization of a University Hospital: A Preliminary Step to Data-Mining-Based Hospital Management Using an Exploratory Univariate Analysis of a University Hospital. Rev. Socionetwork Strateg. 4, 47–63. https://doi.org/10.1007/s12626-010-0014-x

Xu, Y., Li, H., Chen, Q., Zhao, J., Ouyang, Q., 2015. Rapid Detection of Adulteration in Extra-Virgin Olive Oil using Three-Dimensional Fluorescence Spectra Technology with Selected Multivariate Calibrations. Int. J. Food Prop. 18, 2085–2098. https://doi.org/10.1080/10942912.2014.963869

CHAPTER III: JAPANESE DACE (*Tribolodon hakonensis*) FISH FRESHNESS ESTIMATION USING FRONT-FACE FLUORESCENCE SPECTROSCOPY COUPLED WITH CHEMOMETRIC ANALYSIS

3.1 Introduction

It has been demonstrated that fish and its products are essential for the human diet because it has proved to be a good source of proteins. As a result, the estimated number of fish consumed globally has dramatically increased from ≈27 million tonnes (around the 1960s) to ≈114 million tonnes in early 2000 (Stetinensia, 2011). The overall average fish supply then saw a 3.1% annual growth rate and subsequently increased the per capita fish consumption.

Several attributes influence the quality of fresh fish products like safety, nutritional value, availability, level of freshness, convenience and integrity, and physical features) (Olafsdottir et al., 2004). Of them all, freshness is an ultimate concept that directly affects fish quality. Therefore, most consumers use it as a mark of quality to estimate fish's freshness level and safety before purchasing. There are several characteristics by which the freshness state of fish is defined based on postmortem changes that affect the physical, chemical and biochemical and microbiological fluctuations (Bremner & Sakaguchi, 2015). Sensory (Özogul, Özyurt, Özogul, Kuley, & Polat, 2005) and bacteriological analyses (Dalgaard, 1995; Koutsoumanis & Nychas, 2000) have proved effective for fish freshness evaluation; however, they are time-consuming, subjective in nature, and expensive techniques. The evaluation of freshness using the biochemical examination technique reported by Itoh et al. (2013) and Elmasry et al. (2015) has been widely accepted as a conventional technique for evaluating the quality of meat and fish products. This is because the method can quantitatively track down the disintegration of adenosine triphosphate (ATP) compounds to its metabolites: adenosine di-phosphates (ADP), adenosine monophosphates (AMP), inosine monophosphates (IMP), inosine (H_xR), and hypoxanthine (H_x) and uric acid as a final product (Cheng et al., 2016; Watanabe, Tsuneishi, & Takimoto, 1989). To tell the freshness of the fish, a ratio of non-phosphatic ATP to the total ATP-related compounds including decomposition products expressed as a percentage is widely accepted as a standard freshness indicator for meat products. The resultant value (see Eqn. 3.1) is commonly referred to as *K* value.

$$K \text{ value} = \frac{H_xR + H_x}{ATP + ADP + AMP + IMP + H_xR + H_x} \text{ x } 100 \qquad \dots \qquad (Eqn\ 3.1)$$

The freshness is further ranged in different categories depending on various factors extending to but not limited with fish type and ecological environment (saline or freshwater types). For most freshwater fishes, K value <20% is regarded as prime fresh stage, and therefore the fish can be consumed raw; when the value is ranging between 20% and 40%, the fish can only be consumed after cooking, but when the value is >40%, the fish is not safe for consumption because it already spoiled (Kato, Kunimoto, Koseki, Kitakami, & Arai, 2009). However, this method is laborious, destructive, and slow thus, not suitable online monitoring of fish. From the above methods, it is evident that there is a need for a new technique that is quicker and non-destructive for freshness evaluation. Various techniques have been suggested as alternative ways to the complex chemical analysis (K value measurement) for estimating fish freshness.

The fluorescence technique has been attracting much research in the food industry for quality evaluation because it is highly sensitive, relatively cheap to implement, and user-friendly (Christensen, Nørgaard, Bro, & Engelsen, 2006). For instance, Japanese dace (*Tribolodon hakonensis*) fish eye-fluid (Liao, Suzuki, Shirataki, Kuramoto, & Kondo, 2018) and red sea bream (*Pagrus major*) eye-fluid and scales (Liao et al., 2017a) excitation-emission matrix (EEM) characteristics acquired using right-angle fluorescence spectroscopy demonstrated potential in fish freshness monitoring during storage. The spectra characteristics from both fishes showed that the fish contains fluorescent substances with distinct excitation and emission wavelengths and whose fluorescence intensity changes as freshness deteriorates. This technique was a good step in the right direction, but it posed some challenges such as: destructive in nature (during eye fluid abstraction with a needle and syringe); tiresome (carefully targeting the eye fluid to avoid mixing with other compounds in the eye) and limited to industrial applicability. The samples used during the research required some pre-treatment (chemical extraction and centrifuging before the actual measurement was conducted), thus challenging to adopt it for highly concentrated compounds due to strong inner filter effects (Ruoff et al., 2006).

Various chemometrics methods which are based on statistics have previously been applied for the authentication of food. However, every method could be limited to a particular commodity; thus, the method selection is based on the specific need (Granato et al., 2018). Among the analytical methods, partial least square regression (PLSR) is widely adopted for authentication and regression. Furthermore, the PLS loading plot refolding to a 3D map is useful to recognize the important regions of the fluorescence EEM as described by Al Riza, Kondo, Catalano, & Giametta,

2019. Selecting a single or few excitation wavelength-based method can be useful for developing simple sensors based on the spectrofluorimetric principle (Betemps et al., 2012; Bro, 1996; Mehretie, Riza, Saito, & Kondo, 2018; Oztekin & Hahn, 2016; Patra & Mishra, 2002)Therefore, this study implements the approach to select variables of fluorescence EEM..

Based on the existing conditions and preliminary findings from right-angle fluorescence techniques, it is evident that a more easy and precise method is required. However, despite looking promising, right-angle fluorescence spectroscopy posed some challenges on sample pre-treatment (especially for concentrated samples) before measurement to avoid inner filter effects (Hammami et al., 2013; Ruoff et al., 2006) and limitation to industrial application. Therefore, in this research, front-face fluorescence spectroscopy techniques are used because they demonstrate considerable promise since sample pre-treatment is not necessary, hence avoiding inner filter effects and it is near industrial application.

In this study, front-face fluorescence technique was used to acquire the EEM of fish samples (eyeball and skin containing scales). Plus, PLSR analysis has been applied to predict fish freshness from the EEM datasets, and to evaluate the potential excitation wavelengths. The selection of variables with higher contribution (positive and negative principal coefficients) to freshness deterioration was utilized by loading of the analysis to select the most important regions to be adopted as input variables for the simplification of spectroscopy techniques.

3.2 Materials and Methods

Sample information

The Japanese dace fish were procured from the Hamaichi Bait Company (Wakayama Prefecture, Japan), during which they were about ten months old. During this experiment, the fish were kept in well-aerated laboratory acrylic tanks at Kyoto University, Japan. The fish were delivered alive in a plastic bag aerated with water.

Sample preparation

During the experiment, about 120 fish with a length averaging 120±20 mm was selected, killed, and refrigerated at about 5 ℃ for about 2 hours before starting the experiment. The experiments were conducted in three phases, 2018, 2019 and 2020. During measurements the eyeball, surface containing scales and meat were acquired. In every measurement interval, two

measurements were carried out: fluorescence excitation-emission matrix (EEM) of the eyeball and surface containing scales (for some fish and biochemical analyses to inspect the quality of meat for about two days; this is because a maximum of two days is the recommended time for Japanese dace fish to remain in its freshness period (Omwange et al., 2020, 2021).

Biochemical analysis (K value measurement)

The dorsal part of the fish flesh was cut (just below the surface containing scales was sampled) and sliced into tiny pieces with a pair of scissors. Using a plastic hand bottle sprayer, a buffer solution was sprayed on an electrophoresis paper for uniform wetness before adding about 3 µL of a supernatant solution on the circular spots marked on the electrophoresis paper examination. Approximately 200 mg was taken and mixed with extraction reagent A (0.6 mL) from QS-Solution Company, Japan. Potassium hydroxide reagent C (5.61 mL/100 g) from QS-Solution company, Japan, was added to neutralize the solution. The paper was then placed in the Freshness Checker (QS-3201, QS-Solution, Japan) with a parameter set at 800 V for 5 minutes. The freshness checker machine utilizes the paper electrophoresis measurement principle when examining meat products' freshness/quality levels (Kato et al., 2009). After electrophoresis measurement, the paper was dried using a forced air convection paper drier (Paper dryer QS 4201, Japan) set at 100 ℃ for 5 min. Using a 254 nm lamp inside the freshness checker machine, the developed spots were illuminated for recording freshness results by a digital camera (Color EOS M3, Japan). With Spot Analyzer software (QS-Solution, Tokyo, Japan), the spots were digitized to calculate the corresponding *K* values (Omwange et al., 2020, 2021).

Fluorescence EEM measurement

The excitation-emission matrices (EEMs) were attained from different fish samples (eyeball and surface containing scales). The eyeball was detached from its socket, whereas the surface containing scales were cut from the fish's dorsal part. The samples were directly placed used for raw EEM acquisition. The front-face fluorescence spectroscopy (FFFS) method was employed using a spectrofluorometer (FP-8300, JASCO Co., Tokyo, Japan); in the FFFS technique, the excitation light meets the sample at 30° to the normal line. The parameters of EEM acquisition were set as excitation/emission ranges 220-585/250-600 nm, with a low sensitivity of the photomultiplier tubes (PMT) and a scanning speed of 5,000 nm min^{-1}; and the response time of 50 ms. The Ex/Em interval and bandwidths measurements were recorded at 5 nm, respectively.

The excitation beam size was rectangular-shaped, measuring 1 mm by 10 mm. The experiment was conducted at room temperature, set at 20±1 °C. With a standardized light source and response detector, the raw EEM was corrected as per the calibration spectra protocol outlined by JASCO Company before converting the files from arbitrary units (A.U.) to Raman units (R.U.) (Lawaetz & Stedmon, 2009).

3.3 Data analysis

Determining principal components for partial least squares regression (PLSR) analysis

In the preceding studies, the eye-fluid was used to show the freshness changes in Japanese dace fish during storage using right-angle fluorescence spectroscopy (Liao et al., 2018). The use of right-angle spectroscopy on the fisheye fluid EEM for freshness monitoring is subject to various challenges around the destructive sampling method and limited to industrial applicability. This study explores the potential of front-face fluorescence spectroscopy to estimate fish freshness during storage using an intact fish eyeball and surface containing scales; and define a more specific EEM region that can define freshness precisely. Data processing and analysis were done using MATLAB R2020b (MathWorks, USA).

EEM for each sample was unfolded and concatenated into one vector data type as described by (Al Riza, Widodo, Purwanto, & Kondo, 2019) for PLSR analysis. The PLS component analysis was adopted on the unfolded data. This data analysis was split into two (75% training and 25% testing). Regression results were presented as root mean square error (RMSE and coefficients of determination (R^2) for different categories; eyeball's whole excitation-emission range; eyeball selected region around the peaks; surface containing scales whole excitation-emission range; surface containing scales' selected region around the peaks; a combination of eyeball and surface containing scales for whole EEM range and that of the selected important variables. The PLS loading vectors were then refolded into an EEM like data for easy recognition of significant regions on the EEM (see Fig. 3.2), which can be adopted for assessing freshness.

The PLSR analysis functions on MATLAB have been used to develop the prediction model. Investigative data analysis, selection of features, data training, and testing of the model, and assessment of the results were made using these functions. Four sets of input variables were conducted and compared: Ex./Em pairs of peaks, highlighted important excitation wavelengths

considered in the whole emission spectrum were adopted with 6 PLS components (see Fig. 3.1), and a 5-fold cross-validation method was used to avoid overfitting.
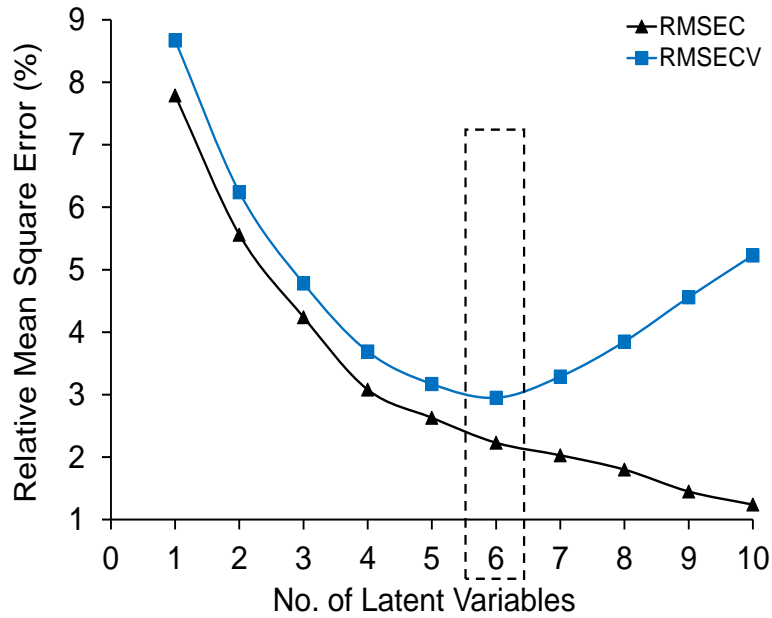

Fig. 3.1: Selection of PLS components for data processing.

3.4 Results and Discussion

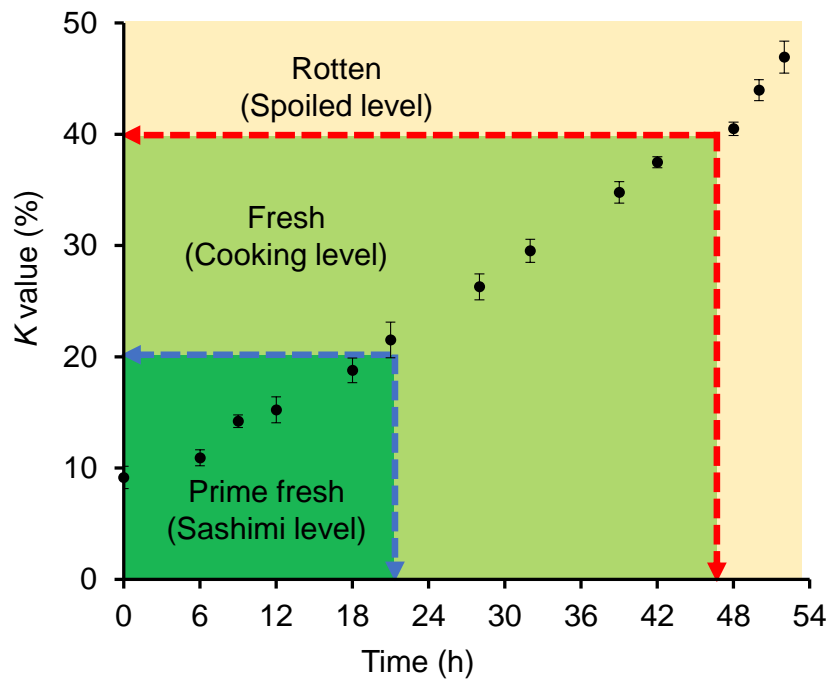*Conventional freshness evaluation (Electrophoresis or K value measurement)*

Fig. 3.2: Time series fish freshness (*K* value) change during storage.

Japanese dace fish's *K* value ranged between 8 - 47% in a span of 48 hours when kept under 4 ±1 °C (see Fig. 3.2). Prime fresh samples showed a *K* value of about 8%, but due to sample variation and different biological activities, some could range from 9 - 10%. The 2 hours spent in the refrigerator after killing before the experiment could potentially affect the initial *K* values since the fish could not die instantly at the same time. From Kato et al. (2009) fish freshness classes; *K* value <20% represented prime fresh samples, where fish can be eaten raw, 20%>*K* value<40% defined the new stage where fish can only be consumed after cooking; *K* value >40% denotes spoiled fish which can only be discarded (wasted). From our analysis, this fish could last in the prime fresh for about 20 hours; after this, the rest of the storage time (until 48 hours) remained in the 'fresh stage' with a *K* value >20% but < 40%.

Japanese dace fish Fluorescence features for eyeball, scales, and meat

Compared to biochemical fish freshness evaluation using electrophoresis analysis (*K* value measurement) (Elmasry et al., 2015; Itoh et al., 2013), the fluorescence EEM provides a direct connection with quality and sensory traits. This is because fluorescence fingerprints represent a sample's chemical composition profile. Chemical substances conforming to the EEM regions have been introduced in previous studies on fish eye fluid using right-angle fluorescence spectroscopy (Liao et al., 2018) and eyeball (Omwange et al., 2020, 2021). However, it is worth highlighting it again for better reasoning in selecting variables for regression.

From Fig. 3.3 above, each body part (eyeball surface containing scales and meat) measured during this experiment depicts EEM with distinct peaks. The fluorescence EEM for eyeball can be characterized into three regions (see fig. 3.4i). For the eyeball, Region A and B with excitations ranging between 210 and 240 nm, and 240 and 315 nm and emissions ranging 280 and 380 nm and 280 and 450 nm, respectively, are associated with proteins and amino acids: Tyrosine, Tryptophan, and Phenylalanine (Ringvold et al., 2003). Ringvold et al. (2003) indicated that the fisheye is rich in proteins and little amounts of aromatic amino acids in live fishes than those that have died. These peaks play a vital role in freshness evaluation using biochemical analysis because, during the breakdown, the ATP compounds can be quantified. Region C with excitation stretching between 310 and 385 nm and emission 370 and 490 nm is suspected to be uric acid, a final product of ATP disintegration and purine metabolism processes in fish. Several enzymes convert purine nucleic acids, including guanine and adenine, to uric acid substances (Cameron, Moro, &

49

Simmonds, 1993; Ridi & Tallima, 2017). The ATP decomposition process results in large amounts of uric acid, which accumulate gradually during storage. Fish tissues and muscles are rich in ATP compounds and the second most abundant metabolite after amino acids. They are responsible for providing energy for muscle contraction and relaxation. This peak was reported in the fluorescence EEM of Japanese dace fish eye fluid observed by Liao et al. (2018), and it demonstrated the great potential of acting as a freshness indicator in fish.
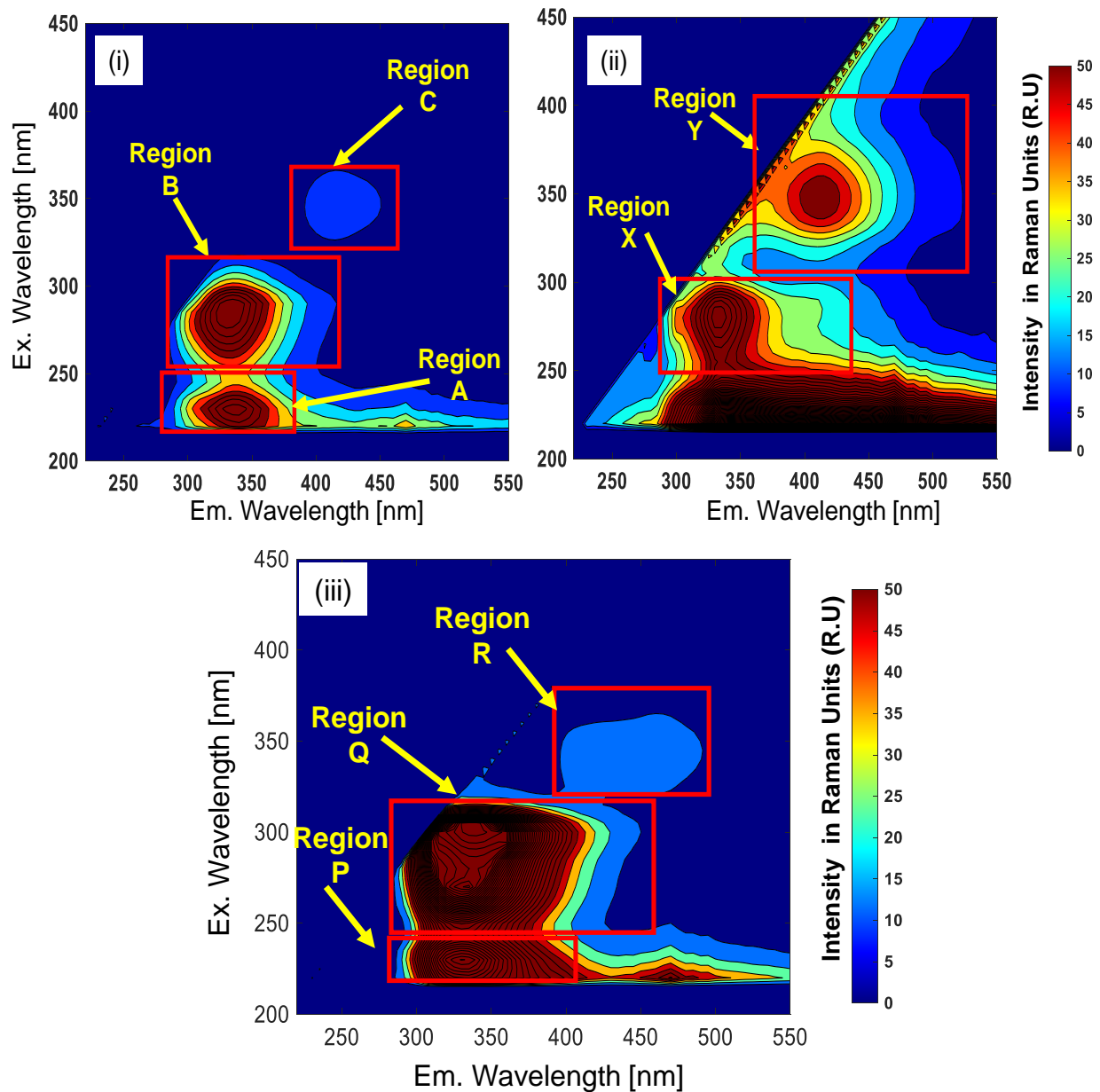

Fig. 3.3: Fluorescence EEM for fish (i) Eyeball, and (ii) Surface containing scales.

The fish surface containing scales shows two distinct regions X and Y, with much noise below 240 nm excitation (see fig. 3.4 (ii)). This noise is because of the rough nature of the scale surface, which causes diffused reflection of the stray light on the surface. As a result, this noise will make some of the important information (especially if it has lesser intensities) of the EEM to be submerged. Region X has excitation ranging 240 and 300 nm and emission 285 and 450 nm: and with a maximum at 280/330 nm. This peak is also said to contain proteins, especially free tyrosine substances (Lakowicz, 2006), which are in abundance in fish. Region Y with excitation between 305 and 390 nm and emission between 365 and 500 nm and maximum at 350/415 nm is said to be containing Type I collagen compounds. Villette et al. (2006) reported that Type 1 collagen is a reduced form of vitamin compounds and nicotinamide adenine dinucleotide, NADH. After untreated mucus from fish surface containing scales for fish proved to contain vitamins or NADH (Georgakoudi et al., 2002). The fact that the strength of peak X (for surface containing scales) is lower than that of peak B (eyeball); is consistent with the fact that collagen substances contain little amount of aromatic amino acids, which is lower than that of other parts of the living body (Eastoe, 1955; Eyre, 1987; Gauza-Włodarczyk, Kubisz, & Włodarczyk, 2017). These substances are essential, especially for rejuvenating tissues for better flexibility and elasticity ability of fish that enhances its easy swimming ability when alive.

Fish meat produced three fluorescence peak regions P, Q and R with excitation/emission maxima at 230/330, 280/330 and 350/415 nm respectively as seen in see Fig. 3.3iii above. All the three peaks for the meat part had almost a constant value which showed slight deviation from the original value. Just like peaks A and B from eyeball and peak X for surface containing scales, peaks P and Q for meat EEM are also associated with aromatic amino acids, nucleic acids (characterized with excitations at around 250 nm and emission ranging 280-480 nm) and proteins mainly tryptophan compounds with excitation at around 290 nm and emission at 330 nm (Dufour, J.P. Frencia, & Kane, 2003; Karoui, Thomas, & Dufour, 2006). According to Dufour et al., (2003), region R in fish meat is suspected to be containing NADH compounds, because the excitation wavelength for standard NADH is at 340 nm and emission ranges 410-455 nm.

Since the same peaks corresponding to every part selected (eyeball, surface containing scales and meat) were observed for all fish samples at different storage times, they showed significantly different tendencies and fluorescence properties as seen from. The fluorescence

spectra of these compounds recorded for Japanese dace fish for about two days of storage time were all fingerprints that could potentially track freshness deterioration in fish.

Time series fluorescence EEM changes during storage

The freshly killed fishes have higher freshness quality free from pathogens, and that is why they are consumed raw in the form of sushi or sashimi, as commonly referred to in Asian countries. However, the fish properties will gradually start changing after being stored for some time due to quality deterioration; some substances in their body get decomposed, thereby accumulating spoilage elements that can show some physical, chemical, or biological changes during storage. The rate of change of visible properties on the fish is affected by the initial handling technique and storage conditions. The changes in the fish's body will affect the fluorescence features of the fish's EEM (Karoui et al., 2006).

Regions A and B (Fig. 3.3 i); X (Fig. 3.3 ii) and P and Q (Fig. 3.3 iii) have been associated with aromatic amino acids, nucleic acids, and its pigments, tryptophan, and tyrosine compounds. The destruction of aromatic amino acids, subsequent protein deposition, and enzymatic activities through metabolism could easily act as biomarkers for fish freshness. The primary cause of initial deterioration in the freshness of fish in the prime stage (freshly killed fish) is associated with catabolic reactions in saccharides and nucleotides, which are immediately followed by decomposition of nitrogenous substances like proteins and amino acids, and finally hydrolysis and peroxide-oxidation of lipids. During this stage, the processes are facilitated by endogenic enzymes. When the storage time is extended, the deteriorative processes are followed by microbial activities (Gram & Huss, 1996). Additionally, the breakdown of polyunsaturated fatty acids (PUFA) could produce primary (such as hydroperoxides) and secondary (like malondialdehyde and aldehydes) products. This generates fluorescent compounds and greatly influences freshness loss (Karoui & Blecker, 2010). Chemical and biological processes act upon the secondary metabolites that come from proteins and decompose them into biogenic amines. In return, this triggers the breakdown of existing proteins and form skatole, tyrosine, indole, putrescine cadaverine & other substances (Gram & Huss, 1996). The fluorescence intensities of the peaks A, B (see Fig. 3.4a and b), X (Fig. 3.5a) and P and Q (Fig. 3.6a) and (b)) are high because they are a product of the total accumulated intensity of protein compounds containing aromatic amino acids and their residuals. This causes the observed intensity variation associated with these peaks. Since the breakdown and formation

of proteins and amino acids involve some complex processes, it becomes difficult to account for the total fluorescence intensity changes and associate them to either individual proteins and/or amino acids.
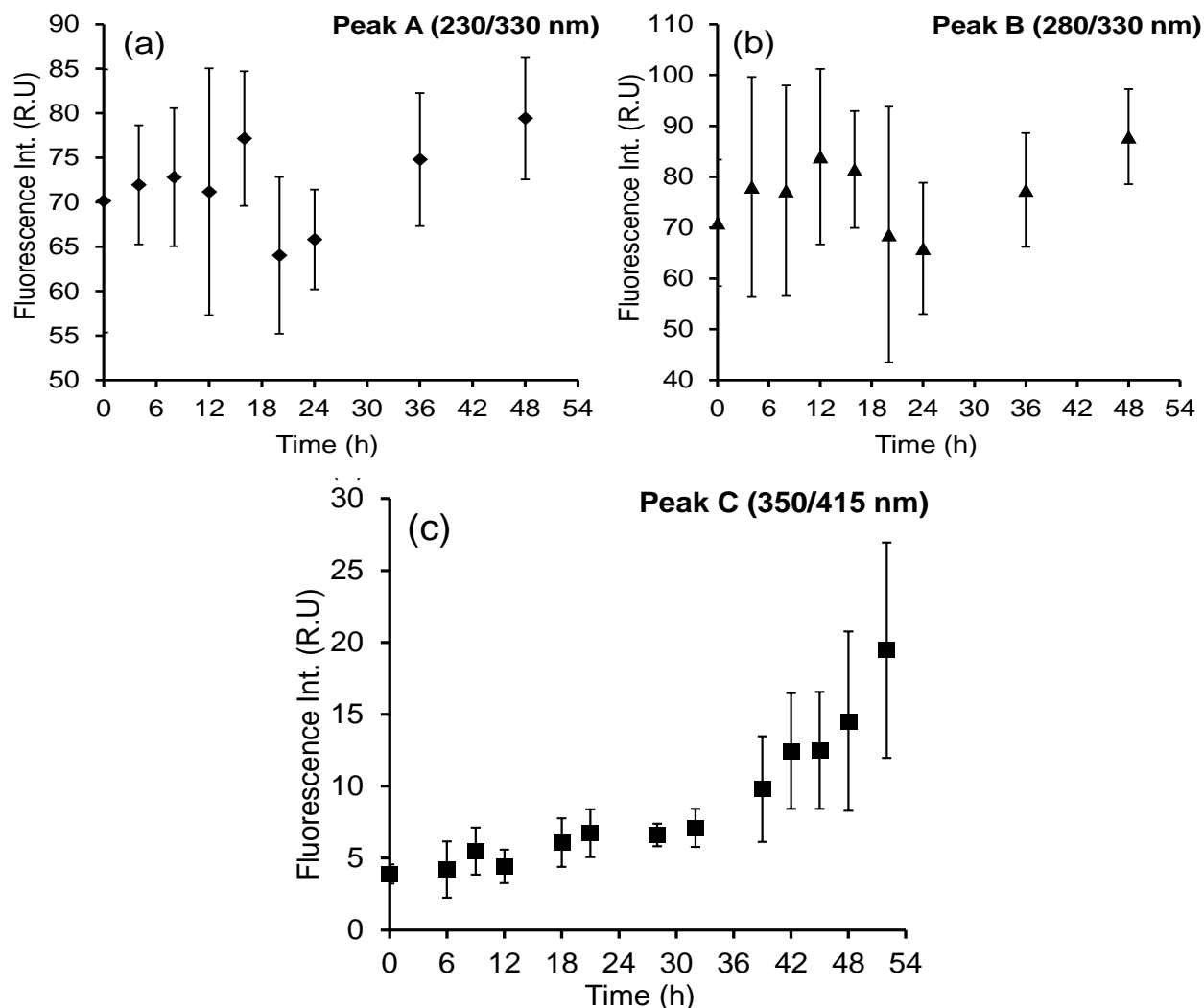
Fig. 3.4: Time series EEM for fish eyeball during storage.

In a live fish, the muscle ATP is hydrolyzed to ADP and is continuously re-synthesized by the mitochondrial respiratory chain, keeping the concentration levels of AMP and IMP low. After the fish dies, the hydrolysis process of ATP to ADP is maintained by contracting muscles but reverse by mitochondrial ATP-synthetase is impossible due to respiratory arrest. Therefore, ATP is resynthesized in inefficient ways; creatine kinase, anaerobic glycolysis, and myoadenylate kinase, which drops its concentration, thus accumulating ADP. ADP is quickly dephosphorylated into AMP and later deaminated to IMP by AMP-deaminase enzymes. IMP is the dominant

nucleotide in the rigor-mortis stage (Wang, Tang, Correia, & Gill, 1998). The decompose of IMP to H_xR, and later H_x is a product of both autolytic and bacterial enzymes. The rate at which IMP will decompose vary significantly between fish species and relies upon the handling and storage parameters (Surette, Gill, & LeBlanc, 1988). The purine metabolism process in the fish converts purine nucleic acids through enzymatic activities (Cameron et al., 1993). These two processes generate the end-product associated with the fluorescence of region C (fish eyeball) with a maximum excitation/emission at 345/415 nm (Fig. 3.4 c).
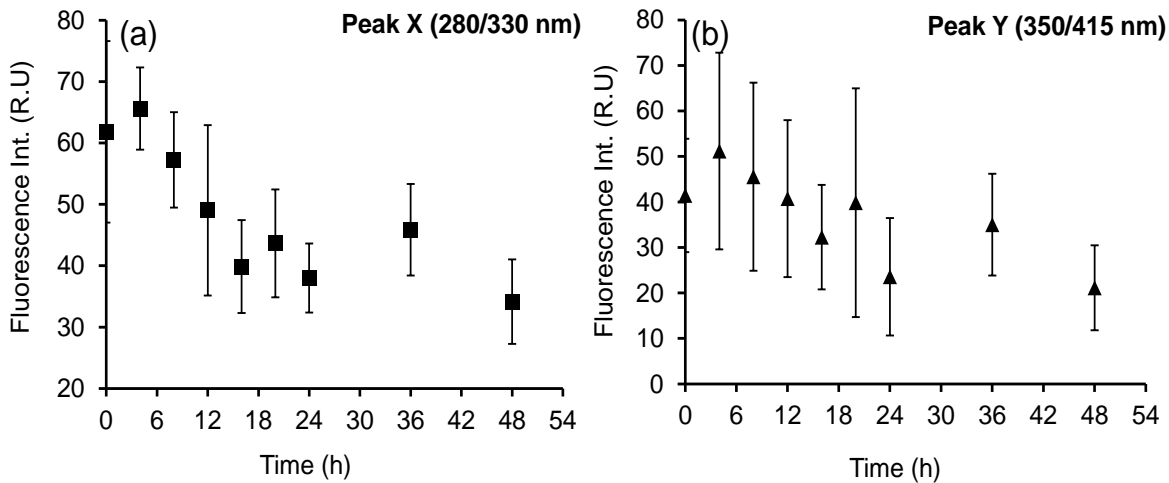

Fig. 3.5: Time series EEM intensity variation for fish scales during storage.

The fluorescence observed on the fish surface containing scales EEM for region Y (Fig. 3.3 ii and 3.5 b) is associated with collagen compounds, which is a type of protein present in the fish for maintaining the skin tissues by providing strength and structure. This was in agreement with the findings of Santana et al. (2016), who reported that collagen for *A. lacustris* fish fluorescence peak recorded at excitation range between $270 - 420$ nm and` emission range between $370 - 600$ nm wavelength and with a maximum at 360/405 nm. On the fish's surface containing scales, a decline in moisture levels was observed by the fact that the fish surface containing scales started becoming less moist, and this could explain the reason why its associated peaks (X and Y) showed a declining tendency during storage. This is because dry samples tend to exhibit less fluorescence intensity compared to those that tend to be wet/moist. This affirms the fact that water condition influences the fluorescence intensity of substances.

The existence of nicotinamide adenine dinucleotide as oxidized and reduced forms; (NAD^+ and NADH respectively are critical enzymes for postmortem metabolic processes of fish meat.

When fish dies, the transformation of NAD$^+$ to NADH and vice versa and rapid anaerobic glycolysis processes begin (Hong, Regenstein, & Luo, 2017). The reverse reaction processes of NADH are responsible for region R (Fig. 3.3 iii and 3.5 c) observed on the fish meat with a maximum peak at 345/410 nm. This is in agreement with the findings of Dufour et al., (2003), where they recorded the NADH fluorescence emission spectra at excitation 336 nm and emission at 414 and 438 nm respectively.

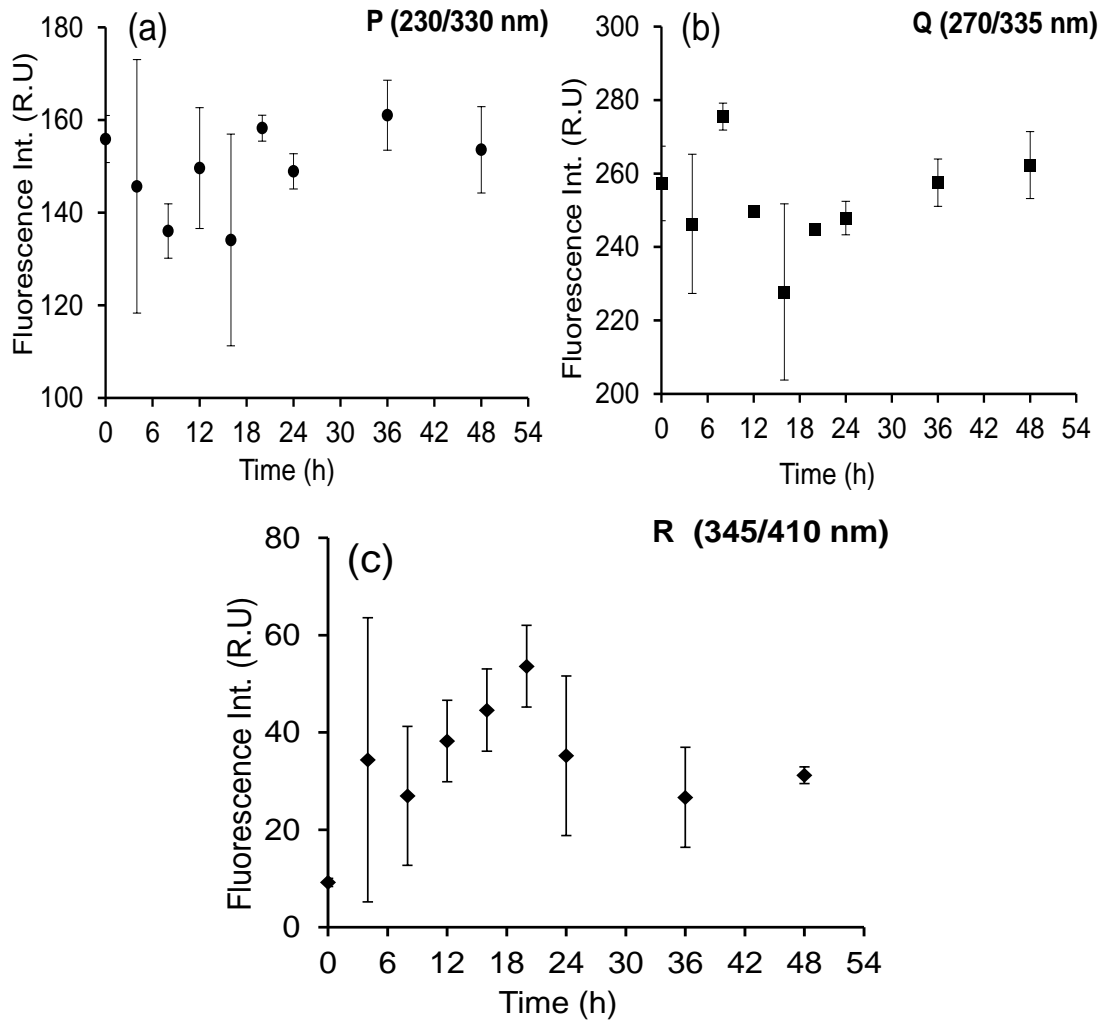Fig. 3.6: Time series EEM for fish meat during storage

Comparing fluorescence EEM region associated with Japanese dace freshness

Based on the findings, the fish eyeball EEM region associated with uric acid (Region C) for Japanese dace fish and scale EEM for collagen (region Y) for Red sea bream (*Pagrus major*) (Liao et al., 2018, 2017b) are both recommended for fish freshness evaluation. Both peaks show

some systematic tendencies (increasing for the eyeball and decreasing for surface containing scales during storage) with unique characteristics that depend on storage time regardless of sample disparity. Additionally, the changes associated with proteins and amino acids have previously been utilized to track down ATP degradation through the biochemical processes (K value). Regardless of the sample variance and storage conditions, and EEM features, it could be possible to use some features to monitor fish freshness changes during storage. All the EEM contain 3D fingerprint features, including the intensity and shape of the spectrum.

Selecting important excitation wavelengths using PLS analysis

Spectra data contain several variables. For fluorescence EEM, several variables depend on both measured wavelength range and interval width. Partial least squares (PLS) regression analysis was adopted to examine the data and locate important variables for freshness evaluation. It was found that 6 PLS components were adequate to represent over 95% of the data variance for both the eyeball and fish surface containing scales by using the combined EEM of different critical excitations highlighted by the model. From Fig. 3.7, the latent variables in PLS (PLS 1 – 6) were ordered in a descending order by their explained variance for K value. The highest latent variables had 35% and 41% explained variances for eyeball and scales respectively.

The values (either positive or negative contribution) of the refolded PLS loadings have been attained in the variable selection. The refolded values of PLS loading 1 to 5 have been summed up, and the values of PLS 1–6 loadings have been plotted for different parts (eye and surface containing scales), as seen in Fig. 3.7i. The higher the absolute value (ignoring the sign of either positive or negative) of the PLS loadings, the higher the contribution of the associated EEM variables for freshness evaluation. Fourteen excitations (8 from eyeball and 6 from scales) were highlighted as most significant excitations for evaluation fish freshness during storage (Fig. 3.7ii). Four approaches to test the applicability of this model were adopted. (i) whole EEM range (Ex.: 220 – 585 Em.: 200 – 550); (ii) Individual excitation fluorescence EEM for important wavelengths considered in the Whole emission range; (iii) combination fluorescence EEM for different excitation wavelengths eyeball and/or surface containing scales and, (iv) Fluorescence EEM for selected important pairs of wavelength peaks (Ex./Em. pairs). For individual peaks with specific pairs of excitation and emission wavelengths in the first scenario could be appropriate for developing multiplex sensor-based devices. For specific excitation wavelengths, it will be useful

for developing a device consisting of Light Emitting Diodes (LEDs) for portable spectrometers (Betemps et al., 2012).
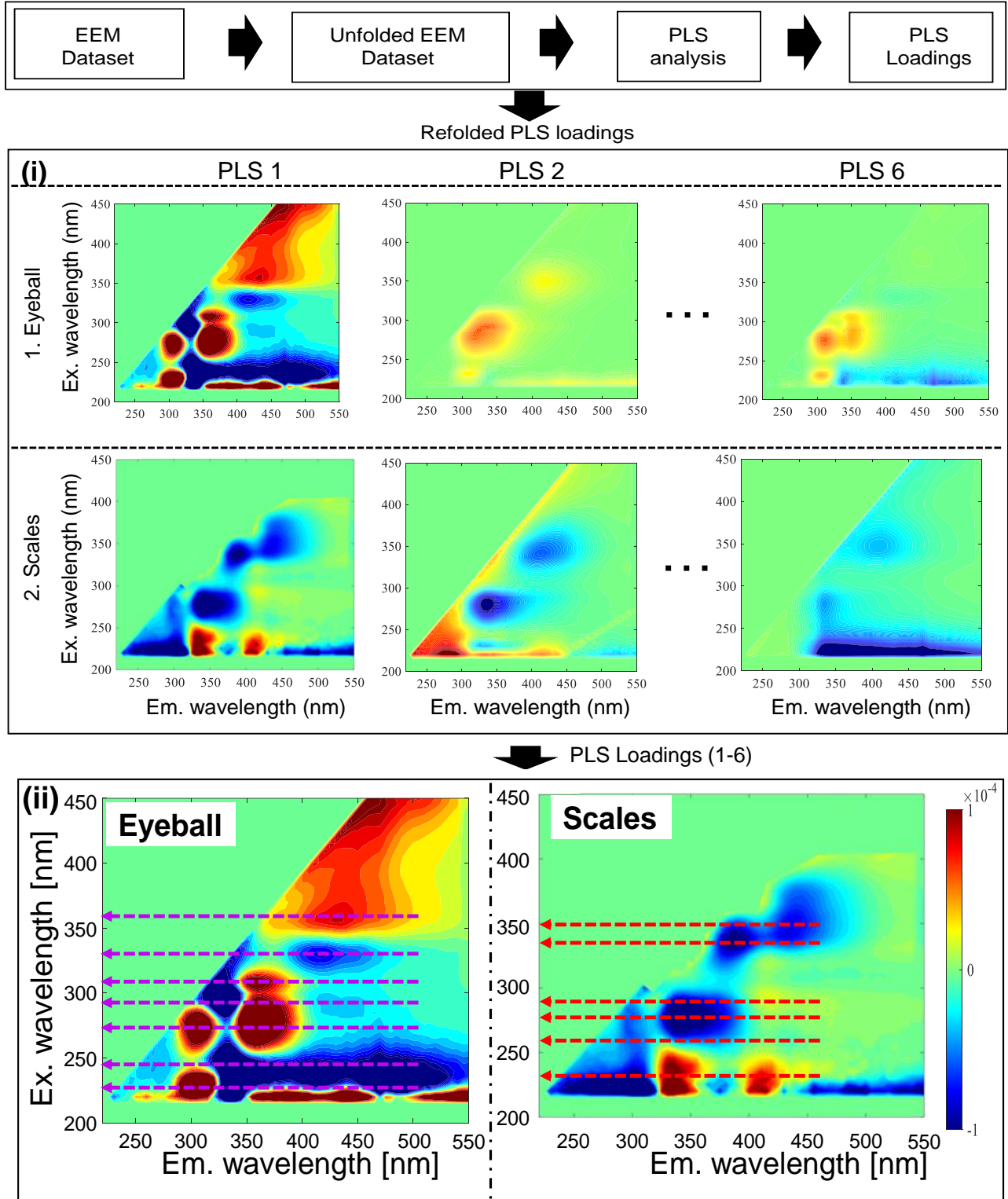

Fig. 3.7: Procedure for selecting important variables.

Freshness evaluation using PLS regression analysis

The prediction models developed consisted of four different categories. Direct EEM intensity values in Raman units (R.U.) were used as input variables for the modeling. When a whole EEM range is considered in this model, an RMSE of 2.97 and 2.92; and R^2 of 0.94 and 0.93 for the eyeball, surface containing scales, respectively. However, the combined results (eyeball and surface containing scales) produced an improvement of the results to 2.67 and 0.95 for RMSE and R^2, respectively (see Fig. 3.8 (i) and Table 3.1). Even though all these regions were adopted in the whole EEM model analysis, it will be more objective to have specific essential areas which are associated with freshness deterioration of fish. This is because, for future applications, it will be easy to develop a multiplex sensor of the specific wavelength to monitor its changes during storage.

From the EEM, the PLSR analysis six regions (eyeball) and five regions (surface containing scales) were highlighted as essential variables contributing either positively (red color) or negatively (blue color) to the freshness changes of fish. The excitations wavelengths of these regions (maximum points of the peak) were recorded as 230, 245, 275, 280, 295, 310, 330, and 355 nm for the eyeball and 230, 275, 280, 295, 340, and 350 nm. In this model, the analysis considered these important excitations in the whole emission range (200 – 550 nm). The study considered three factors: (i) predicting freshness using an EEM for individual excitation wavelengths, (ii) combination of EEM for different excitations for either eyeball or surface containing scales alone, and (iii) combination of different excitations for both the eyeball and scale results. The results showed that even with a single excitation, the results from either the eyeball or surface containing scales could potentially act as a good freshness indicator, as seen from Table 3.2. Using a single wavelength is vital because laser beams could quickly be adopted for monitoring the changes. When different excitations are combined, the model showed a good performance for both the eyeball and surface containing scales. A combination of 230 and 355 nm excitations of eyeball produced 2.81 and 0.96 as RMSE and R^2 as the best (see Fig. 3.8ii), whereas 280 and 355 nm produced 5.09 (RMSE) and 0.85 (R^2) as the least (refer Table 3.4).

For the surface containing scales, all the peak combinations showed high performances with our model, as seen from Table 3.4. However, just the eye or surface containing scales alone might not be ideal; and since all these parts lie on the surface of the, integrating them in one model could quickly realize a better monitoring system. Combining eyeball and surface containing scales will make this idea more robust. The combination of excitations 280 and 355 nm (eyeball) and 280

and 350 nm (surface containing scales) showed a good performance with 2.84 (RMSE) and 0.96 (R^2) (see Fig. 3.8 (iii)). These results demonstrate that simple portable devices like LEDs or laser beams associated with specific wavelengths (multiwavelength technique) can easily track down freshness changes of the fish by just focusing on the eye and surface containing scales from the outside.

With input variables made up of 6 and 5 Ex./Em. pairs (for individual peaks) of the eyeball and surface containing scales, respectively. Using the EEM Ex/Em. pairs associated with the important peak wavelengths highlighted by the model, an RMSE of 4.18; 3.89 and 3.15, and R^2 of 0.89; 0.90 and 0.91 for the eyeball, the surface containing scales, and combination (eyeball and surface containing scales) respectively, as seen in Table 3.3. Fig. 3.8 (iv) shows the model results for the combined datasets from the eyeball and surface containing scales. This result illustrates great potential for establishing a multiplex sensor device that could reveal changes of fluorescence compounds associated with individual peaks during storage.

The individual peaks input variables produced good regression results with this PLSR model. Even with the new data, this model could be updated to retain its efficiency and minimize overfitting due to storage changes, thus working as a non-parametric model. With these results, we highly recommend the development of sensor devices and a protocol based on the combination of at least six selected wavelength pairs (Ex./Em. 230/305; 245/335; 275/305; 280/360; 295/330; 300/325; 330/415 and 350/435 nm for the eyeball) and at least three wavelength pairs (Ex./Em. 240/335, 280/340 and 355/410 nm for the surface containing scales) for fish freshness assessment using PLSR model.
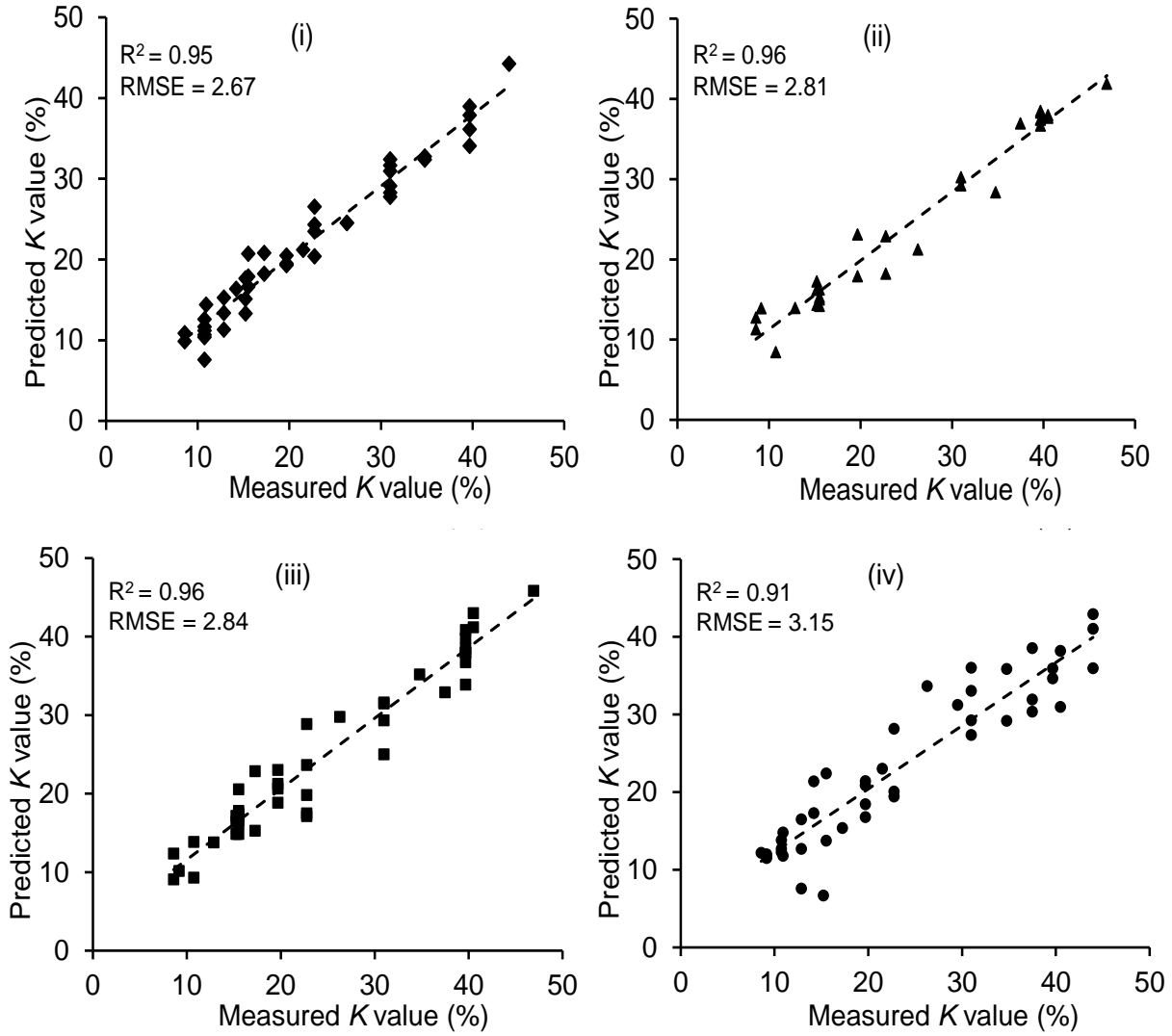
Fig. 3.8: PLSR analysis results for combined (i) EEM intensities in the whole excitation-emission wavelength; (ii) Combined fluorescence EEM for Ex.: 230 and 355 nm for eyeball only considered in the whole emission range; (iii) combination fluorescence EEM for excitation wavelengths 280 and 350 nm for eyeball and 280 and 355 nm for surface containing scales; and (iv) intensities for selected important Ex./Em. pairs.

Table 3.1: PLSR for K value using the whole EEM range.

Body part	Variable		Explained Variance (%)	RMSE (%)	R^2
	Ex. (nm)	No. of Input Variables			
Eyeball		3417	97.0	2.97	0.94
Surface containing scales	220 - 585	3417	86.3	2.92	0.93
Eyeball + Surface containing scales		6834	95.1	2.67	0.95

60

Table 3.2: PLSR for *K* value using Individual excitations.

Body part	Variable		Explained Variance (%)	RMSE (%)	R^2
	Ex. (nm)	No. of Input variables			
Eyeball	230	67	91.9	3.79	0.93
	245		87.6	4.13	0.89
	275		88.9	3.57	0.89
	280		83.9	3.74	0.92
	295		83.4	5.22	0.82
	310		83.8	4.83	0.84
	355		90.4	3.35	0.92
Surface containing scales	230		91.9	2.59	0.93
	275		94.4	2.35	0.93
	295		96.8	1.52	0.96
	340		78.4	3.90	0.79
	350		71.9	5.21	0.70

Table 3.3: PLSR for *K* value using the selected significant (Ex./Em pairs)

Body part	Variable			Explained Variance (%)	RMSE (%)	R^2
	Ex. (nm)	Em. (nm)	No. of Input Variables			
Eyeball	230	305	9	89.7	4.18	0.89
	245	335				
	275	305				
	280	365				
	295	330				
	295	435				
	310	325				
	330	415				
	355	435				
Surface containing scales	230	300	8	89.9	3.89	0.90
	230	335				
	230	415				
	275	300				
	280	350				
	295	415				
	340	390				
	350	435				
Eyeball + Surface containing scales	All Ex./Em. pairs of Eyeball and Surface containing scales combined		17	91.4	3.15	0.91

Table 3.4: PLSR for *K* value using using different excitations for eyeballs and scales.

Body part	Variable		Explained Variance (%)	RMSE (%)	R^2
	Ex. (nm)	**No. of Input variables**			
Eyeball	**230, 355**	134	**91.0**	**2.81**	**0.96**
	245, 355		94.8	2.71	0.95
	280, 355		**85.8**	**5.09**	**0.85**
	295, 355		88.5	4.06	0.89
	230, 280		93.3	3.05	0.91
	230, 295		88.7	2.89	0.90
	245, 280		85.1	3.56	0.87
	245, 295		90.4	3.37	0.89
	230, 280, 295	201	92.1	3.69	0.91
	230, 280, 355		90.7	3.18	0.93
	230, 295, 355		93.9	3.46	0.92
	245, 280, 355		91.8	3.54	0.91
	245, 295, 355		92.9	3.27	0.93
	230, 245, 280, 295, 310, 355	402	91.0	3.09	0.94
Surface containing scales	275, 295, 340	201	91.0	1.57	0.96
	275, 295, 350		94.2	1.99	0.94
	230, 275, 350		97.7	1.80	0.96
	230, 295, 350		96.8	1.77	0.95
	230, 275, 295, 340	268	82.5	3.64	0.81
	230, 275, 295, 350		82.8	3.62	0.81
	230, 275, 295, 340, 350	335	82.7	1.75	0.97
Eyeball + Surface containing scales	280, 350	402	95.9	2.84	0.96
	230, 280, 350		97.2	2.86	0.93
	230, 245, 290, 350		92.5	4.50	0.84
	All Excitations wavelengths combined (Eyeball and Surface containing scales)	737	90.2	3.70	0.89

Understanding the contributuion of emmision wavelenghths using PLS Weights

PLS weights were used to evaluate the contribution of each emission wavelengths by evaluating the highest PLS component. The model of the combined data for both the eyeball (excitations 280 and 355 nm) and surface with scales (excitations 275 and 350 nm) was plotted as shown in Fig. 3.9. The performance of the model showed that for 280 nm excitation of the eyeball, the critical emission wavelength with a broad range between 285 – 400 nm emission contributed positively, as seen from Fig. 3.9 i. For 355 nm excitation, six peaks were observed; two with positive contribution (one major at 375 nm and one minor resting at 435 nm. The other four with a negative contribution comprised of one major peak with a sharp maximum at 365 nm and the other three that looked small with a slightly broader range and with maximum points at 390, 405, and 455 nm (see Fig. 3.9 ii)

For a surface with scales, the best combination is comprised of 280 and 350 nm excitation. When the PLS weights for 280 nm excitation were plotted, two prominent peaks with positive and negative contributions were observed (see Fig. 3.9 iii). The positive peak had a maximum of 285 nm emission with a shorter range between 280 – 305 nm. The second peak with a negative contribution was stationed at 340 nm emission wavelength but with a broad range stretching between 305 – 550 nm. Fig. 3.9 iv shows the 355 nm excitation results which generated two peaks complementing each other and with a negative contribution. They have maximum points at 360 and 420 nm with a broad range covering 360 – 550 nm emission wavelength.

From this, we can say that a combination of excitations 280 and 350 nm for the eyeball and 280 and 355 nm for the surface with scales could potentially act as a good fish freshness indicator during storage. However, for industrial application that involves the use of laser beams, LEDs, or portable spectrometers, a small number of wavelengths is highly encouraged because it will reduce the number of devices, thus making it cheap. Therefore, one monitoring device at 280 nm can be made for both the eyeball and surfacecontaining scales. Additionally, 350 nm (eyeball) and 355 nm (surface with scales) can be made into one by having one monitoring a spectral range of about 20 nm to accommodate both the wavelengths. This means, to monitor the freshness changes of fish, two devices will be sufficient to track the changes for both the fish eyes and scales.
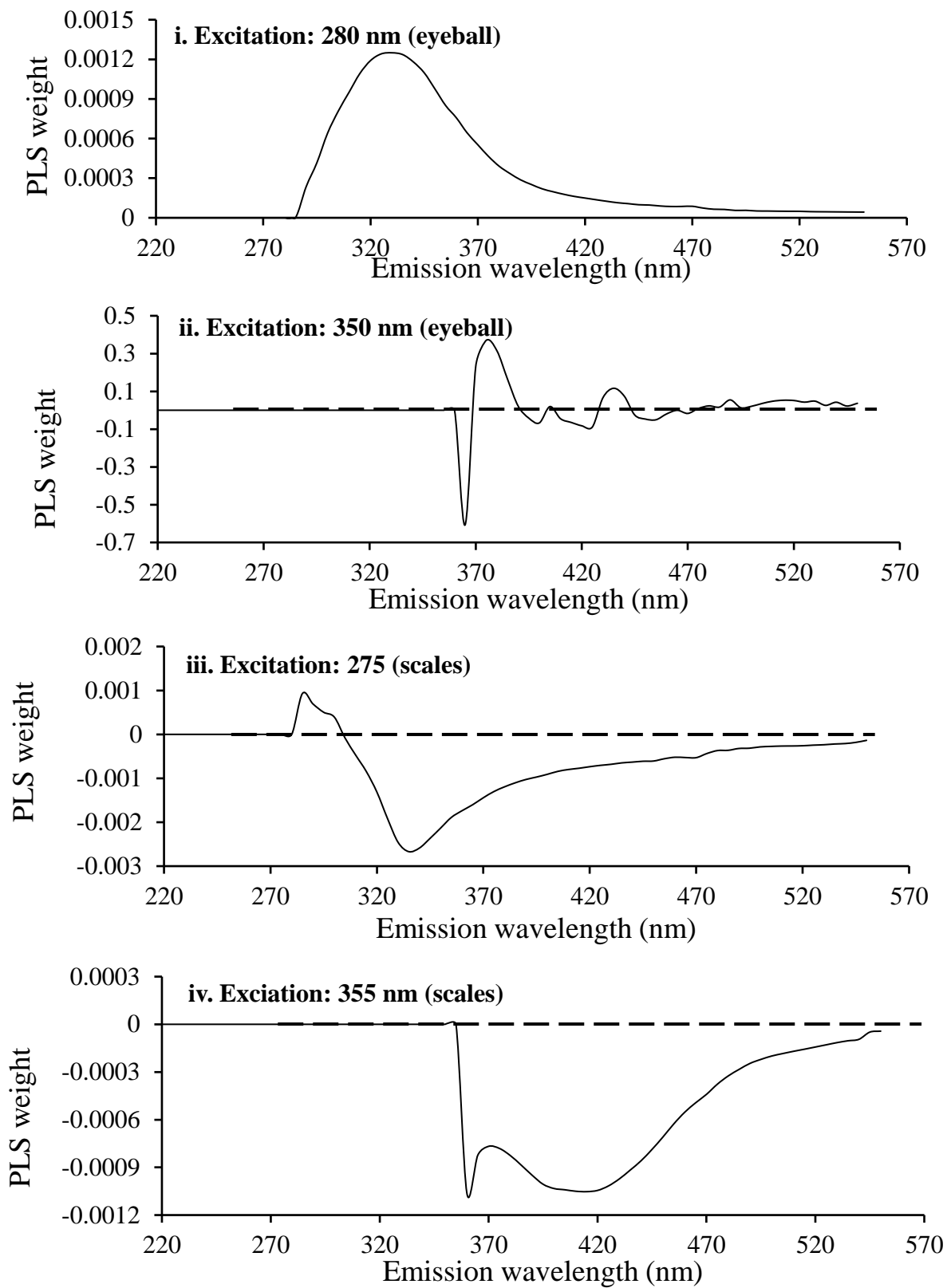
Fig. 3.9: PLS Weight results showing the important emission wavelengths.

3.5 Conclusions

Front-face fluorescence spectroscopy technique was used to acquire EEM features of Japanese dace fish during storage at about 4 °C. Investigative data analysis was conducted to examine fingerprints (potentially sensitive spectral regions) for monitoring fish freshness during storage. Specific wavelengths of the EEM associated with proteins and amino acids and uric acid (for fish eyeball) and amino acids and collagen (surface containing scales) are recommended for freshness monitoring purposes. Four approaches were tested for variable reduction: (i) whole EEM range; (ii) Individual excitation fluorescence EEM for important wavelengths considered in the Whole emission range; (iii) combination fluorescence EEM for different excitation wavelengths eyeball and/or surface containing scales and (iv) Fluorescence EEM for selected important pairs of wavelength peaks (Ex./Em. pairs). It was found that two datasets would be sufficient to act as freshness indicator. Firstly, if just one body part, the excitations of 230 and 355 nm will give highest results with 2.81 and 0.96 for RMSE and R^2, with an explained variance of 91%. Combining the fluorescence EEM of the eyeball and surface containing scales for fish freshness monitoring will achieve a more robust results, and even from the results, the best performance was produced by excitations 280 and 350 nm for eyeball and surface containing scales with 2.84 and 0.96 as RMSE and R^2 data respectively with an explained variance of 95.9%. For intact fish freshness evaluation, the combination of the eyeball and surface-containing scales will be important. Since they lie on the fish's surface, there is great potential in adopting non-destructive freshness evaluation during the assessment. Since all the important peaks have an emission below 550 nm, it is possible to establish a multi-imaging system to capture these images changes with just one camera with a sensitivity ranging between 300 – 550 nm with several rotating filters for different excitation wavelengths. These results, therefore, demonstrate demonstrates two excitation wavelengths are the most important to monitor Japanese dace fish freshness. For industrial application, this research clear indicates that with just two light sources, new freshness indices for fish could be defined in terms of color, thus, non-destructive evaluation.

REFERENCES

Al Riza, D. F., Widodo, S., Purwanto, Y. A., & Kondo, N. (2019). Authentication of the geographical origin of patchouli oil using front-face fluorescence spectroscopy and chemometric analysis. *Flavour and Fragrance Journal*, *34*(1), 15–20. https://doi.org/10.1002/ffj.3473

Betemps, D. L., Fachinello, J. C., Galarca, S. P., Portela, N. M., Remorini, D., Massai, R., & Agati, G. (2012). Non-destructive evaluation of ripening and quality traits in apples using a multiparametric fluorescence sensor. *Journal of the Science of Food and Agriculture*, (September 2011), 1855–1864. https://doi.org/10.1002/jsfa.5552

Bremner, H. A., & Sakaguchi, M. (2015). A Critical Look at Whether ' Freshness ' Can Be Determined. *Journal of Aquatic Food Product Technology*, *9:3*(April 2015), 37–41. https://doi.org/10.1300/J030v09n03

Bro, R. (1996). Multiway Calibration. multilinear PLS. *Journal of Chemometrics*, *10*(March 1995), 47–61.

Cameron, J. S., Moro, F., & Simmonds, H. A. (1993). Gout, uric acid and purine metabolism in paediatric nephrology. *Pediatric Nephrology*, *7*(1), 105–118. https://doi.org/10.1007/BF00861588

Cheng, J. H., Sun, D. W., Qu, J. H., Pu, H. Bin, Zhang, X. C., Song, Z., … Zhang, H. (2016). Developing a multispectral imaging for simultaneous prediction of freshness indicators during chemical spoilage of grass carp fish fillet. *Journal of Food Engineering*, *182*, 9–17. https://doi.org/10.1016/j.jfoodeng.2016.02.004

Christensen, J., Nørgaard, L., Bro, R., & Engelsen, S. B. (2006). Multivariate Autofluorescence of Intact Food Systems. *American Chemical Society*, *106*(6). https://doi.org/10.1021/cr050019q

Dalgaard, P. (1995). Modelling of microbial activity and prediction of shelf life for packed fresh fish. *International Journal of Food Microbiology*, *26*(3), 305–317. https://doi.org/10.1016/0168-1605(94)00136-T

Dufour, E., J.P. Frencia, A., & Kane, E. (2003). Development of a rapid method based on front-face fluorescence spectroscopy for the monitoring of fish freshness. *Food Research International*, *36*(5), 415–423. https://doi.org/10.1016/S0963-9969(02)00174-6

Eastoe, J. E. (1955). The amino acid composition of mammalian collagen and gelatin. *The Biochemical Journal*, *61*(4), 589–600. https://doi.org/10.1042/bj0610589

Elmasry, G., Nagai, H., Moria, K., Nakazawa, N., Tsuta, M., Sugiyama, J., … Nakauchi, S. (2015). Freshness estimation of intact frozen fish using fluorescence spectroscopy and chemometrics of excitation-emission matrix. *Talanta*, *143*, 145–156. https://doi.org/10.1016/j.talanta.2015.05.031

Eyre, D. (1987). Collagen Cross-Linking Amino Acids. *Methods in Enzymology*, *144*(C), 115–139. https://doi.org/10.1016/0076-6879(87)44176-1

Gauza-Włodarczyk, M., Kubisz, L., & Włodarczyk, D. (2017). Amino acid composition in determination of collagen origin and assessment of physical factors effects. *International Journal of Biological Macromolecules*, Vol. 104, pp. 987–991. https://doi.org/10.1016/j.ijbiomac.2017.07.013

Georgakoudi, I., Jacobson, B. C., Müller, M. G., Sheets, E. E., Badizadegan, K., Carr-Locke, D. L., … Feld, M. S. (2002). NAD(P)H and collagen as in vivo quantitative fluorescent biomarkers of epithelial precancerous changes. *Cancer Research*, *62*(3), 682–687.

Gram, L., & Huss, H. H. (1996). Microbiological spoilage of fish and fish products. *International Journal of Food Microbiology*, *33*(96), 121–137. Retrieved from http://www.ncbi.nlm.nih.gov/pubmed/8913813

Hammami, M., Dridi, S., Zaïdi, F., Maâmouri, O., Blecker, C., Karoui, R., … Blecker, C. (2013). Use of Front-Face Fluorescence Spectroscopy to Differentiate Sheep Milks from Different Genotypes and Feeding Systems. *International Journal of Food Properties*, *2912*(May). https://doi.org/10.1080/10942912.2011.583706

Hong, H., Regenstein, J. M., & Luo, Y. (2017). The importance of ATP-related compounds for the freshness and flavor of post-mortem fish and shellfish muscle: A review. In *Critical Reviews in Food Science and Nutrition* (Vol. 57). https://doi.org/10.1080/10408398.2014.1001489

Itoh, D., Koyachi, E., Yokokawa, M., Murata, Y., Murata, M., & Suzuki, H. (2013). Microdevice for On-Site Fish Freshness Checking Based on K-Value Measurement. *Analytical Chemistry*, *85*, 10962–10968. https://doi.org/10.1021/ac402483w

Karoui, R., & Blecker, C. (2010). Fluorescence Spectroscopy Measurement for QualityAssessment of Food Systems—a Review. *Food Bioprocess Technol*, *4*(2011), 364–386.

Karoui, R., Thomas, E., & Dufour, E. (2006). Utilisation of a rapid technique based on front-face

fluorescence spectroscopy for differentiating between fresh and frozen-thawed fish fillets. *Food Research International*, *39*(3), 349–355. https://doi.org/10.1016/j.foodres.2005.08.007

Kato, N., Kunimoto, M., Koseki, S., Kitakami, S., & Arai, K. (2009). Freshness and Quality of Fish and Shellfish (Supplementary Edition). *Journal of The School of Marine Science and Technology*, *7*(2), 87–99. Retrieved from http://www2.scc.u-tokai.ac.jp/www3/kiyou/pdf/2009vol7_2/kato.pdf

Koutsoumanis, K., & Nychas, G. J. E. (2000). Application of a systematic experimental procedure to develop a microbial model for rapid fish shelf life predictions. *International Journal of Food Microbiology*, *60*(2–3), 171–184. https://doi.org/10.1016/S0168-1605(00)00309-3

Lakowicz, J. R. (2006). Principles of fluorescence spectroscopy. *Principles of Fluorescence Spectroscopy*, (June), 1–954. https://doi.org/10.1007/978-0-387-46312-4

Lawaetz, A. J., & Stedmon, C. A. (2009). Fluorescence intensity calibration using the Raman scatter peak of water. *Applied Spectroscopy*, *63*(8), 936–940. https://doi.org/10.1366/000370209788964548

Liao, Q., Suzuki, T., Shirataki, Y., Kuramoto, M., & Kondo, N. (2018). Freshness related fluorescent compound changes in Japanese dace fish (Tribolodon hakonensis) eye fluid during storage. *Engineering in Agriculture, Environment and Food*, *11*(3), 95–100. https://doi.org/10.1016/j.eaef.2018.01.001

Liao, Q., Suzuki, T., Yasushi, K., Al Riza, D. F., Kuramoto, M., & Kondo, N. (2017a). Monitoring red sea bream scale fluorescence as a freshness indicator. *Fishes*, *2*(3). https://doi.org/10.3390/fishes2030010

Liao, Q., Suzuki, T., Yasushi, K., Al Riza, D., Kuramoto, M., & Kondo, N. (2017b). Monitoring Red Sea Bream Scale Fluorescence as a Freshness Indicator. *Fishes*, *2*(3), 10. https://doi.org/10.3390/fishes2030010

Mehretie, S., Riza, D. F. Al, Saito, Y., & Kondo, N. (2018). Classi fi cation of raw Ethiopian honeys using front face fl uorescence spectra with multivariate analysis. *Food Control*, *84*, 83–88. https://doi.org/10.1016/j.foodcont.2017.07.024

Olafsdottir, G., Nesvadba, P., Di Natale, C., Careche, M., Oehlenschläger, J., Tryggvadóttir, S. V., … Jørgensen, B. M. (2004). Multisensor for fish quality determination. *Trends in Food Science and Technology*, *15*(2), 86–93. https://doi.org/10.1016/j.tifs.2003.08.006

Omwange, K. A., Al Riza, D. F., Sen, N., Shiigi, T., Kuramoto, M., Ogawa, Y., … Suzuki, T.

(2020). Fish freshness monitoring using UV-fluorescence imaging on Japanese dace (Tribolodon hakonensis) fisheye. *Journal of Food Engineering*, *287*(May), 110111. https://doi.org/10.1016/j.jfoodeng.2020.110111

Omwange, K. A., Saito, Y., Zichen, H., Khaliduzzaman, A., Kuramoto, M., Ogawa, Y., … Suzuki, T. (2021). Evaluating Japanese dace (Tribolodon hakonensis) fish freshness during storage using multispectral images from visible and UV excited fluorescence. *LWT*, *151*(May), 112207. https://doi.org/10.1016/j.lwt.2021.112207

Özogul, Y., Özyurt, G., Özogul, F., Kuley, E., & Polat, A. (2005). Freshness assessment of European eel (Anguilla anguilla) by sensory, chemical and microbiological methods. *Food Chemistry*, *92*(4), 745–751. https://doi.org/10.1016/j.foodchem.2004.08.035

Oztekin, E. K., & Hahn, D. W. (2016). Differential Laser-Induced Perturbation Spectroscopy for Analysis of Mixtures of the Fluorophores L -Phenylalanine , L -Tyrosine and L -Tryptophan Using a Fluorescence Probe. *Photochemistry and Photobiology*, *92*, 658–666. https://doi.org/10.1111/php.12618

Patra, D., & Mishra, A. K. (2002). Recent developments in multi-component synchronous fluorescence scan analysis. *Trends in Analytical Chemistry*, *21*(12), 787–798.

Ridi, R. El, & Tallima, H. (2017). Physiological functions and pathogenic potential of uric acid_ A review. *Journal of Advanced Research*, *8*(2017), 487–493. https://doi.org/10.1016/j.jare.2017.03.003

Ringvold, A., Anderssen, E., Jellum, E., Bjerkås, E., Sonerud, G. A., Haaland, P. J., … Kjønniksen, I. (2003). UV-absorbing compounds in the aqueous humor from aquatic mammals and various non-mammalian vertebrates. *Ophthalmic Research*, *35*(4), 208–216. https://doi.org/10.1159/000071172

Ruoff, K., Luginbuhl, W., Kunzli, R., Bogdanov, S., Bosset, J. O., Ohe, K. Von Der, … Amado, R. (2006). Authentication of the Botanical and Geographical Origin of Honey by Front-Face Fluorescence Spectroscopy. *Journal of Agricultural and Food Chemistry*, 6858–6866.

Santana, C. Á., Lima, D. M. V., da Cunha Andrade, L. H., Súarez, Y. R., & Lima, S. M. (2016). Laser-induced fluorescence in fish scales to evaluate the environmental integrity of ecosystems. *Journal of Photochemistry and Photobiology B: Biology*, *165*, 80–86. https://doi.org/10.1016/j.jphotobiol.2016.10.005

Stetinensia, F. O. (2011). Trends and factors of development of the world consumption of fish and

fishery products. *Versita*, *10*(18), 213–227. https://doi.org/10.2478/v10031-011-0012-3

Surette, M. E., Gill, T. A., & LeBlanc, P. J. (1988). Biochemical basis of postmortem nucleotide catabolism in cod (Gadus morhua) and its relationship to spoilage. *Journal of Agricultural and Food Chemistry*, *36*(1), 19–22. https://doi.org/10.1021/jf00079a005

Villette, S., Pigaglio-Deshayes, S., Vever-Bizet, C., Validire, P., & Bourg-Heckly, G. (2006). Ultraviolet-induced autofluorescence characterization of normal and tumoralesophageal epithelium cells with quantitation of NAD(P)H. *Photochemical & Photobiological Sciences*, *5*, 483–492. https://doi.org/10.1039/b514801d

Wang, D., Tang, J., Correia, L. R., & Gill, T. A. (1998). Postmortem changes of cultivated Atlantic salmon and their effects on salt uptake. *Journal of Food Science*, *63*(4), 634–637. https://doi.org/10.1111/j.1365-2621.1998.tb15801.x

Watanabe, A., Tsuneishi, E., & Takimoto, Y. (1989). Analysis of ATP and Its Breakdown Products in Beef by Reversed-Phase HPLC. *Journal of Food Science*, *54*(5), 1169–1172. https://doi.org/10.1111/j.1365-2621.1989.tb05948.x

CHAPTER IV: FISH FRESHNESS MONITORING USING UV-FLUORESCENCE IMAGING ON JAPANESE DACE (*Tribolodon hakonensis*) FISHEYE

4.1 Introduction

Fish are known for their good nutritional value and as a rich source of protein, which has led to their increasing demand in the human diet in recent years (Dale, 1994). In tandem, new consumer patterns like consumption of raw fish, have raised safety and quality concerns regarding fishery products (Dowlati et al., 2013, 2012). After landing, although fish is recommended to be kept below 10 °C (Genigeorgis, 1985), the freshness of fish continuously deteriorates, hence losing its nutritional benefits and economic value. Recently, there has been increasing demand for high quality and fresh fish products, highlighting the need for monitoring fish freshness to guarantee high-quality standards and safety for consumers.

Freshness is one of the main attributes consumers use in assessing fish and fishery products; thus, acting like a mark of quality for evaluating the taste and safety of fish by customers (Özogul et al., 2005). Various techniques, such as sensory analysis (Özogul et al., 2005), and microbial analysis (Dalgaard, 1995; Koutsoumanis and Nychas, 2000) have previously been used to assess fish freshness; however, they have all proved to be subjective, time-consuming and expensive. Biochemical analysis (Elmasry et al., 2015; Itoh et al., 2013) was established as a conventional and the standard way to evaluate fish and meat products because of its ability to monitor the degradation of adenosine triphosphate (ATP) derived products, which directly correlate with biochemical changes in meat.

There have been efforts to develop simple and easier techniques as alternative to the conventional methods of complex chemical analyses for estimating fish freshness. Some of them include colorimeters (Huang et al., 2011) and image analyzers (Murakoshi et al., 2013) both of which use common color images; however, normal color measurement may not be sensitive enough for some fish. Spectrophotometer technique was suggested by Cheng et al., (2013), but was limited to fish fillet. Electronic sensors such as e-nose and e-tongue which mimics human senses of smell and taste (Gil et al., 2008), but they are limited to quantitative analysis. New techniques for estimating freshness target to utilize machine vision systems for commercial grading. But to design such systems preliminary investigations are necessary to come up with proper parameter settings.

Fundamental research using optical tools like fluorescence spectroscopy have shown potential for overcoming these limitations. For instance, right angle fluorescence spectroscopy of fish eye-fluid was used to estimate freshness in Japanese dace (*Tribolodon hakonensis*) (Liao et al., 2018). The eye-fluid was sampled throughout the storage period at 20±2 °C to measure spectra properties and their characteristics. They found out that the eye-fluid contains fluorescent compounds; amino-acids and uric acid, whose fluorescence intensity varies with freshness changes, thus, acting as a potential indicator to track fish freshness deterioration during storage. However, this technique posed some limitations: it is (i) destructive (abstracting the eye-fluid a syringe and needle); (ii) laborious and (iii) limited commercial applicability. Hence, there is a need for an easy, quick, non-destructive and commercially applicable technique for monitoring fish freshness. This spectroscopy-based technique with one-point measurement can further be developed into machine vision system which include spatial information similar to what was reported by Nie et al., (2020) on kiwi fruit.

This research therefore proposes a new technique that can use UV-induced fluorescence imaging to estimate fish freshness non-destructively; by tracking the color changes of the fisheye (pupil and cornea) associated with an excitation/emission of 350/415 nm. The color parameters such as R(red), G(green), B(blue), S(saturation), V(value), L* (lightness) and b*(yellowness) in the images for Japanese dace (*Tribolodon hakonensis*) fisheye were investigated and correlated with *K* value indices during storage.

4.2 Materials and methods

Sample preparation

Japanese dace fish were bought from Hamaichi bait Company (Wakayama Prefecture, Japan), where they had been cultured for about ten months. The fish were delivered alive in a plastic bag with water, and after delivery the fish were kept in laboratory raising tanks (Kyoto University, Japan). During the experiment, 52 fish with an average length 160±15 mm was selected, killed and kept in the refrigerator set at 4±1 °C for about 2 hours to lower body temperature before the experiment started. 52 data were obtained (thirteen data points with four fish used at every measurement). At every measurement frequency, three experiments were carried out: imaging (color and fluorescence) of whole fish, excitation-emission matrix fluorescence of eyeball and *K* value of meat for a period 52 hours.
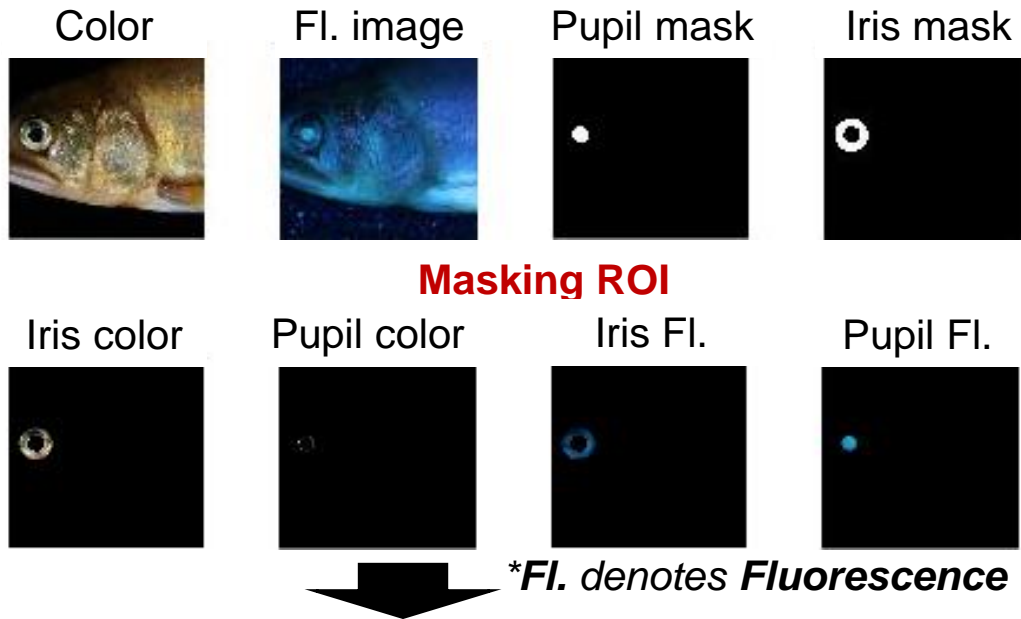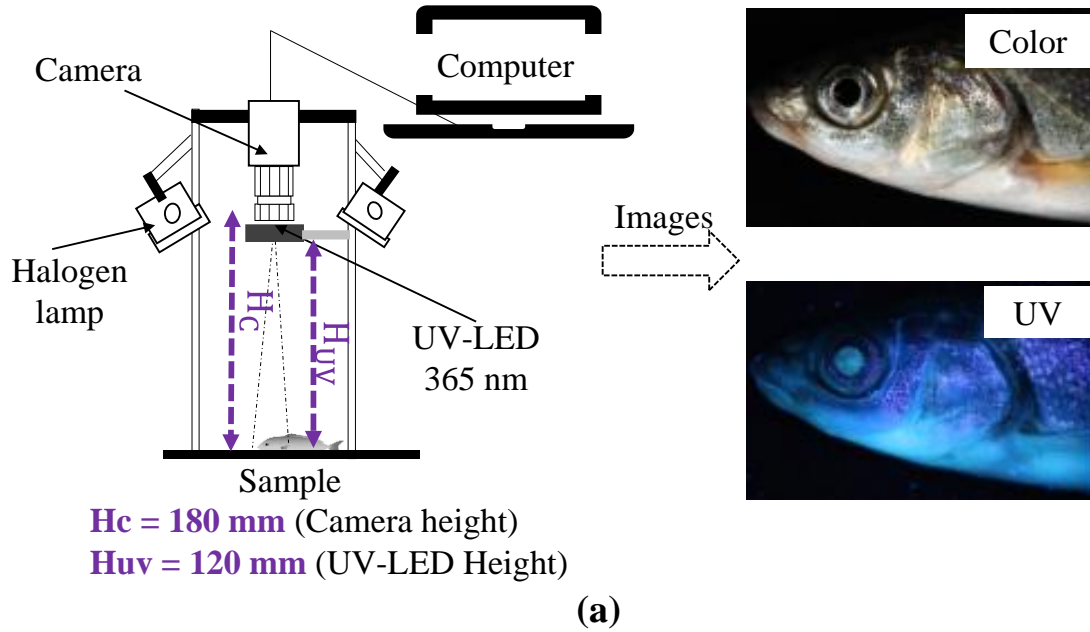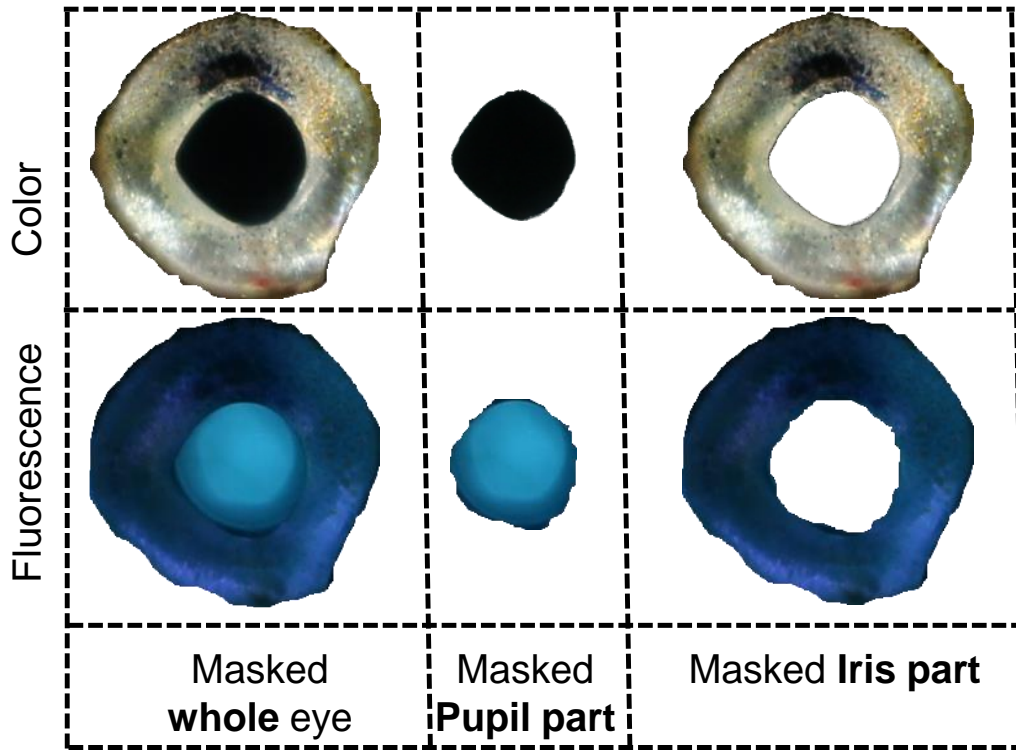
Excitation Emission Matrix (EEM) measurement

The fish eyeball was removed from the eye-socket and placed in a cell holder for fluorescence measurement of the eyeball. Front face measurement technique was used to acquire an EEM using a spectrofluorometer (Jasco FP-8300, Jasco Co., Tokyo, Japan) with parameters: excitation (200-600 nm), emission (220-600 mm), Ex/Em measurements were captured at an interval of 5 nm; 5 nm bandwidth; scan speed of 5,000 nm min^{-1}; a response of 50 ms and with a low sensitivity for the photomultiplier tubes (PMT), at room temperature (20 $\pm$1 $^{\circ}$C). After capturing raw EEM data, correction for light source and response of detector were conducted using calibration spectra obtained by using a standard light source and Rhodamine B calibration following standard calibration protocol provided by JASCO Company, Japan. The corrected data files were later converted from arbitrary unit (A.U.) to Raman units (R.U) to prevent instrument effects on the results (Lawaetz and Stedmon, 2009)**.** Four EEM data at each sampling interval was obtained during the 52 hours storage period. The fluorescence intensity acquired from the fish eyeball was later used for developing *K* value prediction model and selection of the suitable wavelength for fluorescence imaging.
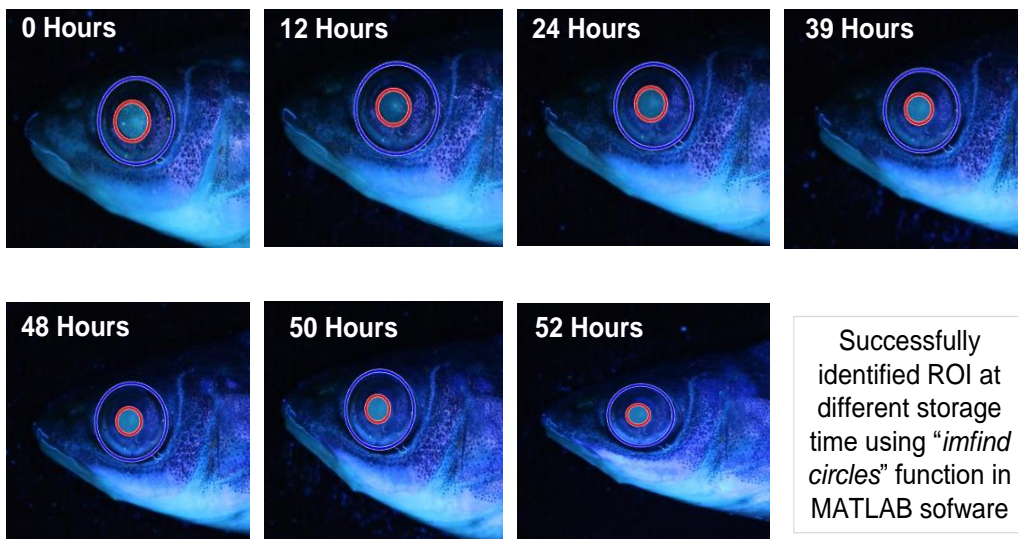
Image acquisition & processing

Fisheye images were acquired in a dark room using EOS DSLR (kiss x7, Canon Inc., Japan) placed at 180 mm above the sample surface with a focal length of 44 mm at room temperature (20 $\pm$1 $^{\circ}$C). Before measurement of fluorescence EEM, color images were taken under the 4 halogen lamps with a shutter speed of 1/10 s, f/6.3 and an ISO of 200. Fluorescence images were acquired using a 365 nm UV-LED excitation source (LDR2-60UV2-365-N, CCS Inc. Japan) with a shutter speed of 4 s, f/6.3 and an ISO of 200. The UV-LEDs were placed 120 mm above the sample surface as seen in Fig 4.1a. 365 nm LED is commercially available and offers stronger power compared to others; it has a wider excitation band ranging from 345-395 nm, and the region of interest has excitation ranging between 310-375 nm, hence it can capture the required information. MATLAB software (MATLAB 9.5 R2018b, MathWorks, USA) was used for image processing. Color images were used to segment the region of interest (ROI); where the pupil and iris were automatically detected using a program code on MATLAB software. Subsequently, the ROI was masked on the fluorescence images by overlaying the corresponding color and fluorescence images (see Fig. 4.1b and c). Original images were in RGB color space but were later

converted to HSV and L*a*b* respectively. Separate color channels (R, G, B; H, S, V; L*, a*, b*) were then extracted and average values were obtained for analysis. Data analysis for all the experiments was done as shown in Fig. 4.1d.
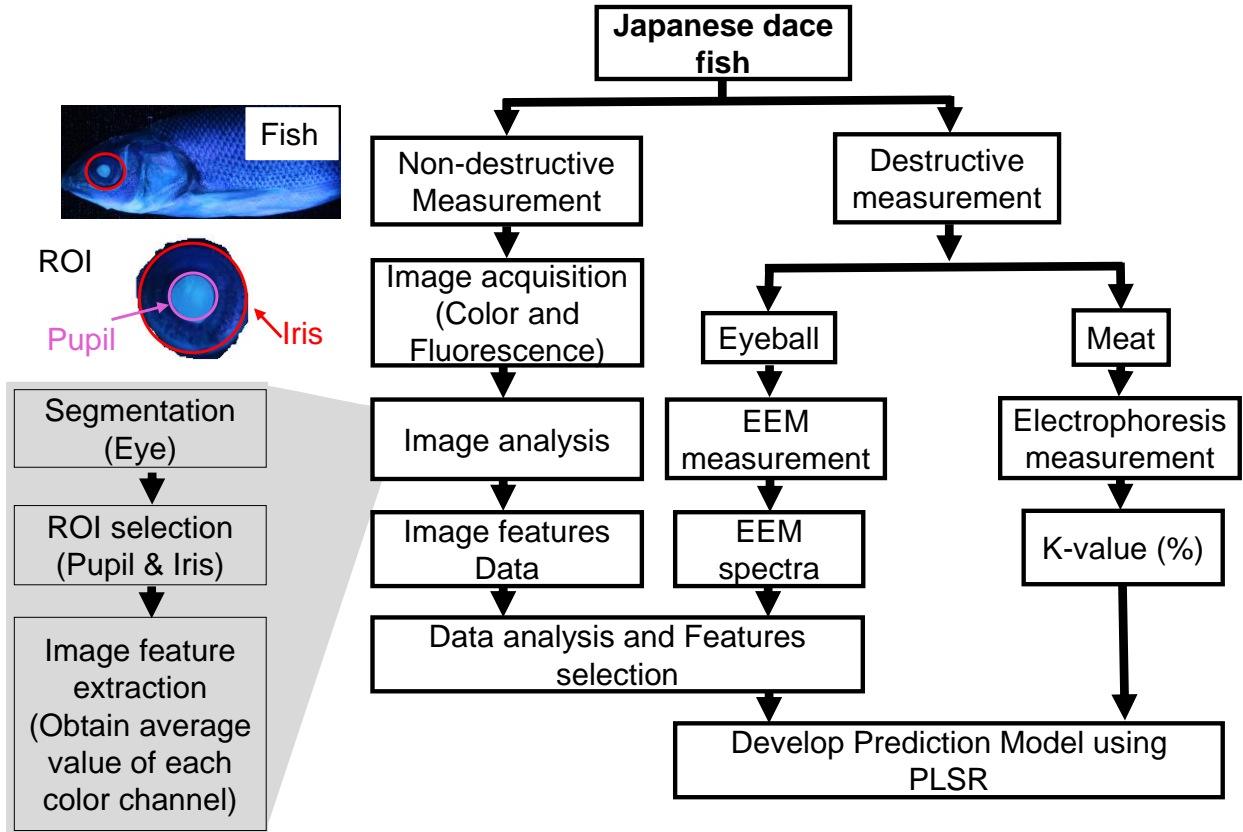

(a)

Masking ROI

FI. denotes Fluorescence

(b)

Successfully identified ROI at different storage time using "*imfind circles*" function in MATLAB sofware

(c)

(d)

Fig. 4.1. (a) Image acquisition system showing the heights of UV LED (H_{uv}) and camera (H_c) (b) steps for masking ROI, (c) ROI successfully detected for all the images and (d) Image processing and multivariate analysis.

4.3 Evaluation of calibration and prediction model Performance

To investigate the suitability of fluorescence imaging to predict *K* value of fish during storage, partial least square regression (PLSR) analysis was conducted using MATLAB R2018a software (MathWorks, USA) by correlating the UV-color parameter changes on the fisheye (iris and pupil) with respect to freshness changes during storage. The performance of calibrated and predicted models for *K* value were evaluated in terms of root mean square error of calibration (RMSEC: Eq. 4.1). or validation (RMSECV: Eq. 4.2) and coefficient of determination of cross-validation, R^2_{cv} (Eq. 4.3) (Cheng et al., 2016).

In this research, a leave-one-out cross-validation technique was applied for validation of the established calibration models (Cheng et al., 2016; Kohavi, 1995). The prediction performance and capability of the PLSR model was evaluated in terms of determination coefficients of

76

calibration (R^2_C) and cross-validation (R^2_{CV}); and root mean square errors of calibration (RMSEC) and cross-validation (RMSECV). A good model depicts a higher R^2_C and R^2_{CV} and lower RMSEC and RMSECV. Their corresponding calculation formula are as below.

$$RMSEC = \sqrt{\frac{1}{n}\sum_{i=1}^{n}(y_{cal} - y_{act})^2} \tag{4.1}$$

$$RMSECV = \sqrt{\frac{1}{n}\sum_{i=1}^{n}(y_{pred} - y_{act})^2} \tag{4.2}$$

$$R^2_{cv} = 1 - \frac{\sum_{i=1}^{n}(y_{cal} - y_{act})^2}{\sum_{i=1}^{n} y_{cal} - y_{mean}^2} \tag{4.3}$$

Where, n is the sample number, y_{act} is the measured value, y_{cal} is the calculated value, y_{mean} is the average value and y_{pred} is the predicted value of the corresponding parameters.

4.4 Results and Discussion

Electrophoresis (K value)

The *K* value for Japanese dace fish varied from about 8% to about 50% over the 52 hours of storage of 4 ±1 °C. Ideally, prime fresh fish has a *K* value starting from about 7% to 8%; however, for this experiment, some samples started from 9% or 10%; and this could be attributed to the two and half hours they spent (30 minutes after killing and 2 hours during refrigeration) before measurement commenced. In this experiment, Japanese dace fish remained within Sashimi and cooking levels for the first 24 hours and 48 hours respectively. Beyond this time, the fish were spoiled and not good for consumption.

Fluorescence

Three peaks A (230/330 nm), B (290/330 nm) and C (350/415 nm) were observed from the EEM fluorescence of the eyeball (see Fig. 4.2) similar to those observed during the investigation of fluorescence properties of the Japanese dace fish eye-fluid by Liao et al. (Liao et al., 2018). Peaks A and B showed higher intensities compared to that of C peak (see Fig. 4.4); this is because A and B peaks are associated with proteins and amino acids which are abundant in fish (Liao et al., 2018). However, these peaks demonstrated unstable tendencies during storage period.

However, for peak C (350/415 nm), the peak is characterized by lower fluorescence intensities which increased gradually during storage. From the previous research on eye-fluid using this particular fish, (Liao et al., 2018) confirmed with HPLC analysis that this peak originates from

77

uric acid. Uric acid is a by-product from two processes: purine metabolism and ATP disintegration processes through enzymatic activities. These processes accumulate uric acid, gradually increasing its intensity during storage. These changes reflected a similar tendency to those of the observed K value changes, thereby suggesting a non-destructive technique that can track these variations non-destructively. Hence, coining the idea for using fluorescence imaging in monitoring the changes related to this peak with excitation 350 nm. Front-face fluorescence spectroscopy has the potential to track fluorescence characteristic changes of a sample (Dufour et al., 2003) nondestructively. Therefore, the fish eyeball (from the surface) fluorescence characteristics were measured using front-face spectroscopy technique and it demonstrates that fisheye EEM could be obtained and related with its freshness.
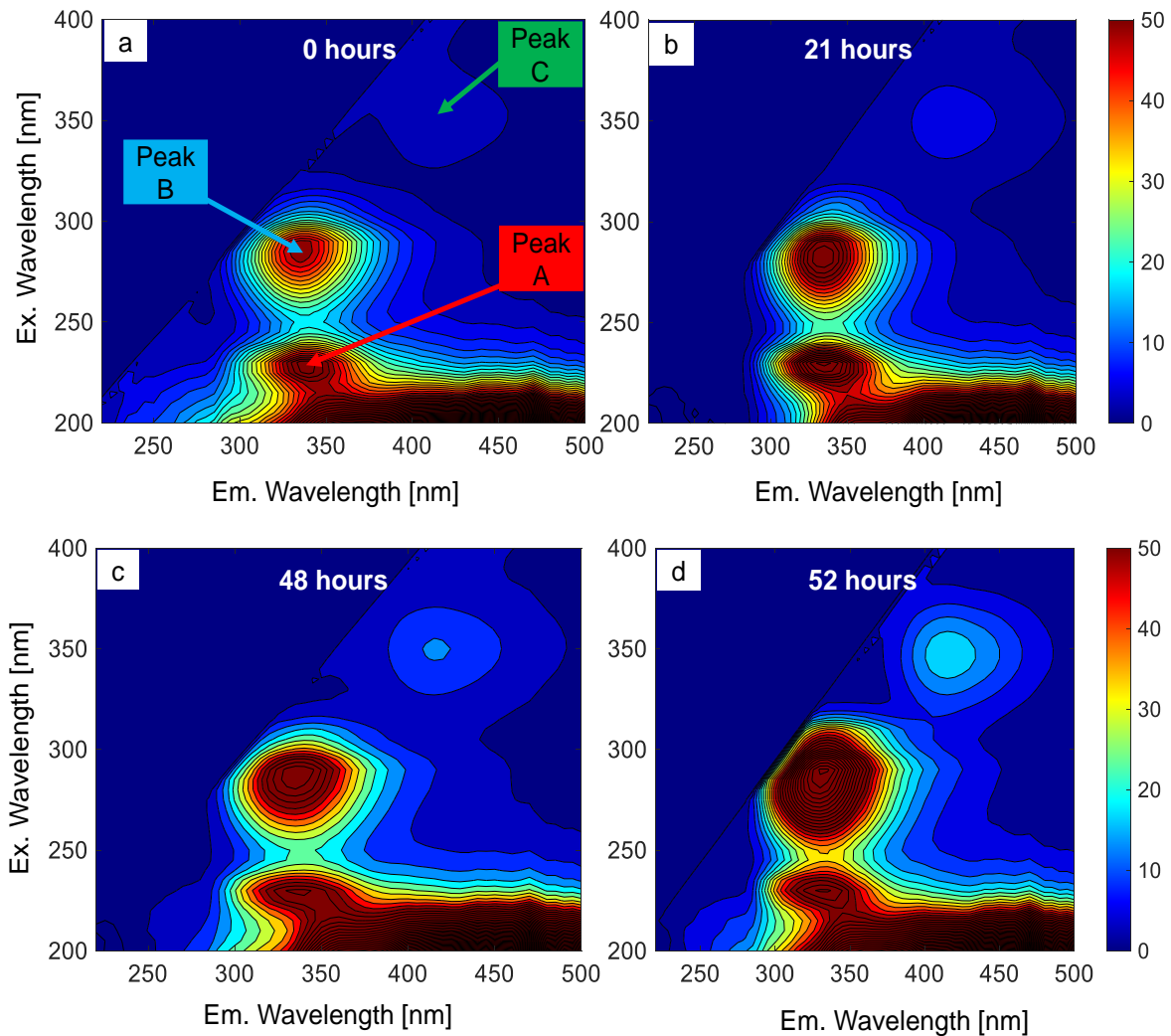

Fig. 4.2. EEM changes for Japanese dace fisheye-ball during storage.
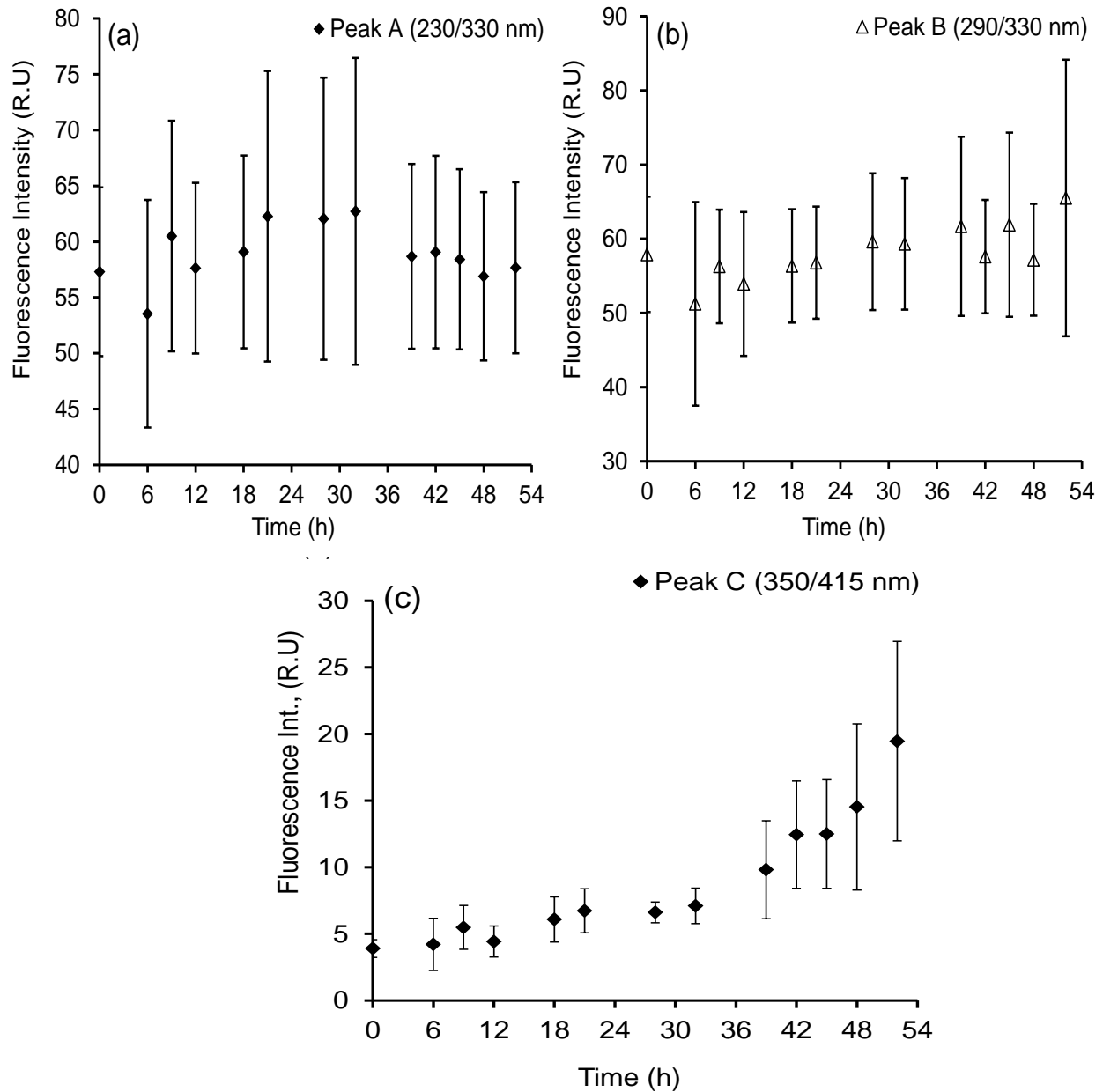
Fig. 4.3. Time-series fluorescence intensity for (a) peak A (230/330 nm) and B (290/330 nm), and (b) peak C (350/415 nm).

The fluorescence intensity changes for the three peaks; A, B and C were used to predict K value of fish during storage. This was meant to analyze the potential of using multispectral wavelengths to estimate freshness variation of fish. Therefore, PLSR analysis was carried out, and from the results, multivariate analysis demonstrated potential to predict fish freshness. The spectra data from individual peaks A, B and C and combination of them all (A, B, and C) showed a higher correlation coefficient and small error (see Table 4.1 below). This implies that for effective freshness prediction using this technique (fluorescence spectroscopy), it is better to combine the

79

data from all the peaks thereby requiring multiparametric optical sensors with different light sources. To come up with such devices/sensors of multispectral wavelengths will be costly, and therefore, there is need for simple and cheaper method to estimate K value of fish during storage. Since the fluorescence intensity changes for peak C was increasing cumulatively (see Fig. 4.3), hence it was selected to establish imaging system to estimate freshness of Japanese dace fish.

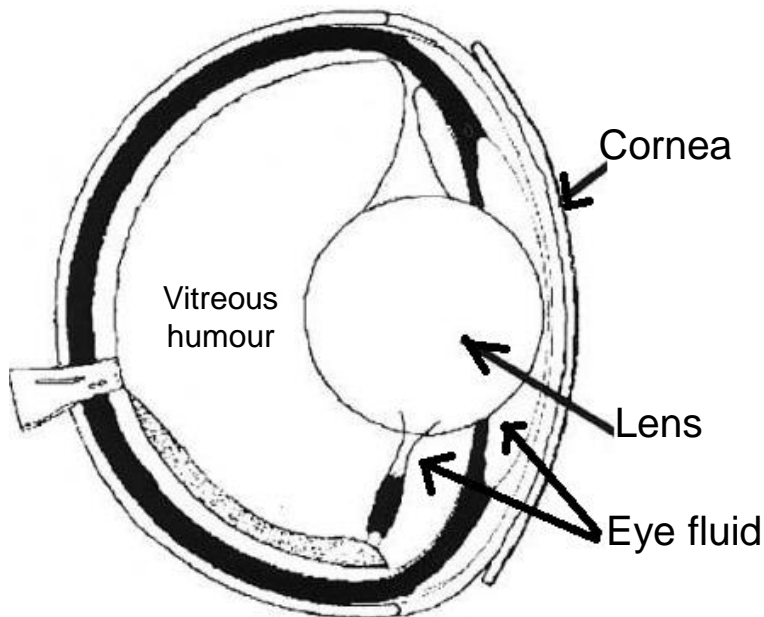*Fluorescence information of fisheye structure*

Fig. 4.4: Fish eyeball and its structure.

Japanese dace fish's eyeballs were removed for investigation of fluorescence properties of different parts (eyeball, lens, cornea, and intact eyeball). The eye fluid was first abstracted from its location (as seen from Fig. 4.5) for internal fluorescence signatures. The eyeball was then dissected to separate the cornea for surface measurement. The fluorescence compounds present in the intact eyeball, eye-fluid and cornea for Japanese fish posted similar fluorescence compounds A, B and C as seen from Fig. 4.5. The corresponding excitation matrices (EEM) for all the parts (intact eyeball, eye-fluid, and cornea) was 230/330, 280/330 and 350/420 for peaks A, B and C respectively. The fisheye lens demonstrated that it is made up of amino acid compounds (See Fig. 4.5). The cornea and lens were given two treatments; (i) measured after dissecting without cleaning (wiping it) it, (ii) wiped and wiped it with kim towels before measuring it. During dissection, some eye fluid residues could be stained on the surface, and this might influence the fluorescence effects from the cornea layers. So, by wiping and washing, all the internal eye components that might

80

have embedded during dissection are assumed to have been fully washed away, so that the EEM observed is taken to be originating from only the cornea layer. In both cases, the EEM properties remained the same (see Fig. 4.6 i and ii), implying that the fluorescence compounds observed on the intact eye is not just from the eye fluid (inside the eye) but from the surface of the eye. This means that despite the lens being sandwiched between eye fluid and vitreous humour (see Fig. 4.4), it does not mix even after the fish has dies.

When the EEM for red sea bream (*Pagrus major*) fish (from sea water) was measured, EEM features like those observed with ayu were evident. However, the intensities for peak C were slightly lower compared to peaks A and B, for time series quantification of the fluorescence changes, a ratio of peak intensities between different peaks can be considered for more robust results. This means that for non-destructive measurement, an intact eye can reveal enough fluorescence information.
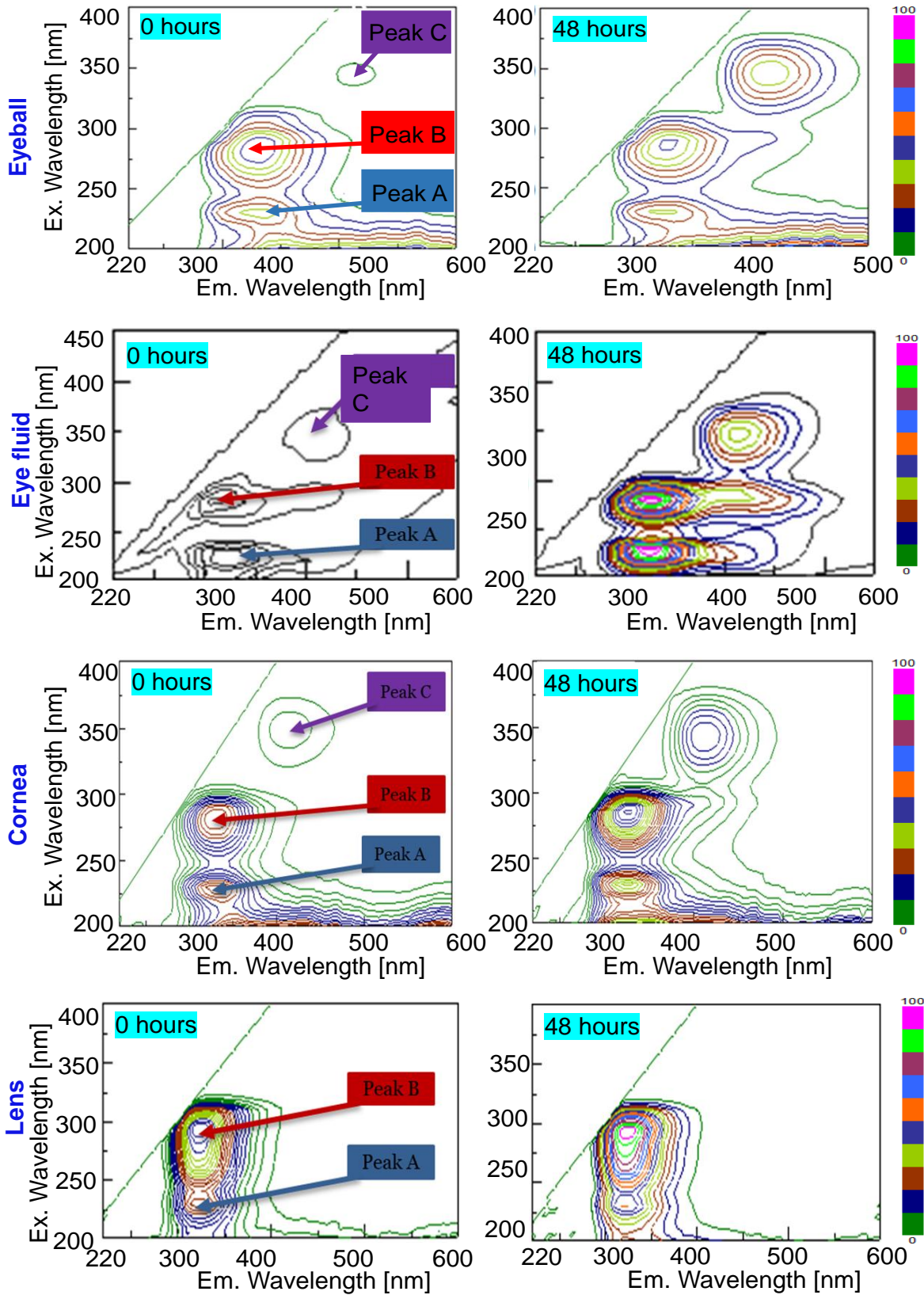
Fig. 4.5: EEM for different parts of the fish eyeball for Japanese dace fish.
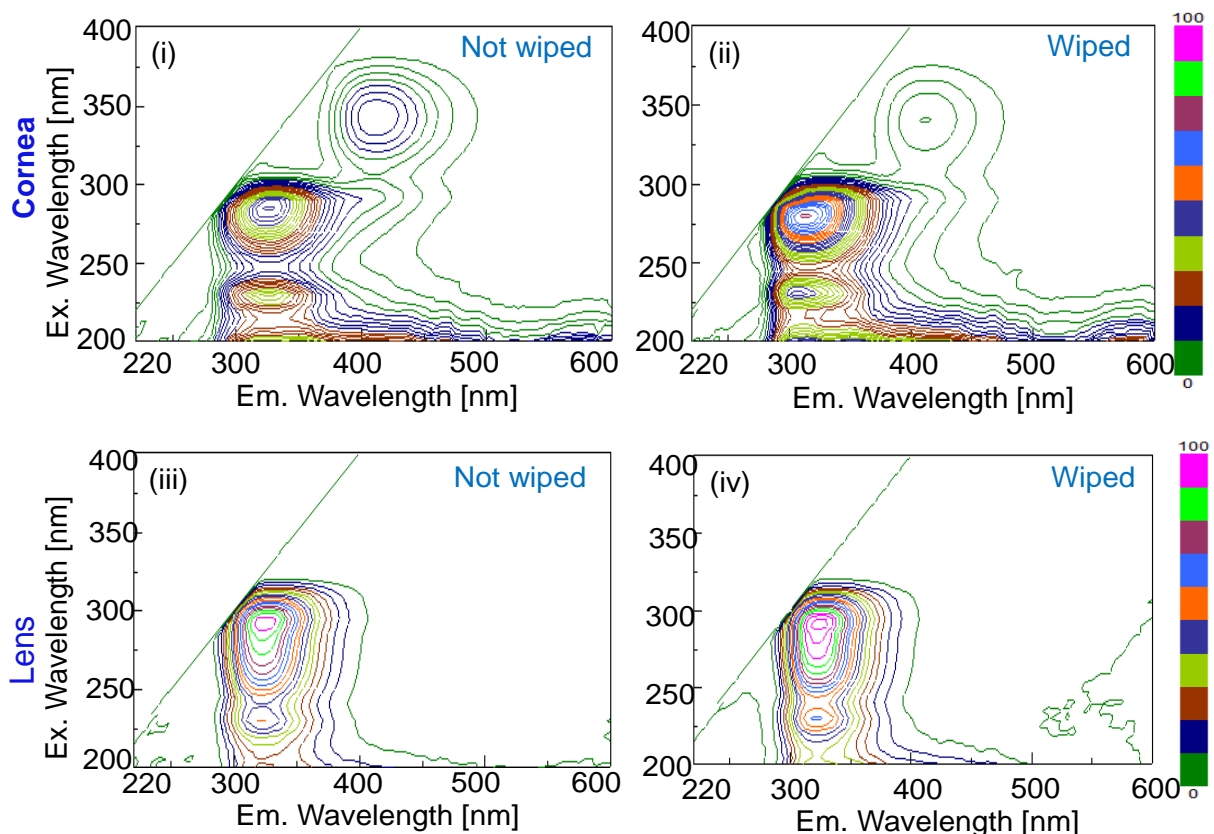
Fig. 4.6: EEM for dissected (i) Not cleaned Cornea, (ii) cleaned cornea, (iii) Not cleaned Lens, and (iv) cleaned Lens obtained from the Japanese dace fish eyeball.

UV-induced fluorescence Imaging

As reported by Murakoshi et al. (2013), the condition of fish eyes plays a critical role when it comes to consumer preference making decisions of whether to buy fish or not. The color changes of fisheyes after death are solely associated with the dynamic changes of organic compounds, like microorganism activity, protein-decomposition, and lipid oxidation. Fig. 4.8a and b show typical changes in fisheye color and fluorescence images for Japanese dace fish during storage at 4±1 °C. Within the visible range clear variation (brightness change) can easily be noted in the fluorescence images in comparison to normal color images. From the EEM data (see Fig. 4.2 above), the fluorescence peak C was located at about 350/415 nm, which is near the blue-color wavelength region. The 365 nm ultra-violet light emitting diode (UV-LED) used has a wider spectrum ranging between 345 nm and 395 nm (see Fig. 4.7) and therefore it can capture peak C characterized with excitations range of 310-375 nm. It therefore can track the fluorescence information changes, and since the range is near the blue color in the electromagnetic spectrum, the emissions from the eye

appear blue as seen in Fig. 4.8b. This is evident from image analysis results where R-, G- and B-channels increased gradually for both the pupil and iris as the freshness deteriorated during the storage (see Fig. 4.9a, b and c).
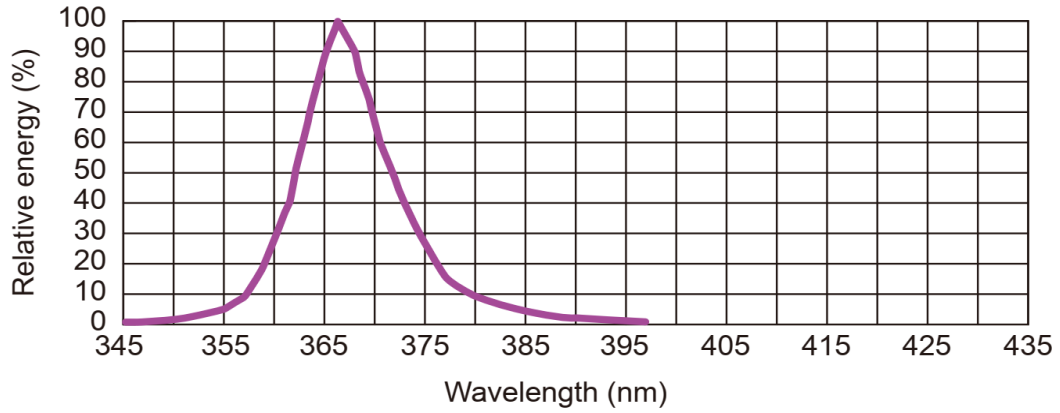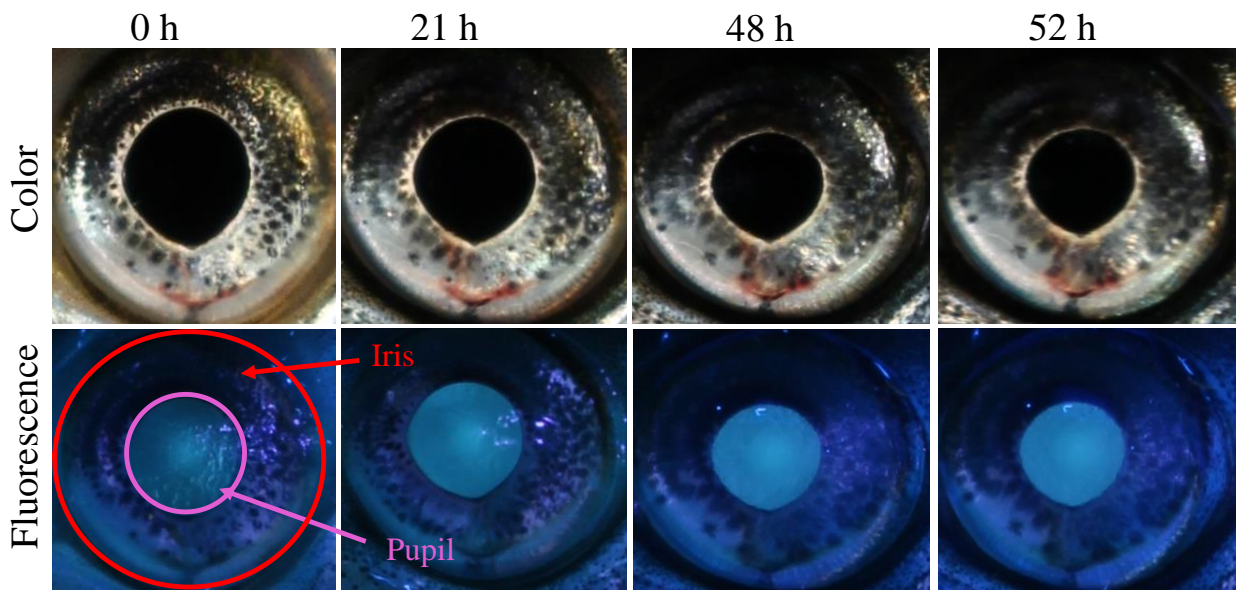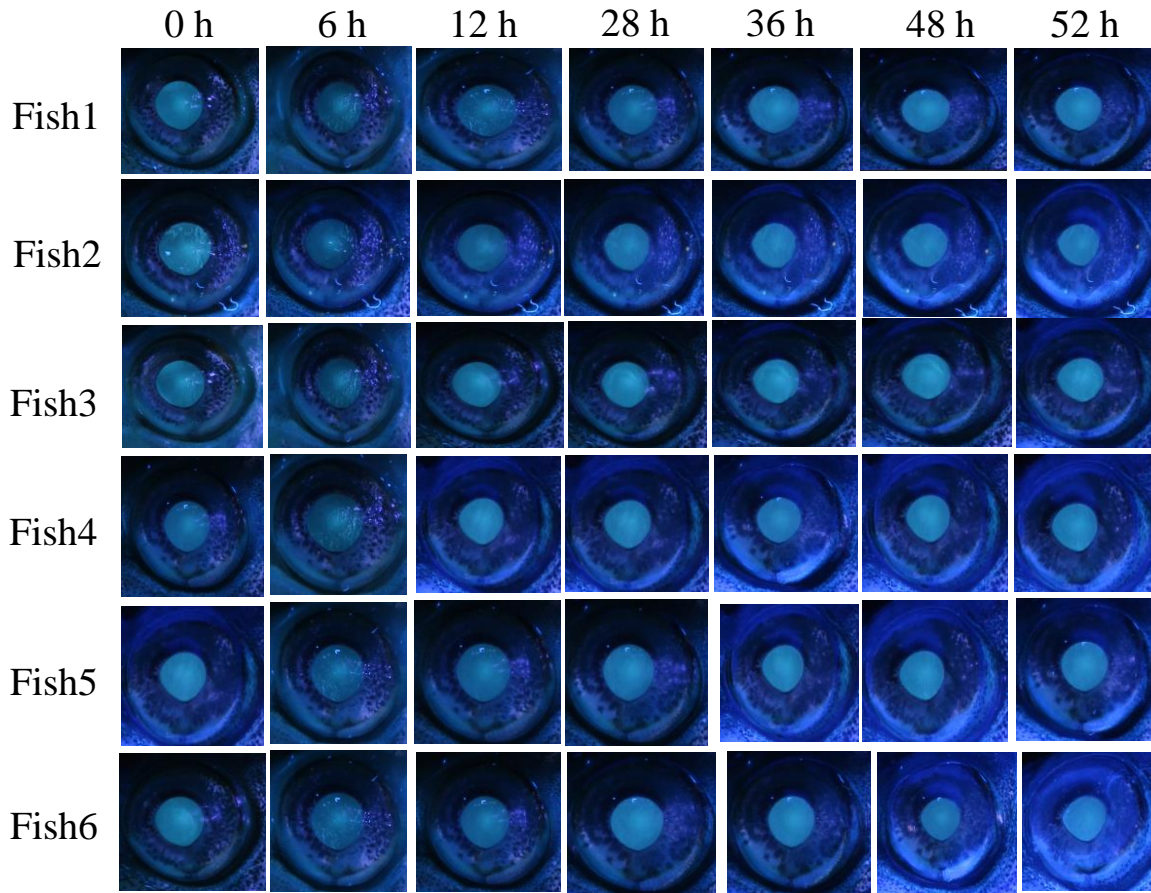

Fig. 4.7: Spectral properties for the 365 nm LED used in this experiment.

(a)

	0 h	6 h	12 h	28 h	36 h	48 h	52 h
Fish1							
Fish2							
Fish3							
Fish4							
Fish5							
Fish6							

(b)

Fig. 4.8. (a) Fisheye color and fluorescence images and (b) time series fluorescence color changes.

Fresh fishes are known for their dark and translucent nature of eyes, especially on the pupil part. From the common color images (Fig. 4.8a), the pupil part of the eye was black and bright in color the beginning of storage, however, this part slowly turned to dull and opaque gray as storage progressed. These changes in the pupil were purely associated with variations in morphological color resulting from fluorescence compounds and biochemical reactions taking place in the eye. In the iris are black pigments parts called melanophores controlled by enzymatic activities and they are responsible for pigmentation, through dispersion and aggregation. After the fish were killed, all biological activities stopped, and enzymatic processes degenerates slowly causing the melanophores to decline with time, hence they faded or bleached. For this reason, they were classified as physiological color changes. When both the morphological and physiological processes were combined, the result was observable color changes in the fisheye (pupil and iris) thus causing the blue color on fluorescence images to become brighter and brighter with time.

From the analysis of common color images, the results indicated no consistent; and when they were used in the prediction model, they gave R^2_{cv} of 0.84 and RMSECV of 5.3% (Table 4.1), this represented a lower correlation with respect to the freshness deterioration during storage. Therefore, this information was not used in the prediction model. However, from what was reported by Dowlati et al., (2013), on the gilthead sea bream (*Sparus aurata*) fisheye, L*a*b* color space changes for normal color images of fisheye showed a positive correlation with its freshness deterioration. In this research, the tendencies observed from the extracted image features (average RGB, HSV and L*a*b* values of iris and pupil parts) depicted a less strong correlation with freshness deterioration during storage. This could be explained by differences in fish species and/or ecological environmental conditions; red sea bream are saline water fish and Japanese dace are freshwater, hence their biological activities are present.

In the fluorescence images (Fig. 4.8b), there was more pronounced variation in brightness intensity for both the iris and pupil. In the EEM data, peak C has its excitation at 350 nm which is within the spectral array of the 365 nm UV-LED used to acquire the images. Therefore, the blue fluorescence is believed to be emanating from this peak. In earlier research investigating the fluorescence of Japanese dace fish eye-fluid, this peak (350/410 nm) was demonstrated to have the potential to track freshness deterioration during storage at 20 ± 1 ^{o}C (Liao et al., 2018). This clearly shows that the observed fluorescence in the images is coming from this peak C (350/415 nm).

The changes observed in the fluorescence images (increased brightness) could be attributed to internal and external chemical changes that produce organoleptic variations like color and appearance in fish after death (Masniyom, 2011), and vary with time as fish undergoes the spoilage stages. Usually, fish contains a lot of lipids and fatty acids, and some of the chemical processes include lipid oxidation, lipolysis and the interaction of the formed products with non-lipidic components, like proteins. For example, yellow pigments are formed when proteins and oxidized lipid react, which in turn are known to speed up the fish spoilage rates, when not stored at proper temperature; below 10 ^{o}C (Genigeorgis, 1985). Fish muscles are rich in long chain lipids with a largest percentage being polyunsaturated fatty acids which undergo a substantial oxidation during processing and storage. Color and texture modification are affected by lipid oxidation rates (Lie, 2001) in fish and it is a major quality problem. Thus, by monitoring the color changes, it is possible to quantify the oxidized lipids. Stoknes et al., (2004) reported that fatty acids and lipids are present in fisheyes and brain, and their breakdown during decomposition of fish can contribute to the

changes in fluorescence compounds within region C characterized by Uric acid. The breakdown of fatty acids in the fisheye can directly affect the degradation of ATP compounds and purine metabolism processes which lead to accumulation of uric acid during storage; thus, affecting color values obtained in our experiment. In general, the biochemical and physiological processes in the of fisheye produce the chemical and physical alterations which subsequently will affect their color changes. Therefore, color changes especially in fluorescence images can act as a primary indicator of freshness deterioration during storage, hence offering a non-destructive means of freshness evaluation.

During image analysis, all the color spaces; RGB, HSV and L*a*b* of the fluorescence images, were considered with the aim of developing a multivariate analysis model for predicting freshness. In this experiment, seven variables; R (red), G (green), B (blue), S(saturation), V (value), L* (lightness) and b* (bluish and yellowish) from both the pupil and iris (total fourteen) showed a linear relationship to freshness changes during storage, and therefore, they were adopted as independent input variables for regression modeling. A linear multivariate analysis tool was developed to investigate their relation to variations in freshness. From the RGB color model, R-, G- and B- values increased for both the iris and pupil parts as storage time progressed (see Fig. 4.9 a, b, c and Fig. 4.12 a, b, c). Changes in pupil lightness could be attributed to concomitant proportional increase of R-, G-, and B- channels (Chmiel et al., 2016). The Blue channel of RGB color space was used in the scatter plots below, because it is easier to visualize the changes from the fluorescence images and a correlation was developed with *K* values.

Fresh fishes are characterized by dark and translucent eyes (Shi et al., 2018). Saturation and b* channel values of both pupil and iris also decreased throughout the storage as seen from Fig. 4.10a and 4.11b for Iris and Fig. 4.13 i and 4.14 ii for Pupil). The reduction observed for S- and b* could be attributed to the reduction of the primary color elements in a color space. The V- and L*-channel values gradually increased during storage (see Fig. 4.10b and 4.11a for Iris and Fig. 4.13 ii and 4.14i for pupil). These outcomes agreed with findings reported by Balaban et al., (2014) and Balaban & Alçiçek (2015). The results significantly display important color changes associated with the fisheye between iris and pupil during storage. The differences in color increase the possibility that the consumer may make wrong decision when deciding the freshness fishes in the market.
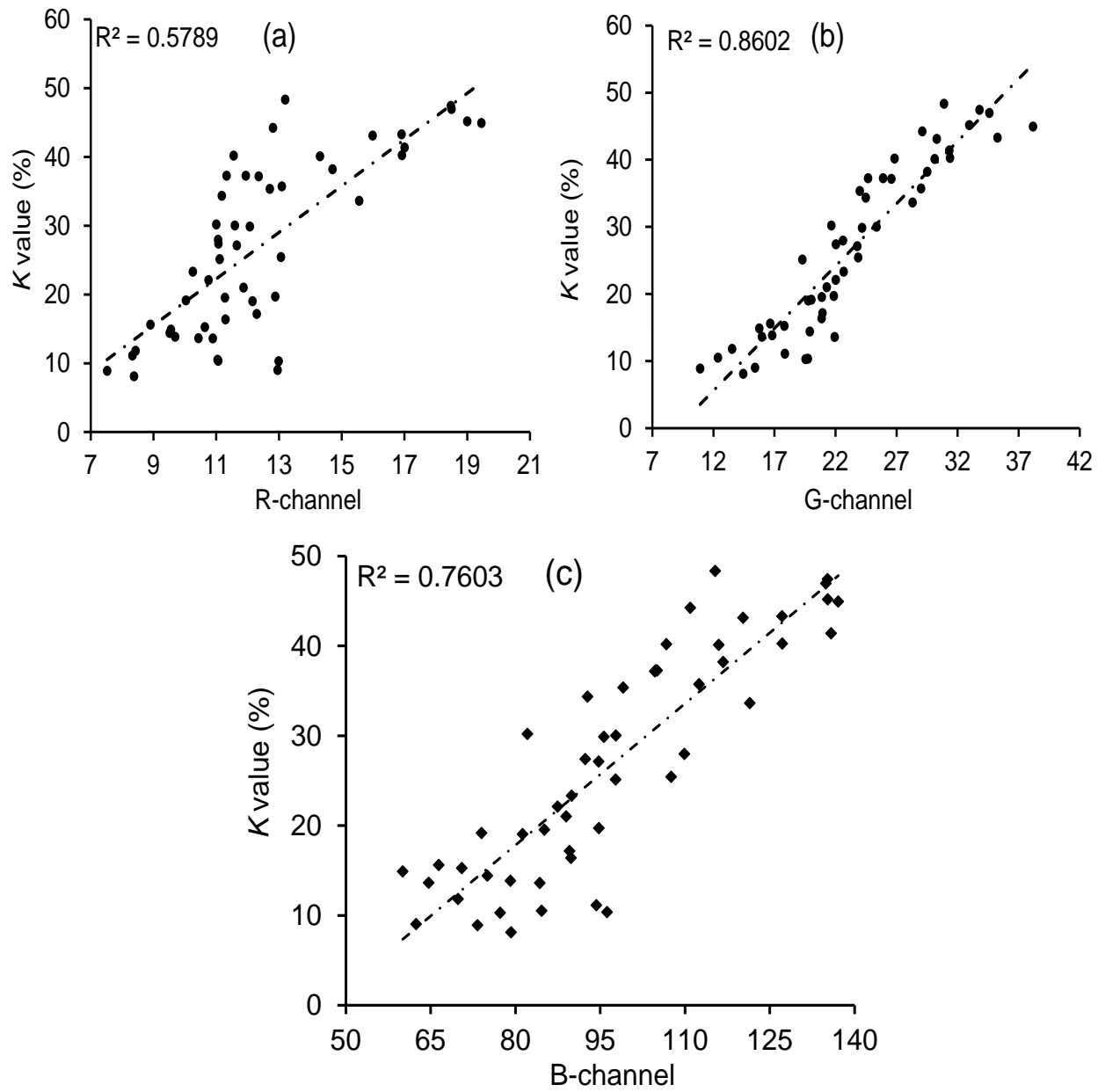
Fig. 4.9. (a) R-, (b) G- and (c) B- color values for fluorescence images of Iris part of the eye.
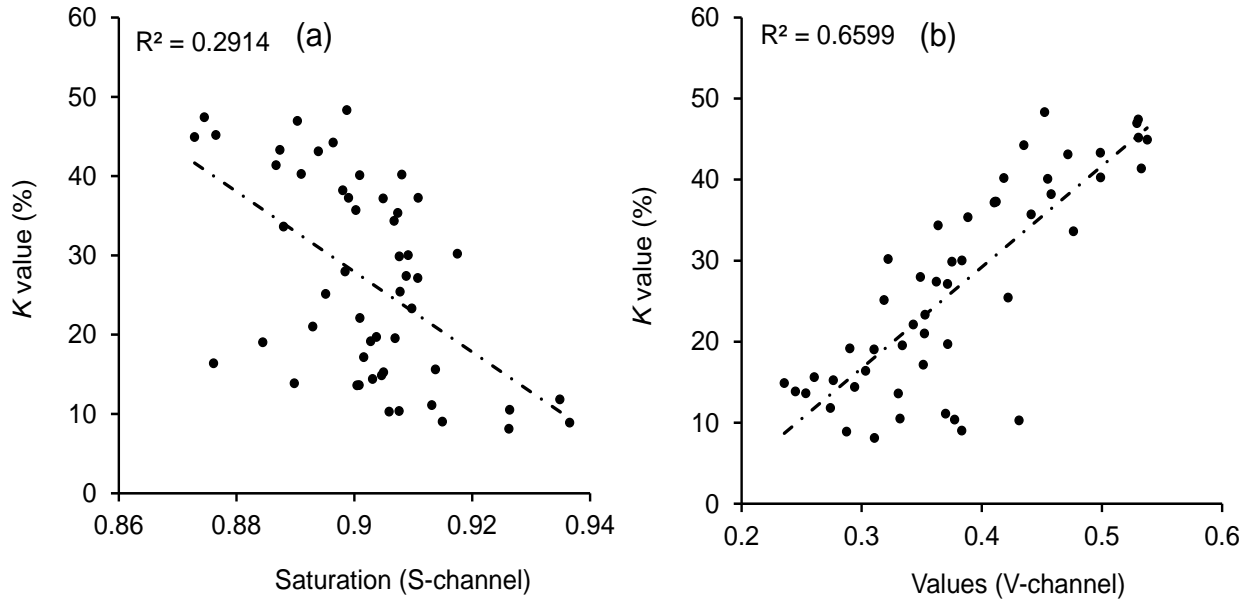
Fig. 4.10: (a) S- and (b) V-channel color values for fluorescence images of Iris part eye.
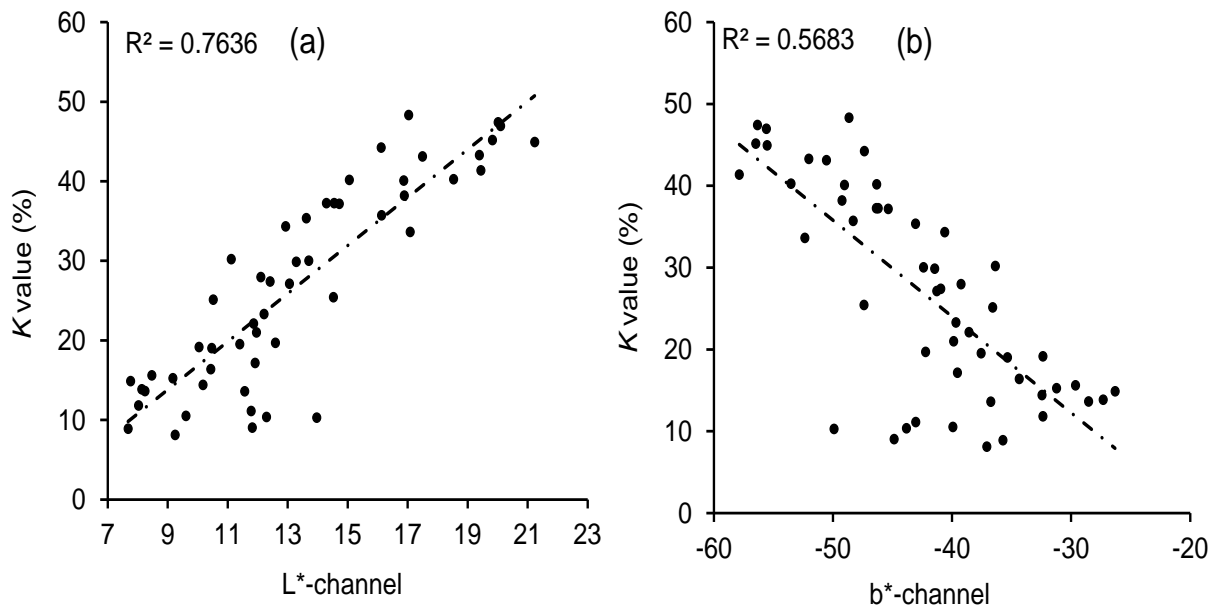

Fig. 4.11: (a) L* and (b) b* color values for fluorescence images of Iris part.
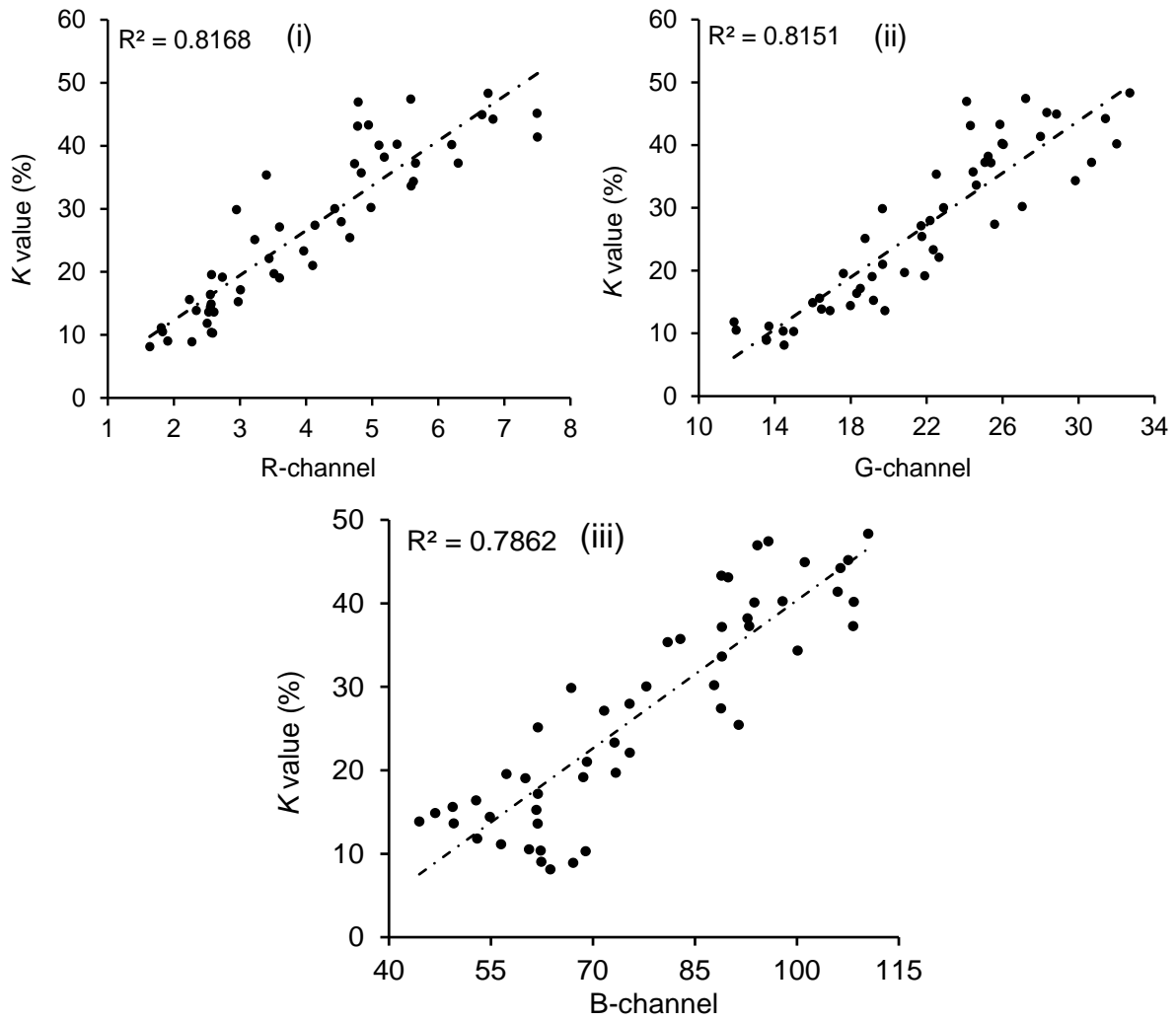
Fig. 4.12: (i) R-, (ii) G- and (iii) B-color values for fluorescence images of Pupil part.
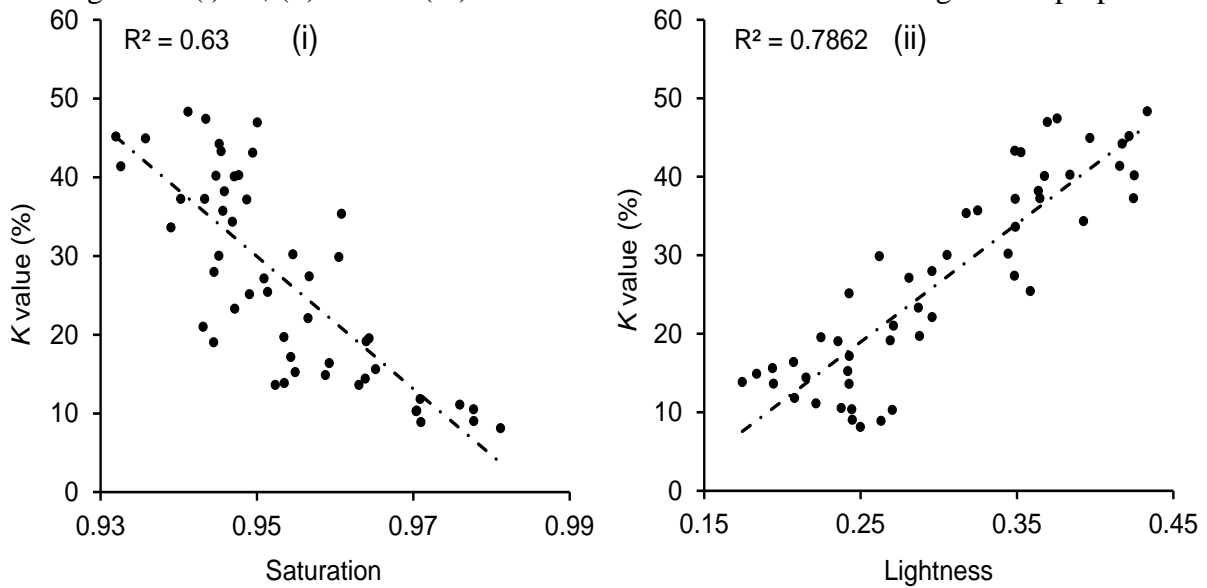

Fig 4.13: (i) S- and (ii) V-channel values for fluorescence images of Pupil part.
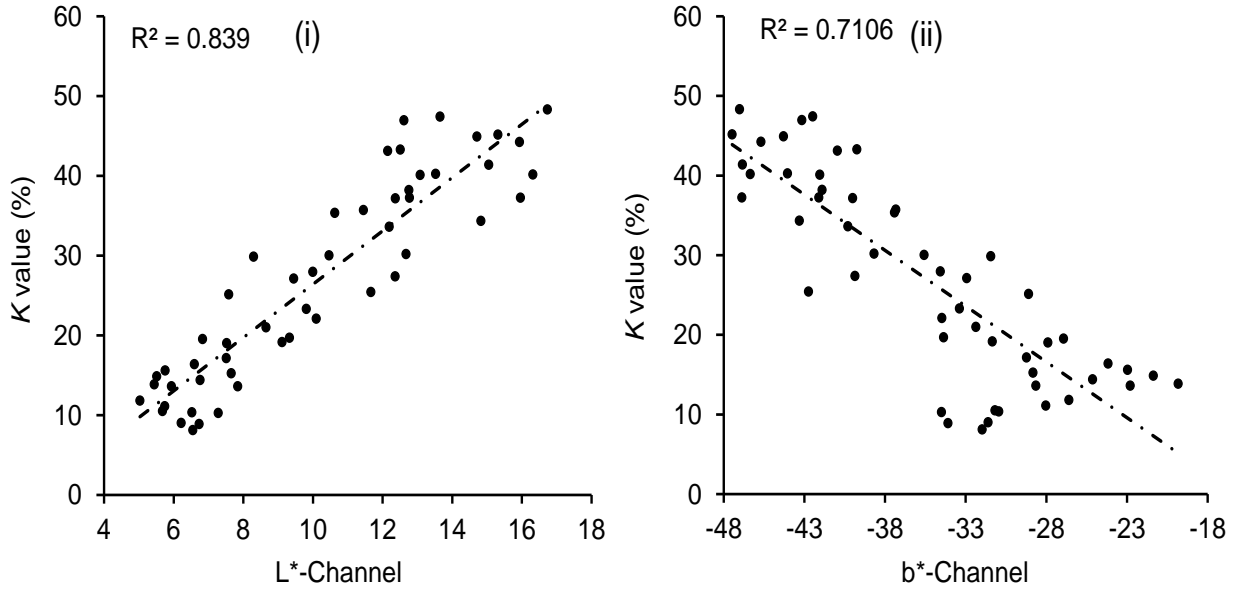
Fig. 4.14: (i) L* and (ii) b* values for fluorescence images of Pupil part.

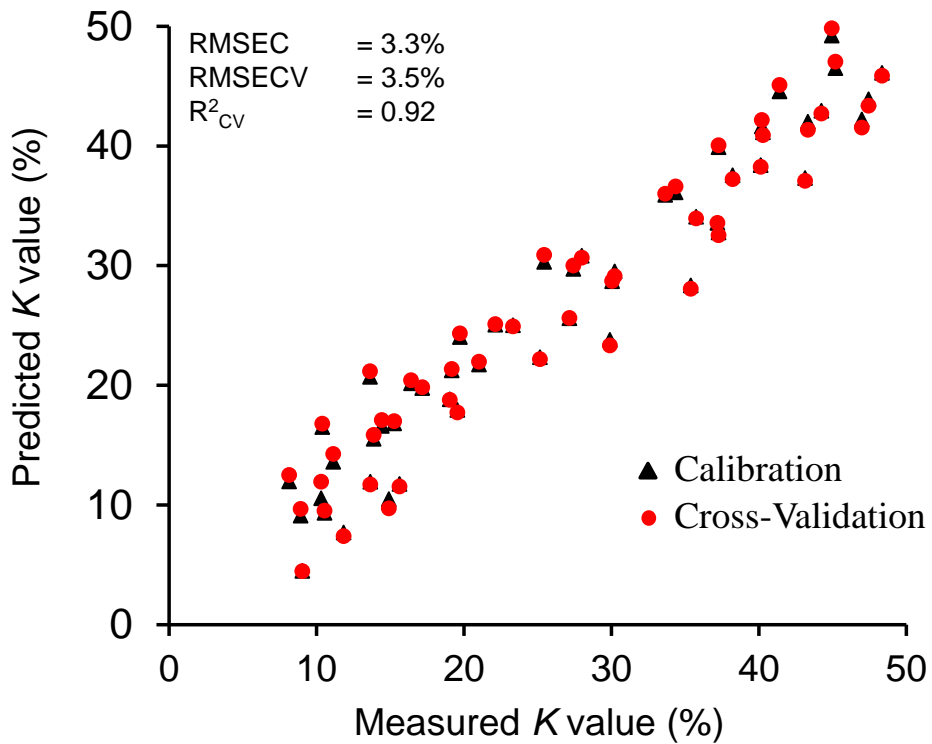**Prediction of K value for Ugui flesh**

Fig. 4.15: Relationship between measured and predicted K value of Japanese dace fish meat.

The fourteen individual variables (R, G, B, S, V, L* and b*) for both the pupil and iris, each separately produced a linear correlation with a coefficient of determination ranging between 0.68 and 0.79. All the significant variables were combined in the prediction model as input variables (predictors) and to generate the corresponding predicted K value as response variable. Eighteen variables (different color spaces; RGB, HSV, and L*a*b* for both the iris and pupil parts) univariate analysis has been conducted to select the variable with the highest correlation. Variables with $R^2 > 0.5$ were selected out of which fourteen (R, G, B, S, V, L* and b*) were adopted in the multivariate analysis. A correlation was made between measured and predicted K value variables and then relationship drawn by R^2 and RMSE. Leave-one-out cross-validation test analysis was used to evaluate the PLSR model to check for overfitting and data selection biasness; where this model gave R^2 of 0.92 and RMSE of 3.5% (see Fig. 4.15).

Table 4.1: PLS Regression model results for predicting K value of fish.

Spectra features	Variable		Latent Variables (LV)		Model	RMSE (%)	R^2
	Ex. (nm)	Em. (nm)	No. of Latent Variables	Explained Variance (%)			
Fluorescence Spectroscopy (EEM)	230 290 350	330 330 415	N/A	N/A	Univariate	12.4 9.7 5.7	0.13 0.44 0.75
Fluorescence Spectroscopy (EEM)	230 290 350 230, 290, 350	240-600 300-600 360-600 240-600	4	99.24 97.90 97.01 98.30	Multivariate	1.1 1.8 2.2 1.6	0.98 0.97 0.96 0.98
Image features	Color channels			Explained Variance (%)	Model	RMSECV (%)	R^2
Normal color images	R, G, B S, V L*, b* R, G, B, S, V, L*, b*		4	83.43 48.03 69.01 83.54	Multivariate	6.0 9.2 6.8 5.3	0.79 0.48 0.69 0.84
Fluorescence images (Ex. 365 nm)	R, G, B S, V L*, b* R, G, B, S, V, L*, b*			91.22 85.74 92.35 91.18		3.8 5.1 3.8 3.5	0.91 0.86 0.91 0.92

In Table 4.1 above, the univariate analysis results of spectra data for the peak with Ex/Em at 350/415 nm showed the for estimating fish freshness with R^2 of 0.75 and RMSE of 5.7%. These results were better than those of the other two peaks of Ex/Em at 230/330 nm and 290/330 nm. Multivariate analysis using PLS regression for spectra data indicates possibility of monitoring fish freshness changes using multiple wavelengths, with a lower RMSEV and higher R^2 values. However, this technique will be costly because it requires many sensors for receiving signals at different wavelengths.

Compared to fluorescence spectroscopy, fluorescence imaging system utilizes one excitation wavelength (365 nm). Despite the emissions being over a wide range of wavelength, all the signals can be captured using a common digital single lens reflex camera in the visible spectrum. This will reduce the cost of the equipment and making technique easier to apply machine vision. From the PLS regression model, results within acceptable limits were realized with R^2 for validation 0.92 with corresponding RMSECV values of 3.5%, respectively (see Fig. 4.15).

While the fluorescence imaging results look promising, it is good to highlight the drawbacks with technique: (i) the source of fluorescence observed in the images is not well defined; whether it comes from the surface (cornea) or inside the eye or both; (ii) the optical properties of fish eyes differ between individual fish, which can affect the error of the results; (iii) the exposure time of 4 seconds for taking the fluorescence images could be too long, especially for handheld devices while shortening the time could result in more noise in the images. A higher-powered light source to address this. The UV-cut filters used in this experiment have lower transmissivity of UV-light, hence higher transmission filters are necessary. Lastly, if there will be any variations in the LED intensity resulting from non-stabilized voltage source, it can be addressed by adopting a calibration protocol to standardize the machine vision system using a standard calibration plate.

Even given the above, this technique has the potential to be used in online monitoring systems. If it is installed in an autonomous refrigeration system for household and commercial use, it updates on the freshness status of the fish. In return, there will be less wastage of fish (consumption prior to spoil).

4.5 Conclusions

In the supermarkets, fish purely depend on the color of the fisheye in guessing the freshness condition of intact fish before deciding to buy. The result from this experiment confirms that there are indeed significant changes that takes place in the fisheye, and this demonstrates the great potential for non-destructive freshness evaluation of whole fishes. With the great advancement in smart technologies like smartphones, integrating these gadgets with UV light will greatly help consumers to decide freshness level of fish objectively by just illuminating the eyes and capturing the eye images and observing them. With the discovery of internet of things (IoT) and artificial intelligence (AI), the UV-based smartphone imaging technique can be synchronized with simple phone-based algorithms/programs/applications for quick image processing. If these programs are already calibrated with K value of different fish (with an option of selecting the type of fish), consumers will quantitatively know the freshness of whole/intact fish by eye images. This is likely to save a lot of time spent in the supermarket thus shaping up the vision of Society 5.0.

REFERENCES

Balaban, M.Ö., Alçiçek, Z., 2015. Use of polarized light in image analysis: Application to the analysis of fish eye color during storage. LWT - Food Sci. Technol. 60, 365–371. https://doi.org/10.1016/j.lwt.2014.09.046

Balaban, M.O., Stewart, K., Fletcher, G.C., Alçiçek, Z., 2014. Color change of the snapper (*Pagrus auratus*) and gurnard (*Chelidonichthys kumu*) skin and eyes during storage: Effect of light polarization and contact with ice. J. Food Sci. 79, E2456–E2462. https://doi.org/10.1111/1750-3841.12693

Cheng, J.H., Dai, Q., Sun, D.W., Zeng, X.A., Liu, D., Pu, H. Bin, 2013. Applications of non-destructive spectroscopic techniques for fish quality and safety evaluation and inspection. Trends Food Sci. Technol. https://doi.org/10.1016/j.tifs.2013.08.005

Cheng, J.H., Sun, D.W., Qu, J.H., Pu, H. Bin, Zhang, X.C., Song, Z., Chen, X., Zhang, H., 2016. Developing a multispectral imaging for simultaneous prediction of freshness indicators during chemical spoilage of grass carp fish fillet. J. Food Eng. 182, 9–17. https://doi.org/10.1016/j.jfoodeng.2016.02.004

Chmiel, M., Słowiński, M., Dasiewicz, K., Florowski, T., 2016. Use of computer vision system (CVS) for detection of PSE pork meat obtained from m. semimembranosus. LWT - Food Sci. Technol. 65, 532–536. https://doi.org/10.1016/j.lwt.2015.08.021

Dale, N., 1994. National research council nutrient requirements of poultry — ninth revised edition (1994), Journal of Applied Poultry Research. https://doi.org/10.1093/japr/3.1.101

Dalgaard, P., 1995. Modelling of microbial activity and prediction of shelf life for packed fresh fish. Int. J. Food Microbiol. 26, 305–317. https://doi.org/10.1016/0168-1605(94)00136-T

Dowlati, M., de la Guardia, M., Dowlati, M., Mohtasebi, S.S., 2012. Application of machine-vision techniques to fish-quality assessment. TrAC - Trends Anal. Chem. https://doi.org/10.1016/j.trac.2012.07.011

Dowlati, M., Mohtasebi, S.S., Omid, M., Razavi, S.H., Jamzad, M., De La Guardia, M., 2013. Freshness assessment of gilthead sea bream (Sparus aurata) by machine vision based on gill and eye color changes. J. Food Eng. 119, 277–287. https://doi.org/10.1016/j.jfoodeng.2013.05.023

Dufour, E., J.P. Frencia, A., Kane, E., 2003. Development of a rapid method based on front-face fluorescence spectroscopy for the monitoring of fish freshness. Food Res. Int. 36, 415–423.

https://doi.org/10.1016/S0963-9969(02)00174-6

Elmasry, G., Nagai, H., Moria, K., Nakazawa, N., Tsuta, M., Sugiyama, J., Okazaki, E., Nakauchi, S., 2015. Freshness estimation of intact frozen fish using fluorescence spectroscopy and chemometrics of excitation-emission matrix. Talanta 143, 145–156. https://doi.org/10.1016/j.talanta.2015.05.031

Genigeorgis, C.A., 1985. Microbial and safety implications of the use of modified atmospheres to extend the storage life of fresh meat and fish. Int. J. Food Microbiol. https://doi.org/10.1016/0168-1605(85)90016-9

Gil, L., Barat, J.M., Escriche, I., Garcia-Breijo, E., Martínez-Máñez, R., Soto, J., 2008. An electronic tongue for fish freshness analysis using a thick-film array of electrodes. Microchim. Acta 163, 121–129. https://doi.org/10.1007/s00604-007-0934-5

Huang, X., Xin, J., Zhao, J., 2011. A novel technique for rapid evaluation of fish freshness using colorimetric sensor array. J. Food Eng. 105, 632–637. https://doi.org/10.1016/j.jfoodeng.2011.03.034

Itoh, D., Koyachi, E., Yokokawa, M., Murata, Y., Murata, M., Suzuki, H., 2013. Microdevice for On-Site Fish Freshness Checking Based on K-Value Measurement. Anal. Chem. 85, 10962–10968. https://doi.org/10.1021/ac402483w

Kohavi, R., 1995. A Study of Cross-Validation and Bootstrap for Accuracy Estimation and Model Selection. Int. Jt. Conf. Artif. Intell.

Koutsoumanis, K., Nychas, G.J.E., 2000. Application of a systematic experimental procedure to develop a microbial model for rapid fish shelf life predictions, in: International Journal of Food Microbiology. pp. 171–184. https://doi.org/10.1016/S0168-1605(00)00309-3

Lawaetz, A.J., Stedmon, C.A., 2009. Fluorescence intensity calibration using the Raman scatter peak of water. Appl. Spectrosc. 63, 936–940. https://doi.org/10.1366/000370209788964548

Liao, Q., Suzuki, T., Shirataki, Y., Kuramoto, M., Kondo, N., 2018. Freshness related fluorescent compound changes in Japanese dace fish (Tribolodon hakonensis) eye fluid during storage. Eng. Agric. Environ. Food 11, 95–100. https://doi.org/10.1016/j.eaef.2018.01.001

Lie, Ø., 2001. Flesh quality – the role of nutrition. Aquac. Res. 1, 341–348.

Masniyom, P., 2011. Deterioration and shelf-life extension of fish and fishery products by modified atmosphere packaging, Songklanakarin Journal of Science and Technology. Mueang, Pattani. https://doi.org/rdo.psu.ac.th/sjstweb/journal/33-2/0125-3395-33-2-181-

192.pdf

Murakoshi, T., Masuda, T., Utsumi, K., Tsubota, K., Wada, Y., 2013. Glossiness and Perishable Food Quality: Visual Freshness Judgment of Fish Eyes Based on Luminance Distribution. PLoS One 8. https://doi.org/10.1371/journal.pone.0058994

Nie, S., Al Riza, D.F., Ogawa, Y., Suzuki, T., Kuramoto, M., Miyata, N., Kondo, N., 2020. Potential of a double lighting imaging system for characterization of "Hayward" kiwifruit harvest indices. Postharvest Biol. Technol. 162, 111113. https://doi.org/10.1016/j.postharvbio.2019.111113

Özogul, Y., Özyurt, G., Özogul, F., Kuley, E., Polat, A., 2005. Freshness assessment of European eel (Anguilla anguilla) by sensory, chemical and microbiological methods. Food Chem. 92, 745–751. https://doi.org/10.1016/j.foodchem.2004.08.035

Shi, C., Qian, J., Han, S., Fan, B., Yang, X., Wu, X., 2018. Developing a machine vision system for simultaneous prediction of freshness indicators based on tilapia (Oreochromis niloticus) pupil and gill color during storage at 4 °C. Food Chem. 243, 134–140. https://doi.org/10.1016/j.foodchem.2017.09.047

Stoknes, I.S., Økland, H.M.W., Falch, E., Synnes, M., 2004. Fatty acid and lipid class composition in eyes and brain from teleosts and elasmobranchs. Comp. Biochem. Physiol. - B Biochem. Mol. Biol. 138, 183–191. https://doi.org/10.1016/j.cbpc.2004.03.009

CHAPTER V: EVALUATING JAPANESE DACE (*Tribolodon hakonensis*) FISH FRESHNESS USING MULTISPECTRAL IMAGES FROM VISIBLE AND UV EXCITED FLUORESCENCE

5.1 Introduction

The demand for fish and its related products in the human diet has been increasing significantly in the recent past, as reported by Dale (1994). Total fish consumption, as well as the number of consumers has been sharply increasing compared to other sources of meats due to the health benefits of fish meat (protein) such as lower cholesterol levels and higher polyunsaturated fatty acids. However, fish is a highly perishable food, which can easily get spoiled and losing its freshness quickly. Hence, storage and handling methods like drying, refrigeration and deep-freezing have become crucial towards ensuring product quality and consumer safety.

Fish spoilage involves multi-processes/factors implicating physical, microbiological and chemical mechanisms and interrelated with changes in color, texture, protein degradation, oxidation of lipids and microbial spoilage (Alishahi & Aïder, 2012; Ghaly, Dave, Budge, & Brooks, 2010). Chemical processes have been widely used to define the freshness indices of meat products. This process involves tracking the changes of total volatile basic nitrogen (TVB-N) (Castro, Padrón, Cansino, Velázquez, & Larriva, 2006). *K* value index is a biochemical process to assess fish freshness based on adenosine triphosphate (ATP) degradation. The *K* value measures degradation of ATP and its metabolites (Cheng et al., 2016; Lowe, Ryder, Carragher, & Wells, 1993), and expresses it as a percentage. These two indices can precisely measure freshness during the inspection process; however, they are time-consuming, laborious, destructive, and costly (require highly skilled personnel). Hence, not suitable for rapid and non-destructive monitoring systems. Therefore, developing a rapid and non-destructive examination imaging system to monitor fish freshness loss will be of great importance in the fish industry.

Recently, the merger between spectroscopic techniques and computer vision into one system has become a center of interest for several kinds of research (Jackman, Sun, & Allen, 2009; Jackman, Sun, Du, & Allen, 2009; Wang & Sun, 2002; Wu & Sun, 2013). Multispectral imaging as an advanced and powerful tool has been explored for rapid and nondestructive evaluation of the quality and consumer safety for agricultural products (Chen, Chao, & Kim, 2002; Cheng et al., 2013; Liu, Sun, & Zeng, 2014; Omwange et al., 2020; Pu, Kamruzzaman, & Sun, 2015; Wu &

Sun, 2013). From previous studies, all researches focused on single freshness indicators with either single selected or full range selected wavelengths (Cheng et al., 2016; Menesatti, Costa, & Aguzzi, 2010). In a normal multispectral reflectance image, the reflection intensity, which is negatively correlated with absorption, is measured at each pixel. Hyperspectral images have been reported to have higher accuracy in classifying between fresh and stale fish samples (Cheng & Sun, 2014), but they require expensive sensors and higher computational load. Since fluorescence spectroscopy has higher selectivity and sensitivity, a cheap imaging system can be built using a few selected excitation wavelengths within ultraviolet to visible, and simple sensors (cameras) for multispectral imaging fish.

The main objective of this study was to evaluate the viability of using multispectral images from visible and UV excited fluorescence for selected wavelengths identify by partial least square regression (PLSR) to assess Japanese dace (*Tribolodon hakonensis*) fish during storage.

5.2 Materials and Methods

Sample preparation

Japanese dace fish were purchased in December 2020 from the Hamaichi Bait Company in Wakayama Prefecture, Japan, where they were bred and raised for about ten months. The fish were delivered alive in a plastic bag with water, and then they were kept in well aerated acrylic tanks at Kyoto University, Japan. During the experiment, 63 fish with an average length 120 ± 20 mm were selected, killed and stored in the refrigerator set at 4 ± 1 ℃ for about 2 hours while the body temperature reached equilibrium with the storage compartment before the commencement of the experiment. Sixty-three measurements were obtained (nine data points with seven fish used at every measurement). At each interval of measurement frequency, three experiments were carried out: imaging (normal color and UV-imaging) of an intact fish, fluorescence excitation-emission matrix (EEM) of the eyeball and surface containing scales (skin), and biochemical/electrophoresis analyses to examine the K value of meat for a period of 48 hours; Fourty-eighty hours is the recommended shelf life for this fish under this storage condition (Omwange et al., 2020). An EEM is a plot with three axes of excitation wavelength, emission wavelength and fluorescence intensity.

Excitation Emission Matrix (EEM) measurement

Two EEM was acquired from every sample (eyeball and scale). The eyeball was removed from the eye socket, and the surface containing scales were cut form the fish's dorsal part. They were then directly placed in a cell holder separately for the acquisition of raw EEM. For the EEM, front-facing fluorescence spectroscopy technique was adopted using a spectrofluorometer (FP-8300, JASCO Co., Tokyo, Japan) with parameters: excitation range (200-600 nm); and emission range (220-600 mm); photomultiplier tubes (PMT) was set at low sensitivity with a scan speed of 5,000 nm min^{-1}; and response time of 50 ms. Ex/Em measurements were recorded at 5 nm for the interval and bandwidths respectively. The experiment was carried out at room temperature (20±1 °C).

The recorded raw EEM was corrected by standardizing the light source and response detector using the calibration spectra protocol as outlined by JASCO Company. The corrected EEM was converted from the arbitrary unit (A.U) to Raman units (R.U) to prevent instrumental effects/biases on the results (Lawaetz & Stedmon, 2009)**.** Fourteen fish EEM data (7 for the eyeball and 7 from the surface containing scales) at each sampling interval (4 and 12 hours) during the 48 hours storage period. The fluorescence intensity acquired from the fish eyeball was later used for building the *K* value prediction model, and selection of the appropriate wavelength for multispectral imaging. To optimize the imaging technique, key excitation wavelengths were selected based on the EEM acquired from the eyeball and surface containing scales. A simple imaging system was constructed based on this EEM information.

Acquisition and processing of images

The images of fish (covering at least 90% of the body from the head) were taken in a dark room using EOS DSLR (kiss x7, Color Inc., Japan) for white, 395 nm and 365 nm LEDs and UV-camera (ARTCAM-407UV-WOM) for 280 nm LED (see Fig. 5.1 (a) and (b). The LEDs were characterized with different images, such as reflectance images from white lighting and fluorescence images excited from 280, 365 and 395 nm. The EOS DSLR camera was placed at 250 mm above the sample surface with a focal length of 55 mm and the UV camera was mounted at 300 mm above the sample. All images were taken with same F-number (f/6.3) and ISO (100). The sample was illuminated using two white bar LEDs (LDL2-80X16SW2, CCS Inc. Japan) with a shutter speed of 1/5 s for normal color images; two 365 nm UV bar LEDs (LDL-71X12UV2-

365-N, CCS Inc. Japan) with a shutter speed of 2.5 s; two 395 nm ring LEDs (HLV-24VL395-4WNRBTNJ, CCS Inc. Japan) with a shutter speed of 1/4 s and a 280 nm ring (LED (LDR2-100UV2-280-W, CCS Inc. Japan) with software filter parameters (brightness: 50, contrast: 0, sharpness: 11, and gamma: 80; global gain 350 and shutter speed 0.1 s). The distance between the sample and the lighting devices was set as; 160 mm (white bar LEDs), 180 mm (365 nm bar LEDs); 120 mm (395 nm LED), for the UV-imaging system, the 280 nm LED was placed 250 mm above the sample. The color camera was equipped with a polarizing filter (PL) to prevent any form of direct reflection from the samples.
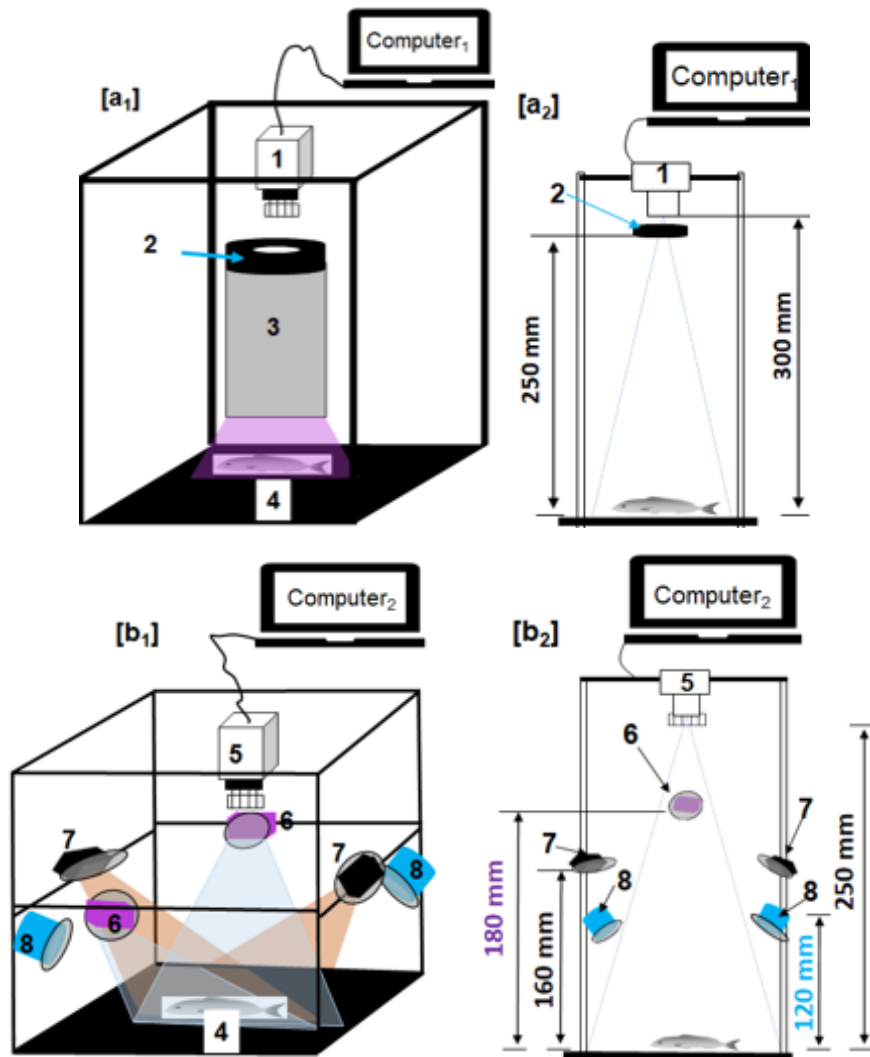

Fig. 5.1: Image acquisition systems: (a$_1$) 3D UV camera imaging system with LED, (a$_1$) 2D UV camera system showing respective LED and camera heights. (b$_1$) 3D color camera imaging system with LEDs, (b$_2$) 2D color camera system with LEDs and camera heights. The numbers denote: 1. UV-camera, 2. 280 nm ring LED, 3. Shield, 4. Sample surface, 5. Color camera, 6. 365 nm bar LED, 7. White bar LED and 8. 395 nm LED.

Image processing was carried out using MATLAB software (MATLAB 9.5 R2020b, MathWorks, USA). The regions of interest (ROIs) comprised of the eye (pupil and iris), belly (fish bottom side), and dorsal part (characterized with more surface containing scales). The eye part was automatically selected using '*imfind circles*' function in MATLAB, whereas the belly and dorsal parts were segmented using grey values for B-channel from images from 365 nm lighting device with a program in MATLAB software. Subsequently, the ROI was masked then overlaid with the corresponding images from different lighting devices (white, 365 nm and 395 nm). Average R, G and B values for RGB color space was extracted for analysis. Data processing for all the experimental data was carried out as shown in Fig. 5.2.
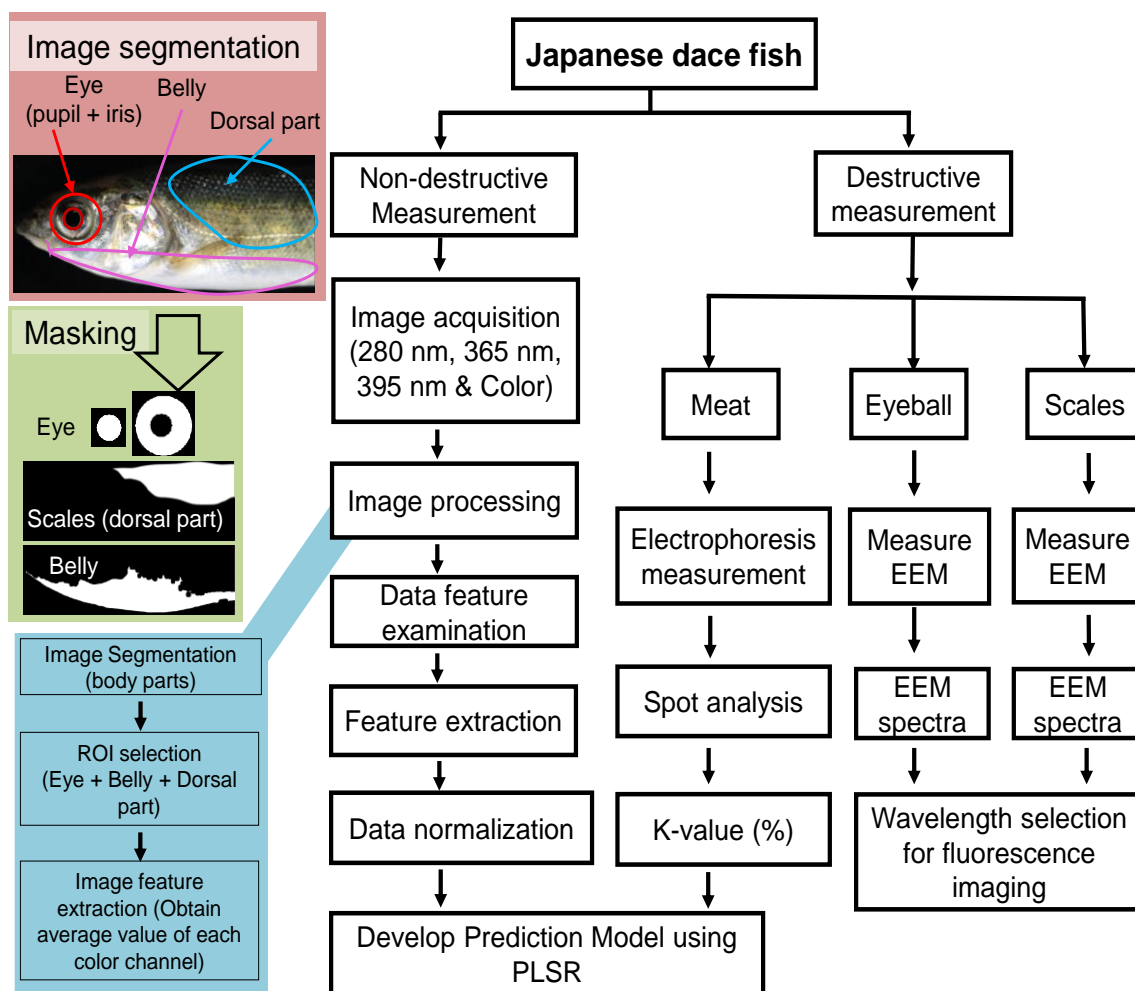

Fig. 5.2. Description of flow diagram image processing and multivariate analysis.

5.3 Multivariate analysis for predicting freshness

Partial least square regression (PLS-R) analysis was used in evaluating the appropriateness and reliability of multispectral imaging in predicting the *K* value of fish. MATLAB R2020b software (MathWorks, USA) was adopted for the PLS-R analysis and building the fish freshness prediction model using imaging data (eyes, belly, and dorsal part) with the meat freshness indices (*K* value) measured by chemical analysis. The accuracy of this model between measured and predicted *K* value was evaluated using root mean square error as seen in the equation (1) below. The coefficient of determination, R^2 and relative mean square error, RMSE were used to identify a good model with higher R^2 and lower RMSE. This research adopted a leave-one-out cross-verification of the model. The calculation formula is as below with eighty-five variables made up of different combination of variables.

$$RMSE = \sqrt{\frac{1}{n}\sum_{i=1}^{n}(y_{predicted} - y_{measured})^2} \ \dots \ (\text{Eqn } 5.1)$$

5.4 Results and Discussion

Electrophoresis (K value)

The *K* value for Japanese dace fish increased dramatically from 8% to about 40% when stored under 4 ±1 °C for 48 hours. Very fresh fish meat has a *K* value of about 8%; however, due to sample variability and difference in biological processes, some can start 9% or 10%. Additionally, the time (about two hours) in the refrigerator after killing (before measurement commenced) can also affect the initial *K* values because the biological activities for individual fish samples do not stop at the same time after killing. Kato et al. (2009) classified fish freshness into three categories; prime fresh (*K* value <20%), fresh stage (20%>*K* value<40%) and spoiled (*K* value >40%). Prime fresh defines the fish meat can be consumed raw (without cooking); fresh stage represents the fish meat which can be consumed only after cooking; spoiled fish is not safe for consumption hence should be discarded. In this experiment, the Japanese dace stayed within the prime fresh stage for about 20 hours with a *K* value of <20%, whereas the rest of the fish had attained the 'fresh stage' characterized with K value >20% but less than 40%.

Fluorescence

i. EEM for fish Eyeball

The EEM spectra obtained from the fisheye ball identified three fluorescence peaks A, B and C with excitations at 230 nm, 280 nm and 350 nm, and corresponding emissions at 330 nm for peaks A and B, and 415 nm for peak C, as seen in Fog. 5.3. These fluorescence peaks were similar to those reported by Liao et al. (2018) and Omwange et al. (2020) for Japanese dace fisheye fluid and eyeballs, respectively. Peaks A and B are suspected to be aromatic amino acids (tyrosine and tryptophan) (Liao et al., 2018). The excitation and emission wavelength pair for peak C at 350/415 nm is associated with uric acid (Lamkin, Unruh, & Pomerranz, 1991). This was later confirmed by Liao et al., (2018), who measured pure uric acid and compared with the HPLC results from fisheye fluid where the peak depicted similar characteristics. The fact that eye fluid and an intact eyeball shows similar fluorescence features, then it is easier to employ non-destructive measurement methods to track their changes during storage.
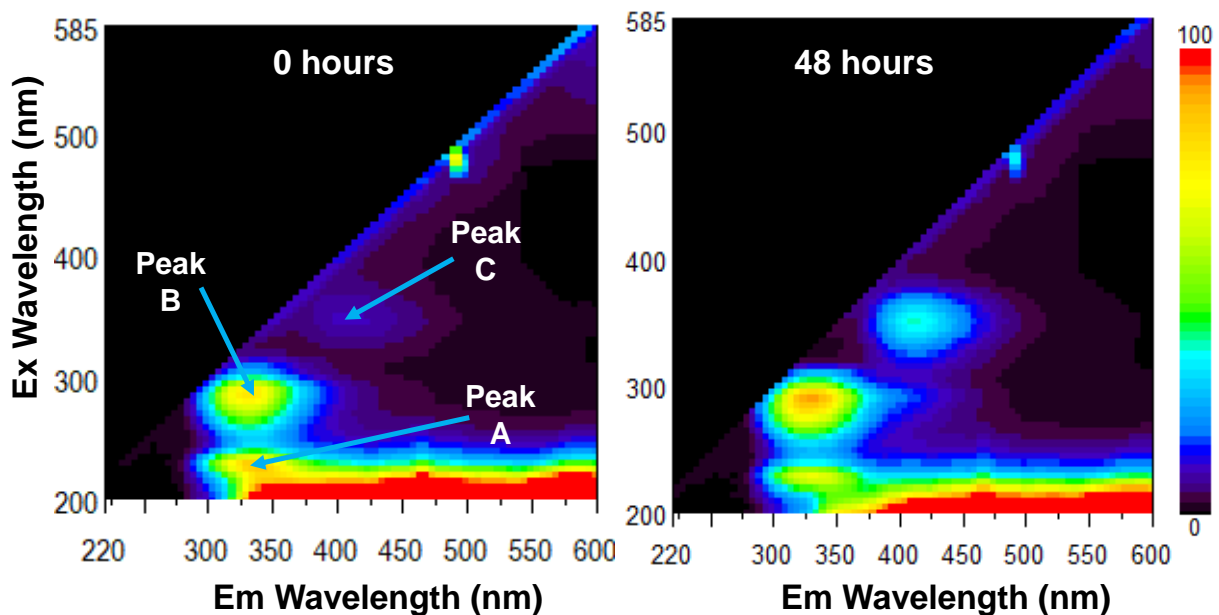

Fig. 5.3: Typical Eyeball EEM for Japanese dace fish.

ii. EEM for fish surface containing scales

Two peaks with clear excitation/emission matrices centered at X (280/330 nm) and Y (350/415 nm) were evident with Japanese dace fish surface containing scales (see Fig. 5.4). Previous studies have linked the fluorescence signal for peak X to protein compounds coming from free tyrosine residuals (Lakowicz, 2006); and it has been reported that fish surface containing

scales contain about 40 - 80% organic protein, made up of 24% (ichthylepidin) and 76% (collagen) (Masood et al., 2015). The organic proteins with residuals from tyrosine are responsible for the fluorescence intensity for peak X. The fish's body is characterized by a mucus layer covering the scale surface. This mucus layer is a complex fluid made up of protein macromolecules (Ángeles Esteban, 2012), and it is responsible for defending the fish by forming a biological barrier (Park et al., 2014). The mucus is characterized by strong absorption within the protein region, and this is caused by the presence of tyrosine residues which forms an essential component in the fish's mucus layer (Chong, Tham, Foo, Lam, & Chong, 2005; Oda et al., 1984).

The second peak Y detected in the surface containing scales with excitation/emission centered at 350/415 nm is associated with type I collagen (reduced form of vitamins or nicotinamide adenine dinucleotide; NADH) (Villette, Pigaglio-Deshayes, Vever-Bizet, Validire, & Bourg-Heckly, 2006). For instance, Ikoma et al. (2003) indicated the presence of type I collagen strands on red sea bream (*Pagrus majo*r) fish surface containing scales with partially hardened internal layers and well-calcified external layers. In their research, they confirmed that the infrared spectra for internal layer collagen of their sample is like the collagen isolated from surface containing scales of other fish species. Georgakoudi et al. (2002) alluded that untreated surface containing scales may contain NADH or vitamins present in the mucus layer, and this could enhance the intensity for peak collagen substances. With this we can affirm that since Japanese dace fish contain surface containing scales, thus the origin of peak Y.
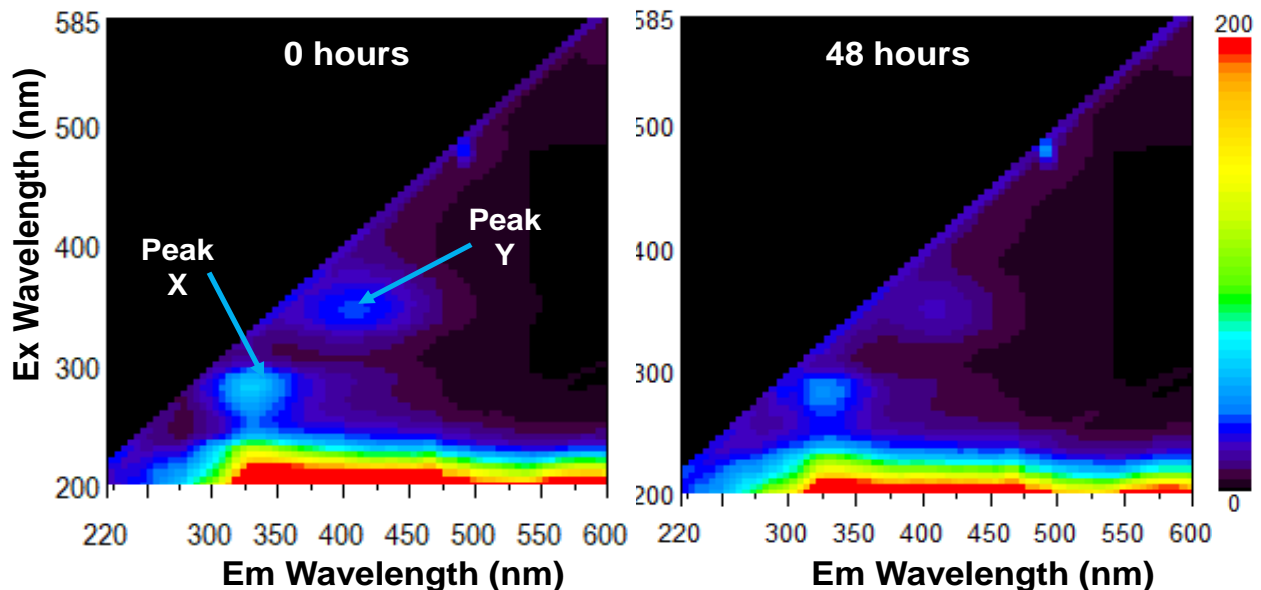

Fig. 5.4: Typical surface containing scales' EEM for Japanese dace fish.

Time dependent fluorescence intensity variations
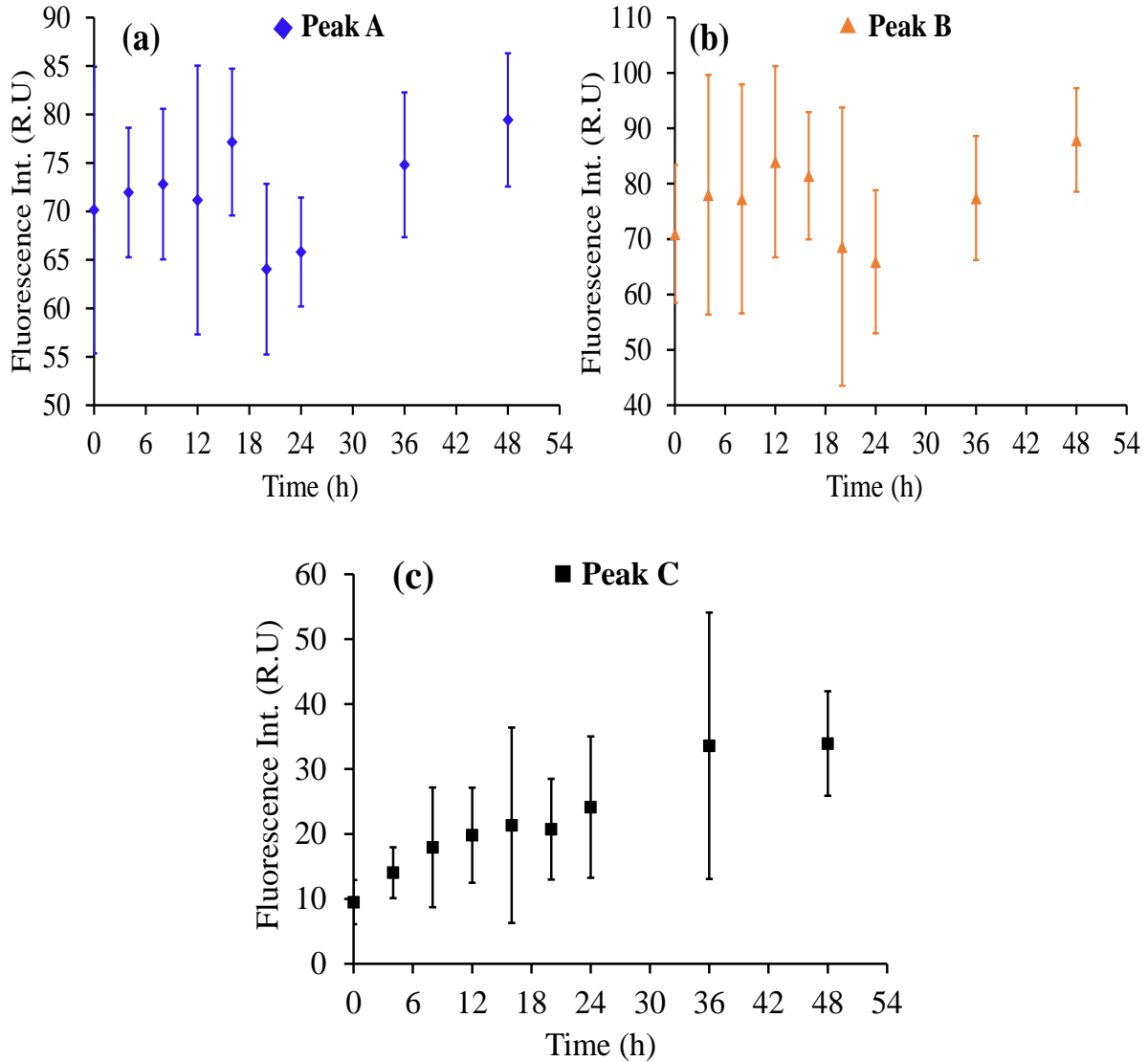
   i. *Fish eyeball EEM*

Fig. 5.5: Time series fish eyeball fluorescence EEM for Japanese dace fish (a) peak A (230/330 nm), (b) peak B (280/330 nm) and (c) peak C (350/415 nm).

The fluorescence intensities associated with aromatic amino acids; peaks A and B showed large variations during the storage period (Fig. 5.5 (a) and (b)). When the fish is alive, the eye is said to contain large quantities of protein and small amounts of aromatic amino acids (Ringvold et al., 2003). For instance, in Salmon fish (*Salmo salar*), 2.64 g/L total proteins contains 18 µmol/L of tryptophan and 74 µmol/L tyrosine (Ringvold et al., 2003). Normally, when fish freshness deteriorates, it undergoes four stages of degradation namely: rigor mortis (pre- and post-rigor), autolysis (self-digestion by enzymatic activities), bacterial spoilage and later chemical spoilage

106

(Ghaly et al., 2010; Ocaño-Higuera et al., 2009). The first two stages (rigor mortis and autolysis) are mostly instigated by biological enzymes (Abbas, Saleh, Mohamed, & Lasekan, 2009). During these two stages, proteins are converted and then decomposed into free amino acids and peptides, this causes a slight increase in their fluorescence intensity (Fraser & Sumar, 1998). When the bacteriological and chemical spoilage processes start, they act upon secondary metabolites resulting from proteins disintegrating them into biogenic amines. This results in significant breakdown of the existing proteins forming tyrosine, skatole, putrescine, indole, cadaverine and many others (Gram & Huss, 1996). This is the reason as to why peaks A and B in Fig. 5.5 (a) and (b) shows some varying intensities during storage.

From Fig. 5.5 (c), peak C with Ex/Em 350/415 nm is increasing likely during storage. The results demonstrated that the fluorescence intensity of uric acid was low when the fish was at the prime fresh stage, and then gradually increased as storage time progressed. As earlier indicated, uric acid is formed from two processes: purine metabolism and decomposition of ATP compounds. These processes accumulate uric acid, increasing its fluorescence intensity during storage.

ii. *Surface containing scales scale*

From the EEM for fish surface containing scales in Fig. 5, there were significant changes witnessed on the fluorescence peak intensities associates with peaks X and Y for two measurement times (start and end of the experiment). Earlier researches have associated these peaks with tyrosine residues and type I collagen. The outer mucus in fish is known for protecting the fish tissues and organs against mechanical damages and regulate the physiology of the cell environment. When the fish is alive, the constant discharge and replacement of mucus inhibit stable colonization of possible dangerous micro-organisms (Guardiola, Cuesta, Arizcun, Meseguer, & Esteban, 2014).

When the fish dies, its metabolism process stops, regeneration of the protein cell substances on the surface containing scales halted thus rendered the fish defenseless. As the microorganisms multiply faster, they consume the free tyrosine and proteins, causing the decrease of intensities observed in both peaks (X and Y), see Fig. 5.6 (a) and (b). In a previous study, Liao et al. (2017), showed a decreasing trend in these two peaks. The peaks are associated with collagen stability in the prime fresh stage before a rapid increase, and then start decreasing drastically. Unlike red-sea bream, this (350/415 nm) decreased gradually, and this could be attributed to: (i) scale thickness; where Japanese dace fish have very tiny surface containing scales compared to red sea bream; (ii) difference in decomposition rates due to different species, culture environment and size; (iii) or

freshwater fish (Japanese dace) show high sensitivity to storage environments rather than saline water fish (red sea bream). Time series EEM data demonstrate that there is some potential to employ a nondestructive technique to quantify fluorescence variation of surface containing scales, especially within the prime stage (<20 hours) and correlate it with fish freshness deterioration.
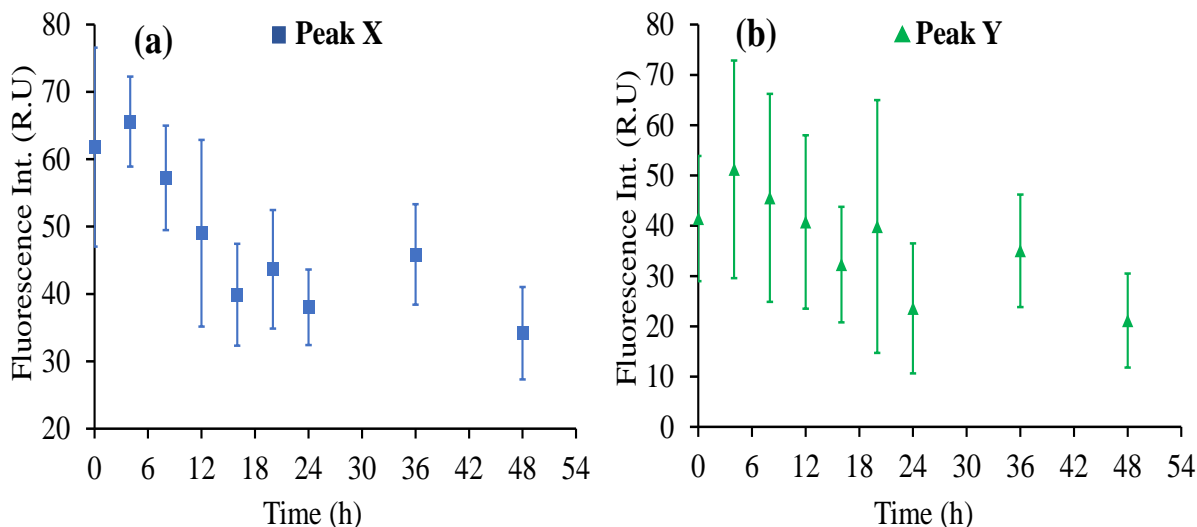

Fig. 5.6: Time series fluorescence intensities of (a) peak X (280/330 nm) and (b) peak Y (350/415 nm) for Japanese dace fish surface containing scales.

Multispectral imaging

From the EEM data, three peaks, A (230/330), B (280/330), and C (350/415) were present on the eyeball; additionally, two peaks X (280/330) and Y (350/415) were detected on the surface containing scales. These peaks were characterized by wider spectra ranges; 250-310 nm (excitation) and 280-400 nm (emission) for B and X, and 315-395 nm (excitation) and 370-520 nm (emission) for C and Y. Existence of already commercialized LEDs with different but defined excitation wavelengths and sensors (cameras) makes it possible to adopt imaging technique in tracking the tendencies of these peaks in terms of color variation during storage. In this experiment, we adopted three UV-LEDs: 280 nm LED, whose excitation crest coincides with the maxima for peaks B and X, 365 nm excitation characterized with a wider spectral range; 345-390 nm and, 395 nm ranging 370-430 nm. Additionally, white LED was essential for white lighting.

Fig. 5.7 a-d shows Japanese dace fish images captured under different illumination lights (white lighting, 365, 395 and 280 nm). Different lighting devices produce different tendencies of images when compared to each other. From the EEM data (seeFig.5.3 and Fig.5.4), every peak has

its independent excitation and emission maxima. The selected UV-LEDs possess different properties and characteristics.

All the images captured produced some significant changes around the ROIs. For instance, from color images Fig. 5.7a, the pupil part of the eye was dark and bright colored at the onset of storage time. The part slowly changed to a dull and greyish with a longer storage time advanced. These changes can be purely attributed to changes in the color morphology caused by biochemical processes taking place within and outside the eye. The other part of the eye is the iris, which houses many melanophores (black pigments). These pigments are enzymatically controlled and whose sole responsibility is to cause pigmentation or fish camouflaging, through the dispersion and aggregation processes (Ángeles Esteban, 2012; Rodionov, Lim, Gelfand, & Borisy, 1994). When the fish dies, its biological processes stop, and but the processes controlled by enzyme-controlled processes degenerate slowly, making the melanophores sizes and/or number to decline gradually with time. This causes fading away of the pigments on the surface through physiological processes, thus making the iris to appear like it is bleached. The combination of both physiological and morphological processes results in observable color variations in the fisheye.

On the fish's body are black pigments called melanophores. The melanophores become more pronounced, and they are the ones responsible for the camouflaging abilities of fish. When the fish dies, these enzymatically controlled pigments aggregate the pigments and retracts it back to the inner tubules, making the grey values to increase with longer storage times (Rodionov et al., 1994). On the fish's body is a mucous layer (viscous colloids comprising of antibacterial enzymes, proteins, commonly known as mucins). This provides the first defense, continuous with the whole-body linings and openings. The mucus can offer protection, disease resistance, respiration, regulation of ionic and osmotic processes, excretion, among others.

From fluorescence images of the 365 nm excitations, all images exhibited a blue color (Fig. 5.5b) but with different intensities on the respective ROI. The pupil and the belly parts showed a deep blue color from the onset of storage time, and they changed to a lighter blue with longer storage times. From Fig. 5.5c, the EEM intensity showed a continuous increase during storage. This was in agreement with the findings of Omwange., (2020) and Liao et al. (Liao et al., 2018). The increasing intensity in EEM implies that blue color starts fading, causing the shift in the color values. The changes here depended on individual samples and the large variation witnessed from the time series EEM of Fig. 5.5c. The tendency was different on the surface containing scales

because the blue color became darker and darker, and this can be seen even from decreasing time-series intensity values of their EEM of Fig. 5.6a and b.
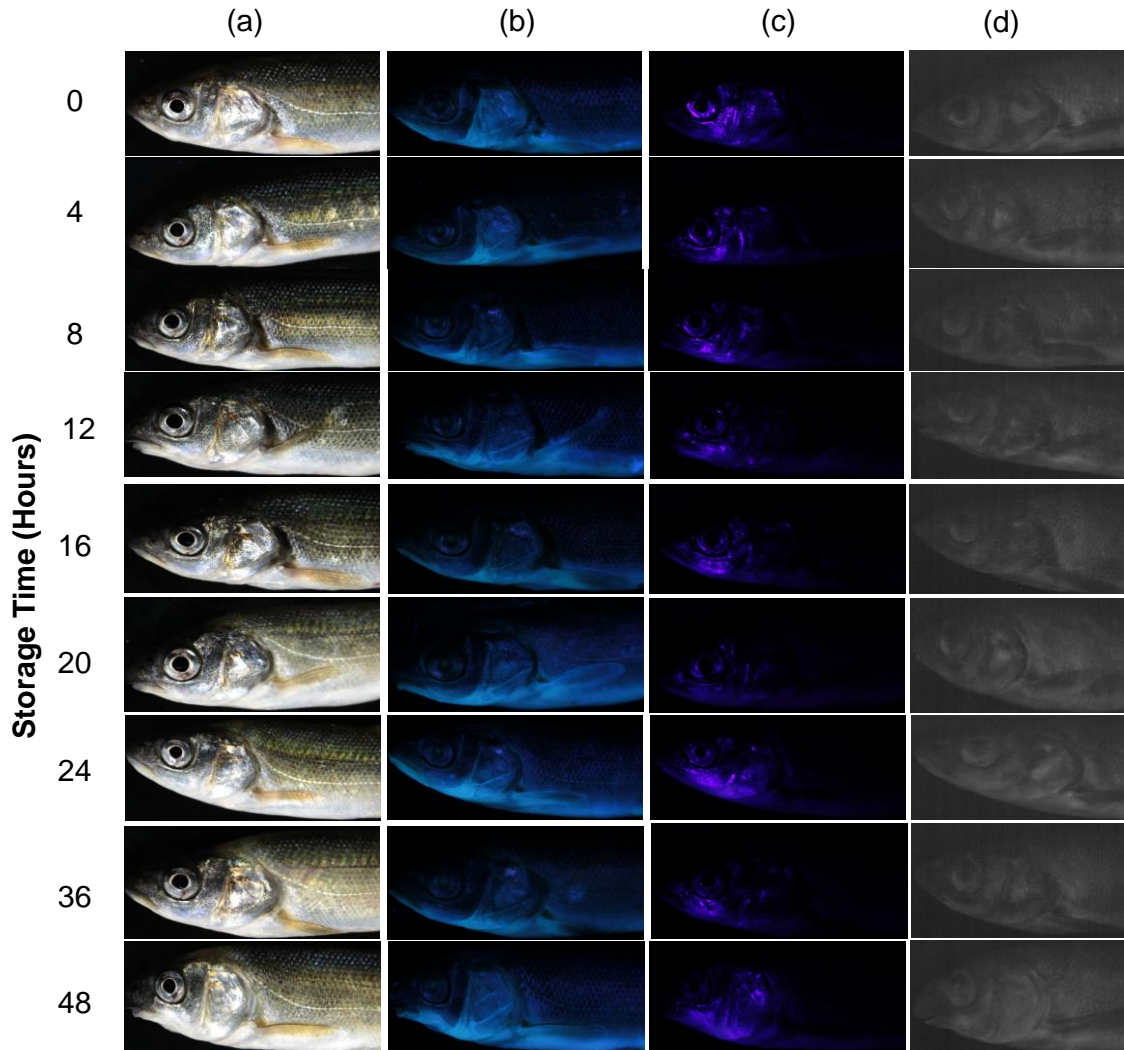

Fig. 5.7: Time series fish images for 5 lighting devices: (a) white lighting, (b) 365 nm, (c) 395 nm; all captured using normal color camera and (d) 280 nm captured using UV-camera.

The 395 nm excitation produced purplish images especially around the head and belly, and especially closer to the head (see Fig. 5.7c. From the images, most samples showed deep purple color at the onset of storage, and it was more observable at the belly and around the operculum. The purple color around the iris of the eye diminished gradually, changing to a deep blue. On the surface containing scales, the samples remained very dark (deep purple) from the onset of storage time, but as storage progressed, the last image can reveal some changes in terms of lighter purplish, where the surface containing scales can be seen. This means that the decreased fluorescence intensity of peak X makes the image color change to violet.

Deep ultraviolet LED (280 nm) was used to capture the fluorescence changes associated with peak B (280/330) for the eyeball and peak X (280/330) for the surface containing scales. This peak is associated with amino acids and proteins, which are in abundance in fish. The images were captured using a monochromatic UV camera; whose images are in one channel (grey images). From these images, grey values and contrast variation could be extracted and thereafter factored in the freshness prediction model. Both the 365 and 395 nm LEDs could manage to capture the information associated with peaks C and Y because of their wide spectral excitation wavelengths.

It has been reported that after the death of fish, internal and external bio-chemical processes are responsible for organoleptic changes in the color and fish appearances after death (Masniyom, 2011). Therefore, the changes witnessed here with the fluorescence images are directly linked with these processes, and they are expected to vary with longer storage times and conditions. Additionally, Stoknes et al. (2004) reported that lipids and fatty acids are abundant in fisheyes and brains, and thus their disintegration when decomposing contributes to the changes in fluorescence compositions. The chemical processes responsible for breaking down these fatty acids within the fish's body can directly influence degradation of processes associated with the ATP compounds and metabolic synthesis of purine substances in the fish's body, thus accumulating uric acid. On the other hand, these processes can directly influence biochemical processes linked to collagen activities. This will be reflected on the changes in color values for samples as storage time advances. The process of physiological and biochemical in the fish will lead to physical and chemical modifications which later will affect color changes. And therefore, all surface changes confirm that an imaging method can objectively quantify and relate them with the freshness deterioration during storage.

Multivariate analysis

During image analysis, RGB color space, contrast (for white color, 365 nm, and 395 nm images), grey values and contrast variation for 280 nm images were considered with the goal of building a multivariate fish freshness prediction model. In the experiment, 85 variables from eyeball (pupil and iris), belly and surface containing scales around dorsal part demonstrated a tendency with freshness deterioration, hence they were adopted in the model. When color changes are combined in the prediction model, it was realized that it could be adopted as a primary indicator

of fish freshness changes during storage. This model can offer an alternative non-destructive method for evaluating freshness.

The average pixel values for eighty-five individual variables [R_{white}, G_{white}, B_{white}; R_{365}, G_{365}, B_{365}; R_{395}, G_{395}, B_{395}; $R_{white-ratio}$, $G_{white-ratio}$, $B_{white-ratio}$; $R_{365-ratio}$, $G_{365-ratio}$, $B_{365-ratio}$; $R_{395-ratio}$, $G_{395-ratio}$, $B_{395-ratio}$; $Contrast_{white}$, $Contrast_{365}$, $Contrast_{395}$] for iris, pupil, belly and dorsal parts respectively and grey values from 280 nm excitation] generated from the images (Fig. 5.7) were adopted in the prediction model. The prediction models considered four data sets: (i) RGB values for all images (R_{white}, G_{white}, B_{white}; R_{365}, G_{365}, B_{365}; R_{395}, G_{395}, B_{395}) with 36 variables; (ii) RGB values (R_{white}, G_{white}, B_{white}; R_{365}, G_{365}, B_{365}; R_{395}, G_{395}, B_{395}), contrast values ($Contrast_{white}$, $Contrast_{365}$, $Contrast_{395)}$ and grey values for 280 nm images with 49 variables; (iii) RGB-ratios for all images ($R_{white-ratio}$, $G_{white-ratio}$, $B_{white-ratio}$; $R_{365-ratio}$, $G_{365-ratio}$, $B_{365-ratio}$; $R_{395-ratio}$, $G_{395-ratio}$, $B_{395-ratio}$) with 36 variables; and (iv) RGB-ratios ($R_{white-ratio}$, $G_{white-ratio}$, $B_{white-ratio}$; $R_{365-ratio}$, $G_{365-ratio}$, $B_{365-ratio}$; $R_{395-ratio}$, $G_{395-ratio}$, $B_{395-ratio}$), contrast values and grey values for 280 nm with 49 variables respectively. Since in the human eye, RGB have color sensitivity receptors for R (red), G (green) and B (blue) color channels, it is hypothetically possible to decompose all visible colors into a combination of three "primary colors", and this explains why we opted for the RGB color palette.

Table 1 Table 5.1: PLSR model results for *K* value fish predicting using imaging data.

	Excitation Light				No. of input variables	RMSE (%)	R^2
	White	365 nm	395 nm	280 nm			
i	RGB			-	36	2.64	0.93
ii	RGB & Contrast			Grey value	49	2.42	0.94
iii	RGB ratio			-	36	2.59	0.93
iv	RGB ratio & Contrast			Grey value	49	2.62	0.92

From these findings, it can be identified that a simple imaging system with LEDs of excitations targeting these fluorescence compounds could easily give information regarding the color changes. The imaging results considered many parameters of several combinations with an aim of finding the best of them as shown in Table 5.1. The results were divided into four parts: (i) RGB values only for all images (white, 280, 365 and 395 nm); (ii) RGB values, contrast values

(both for white, 280, 365 and 395 nm) and grey values for 280 nm images; (iii) RGB-ratios only corresponding to (i); and (iv) RGB-ratios and contrast values corresponding to (ii) with grey values for 280 nm images. This is because, previous researches have demonstrated the greatest potential with 365 nm and white light imaging in evaluating food quality.
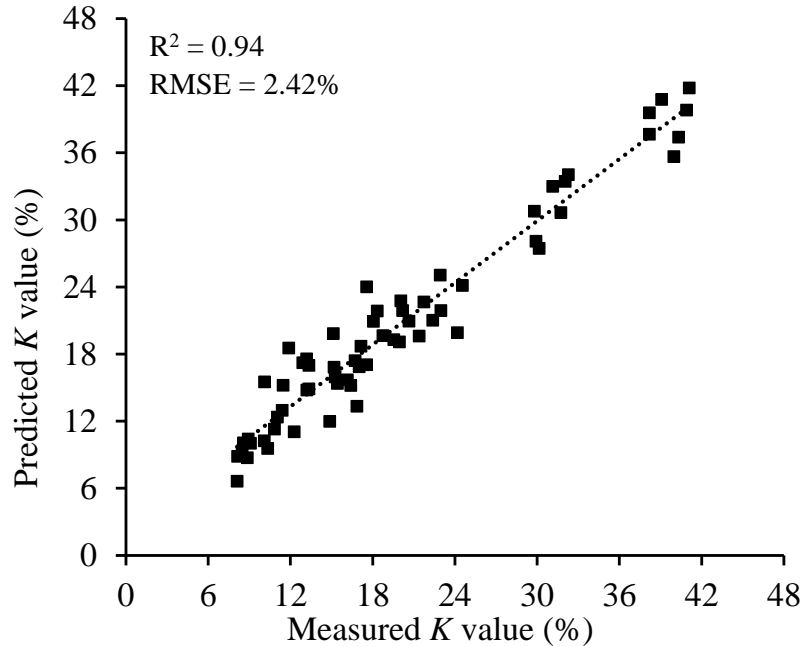

Fig. 5.8: PLSR model results for measured K value using imaging data.

The combination of R, G, and B values for all the ROIs in the model, gave RMSE of 2.64% and R^2 of 0.93. When the contrast of above images and the grey values from 280 nm lighting were incorporated in the dataset, a slight improvement of the results was realized with RMSE of 2,42% and R^2 of 0.94 (Fig. 5.8). This represented the best results from all the models in this research. The color ratios and the combination of these ratios with contrast and grey values from 280 nm UV images produced similar results of 2.59% and 2.62% for RMSE and 0.93 and 0.92 for R^2, respectively (see Table 5.1). These results slightly improves to what was reported by Omwange et al., (2020); where they reported an RMSE of 3.5% and a R^2 of 0.92 from just fluorescence imaging of the fish eyes. During model building and calibration, the combinations factored in the variables from all the ROIs parts. These results indicate that three LEDs (white, 365 nm and 280 nm) are enough to act as freshness indicator in fish, however, adding a 395 nm excitation LED could improve the accuracy of the findings as seen from Table 1. This is evident that adding 395 nm excited images slightly improved the results with less RMSE and a better R^2 value.

113

A loading latent variable diagram was constructed to understand the contribution of each variable to the model created. From the loading weights of the first latent variable, the first and highest principal component was from the three variables showed the highest positive contribution to the model and they include [G_{365}, B_{365} (green-blue channels from 365 nm excitation of pupil part of the eye); and $B_{365\text{-ratio}}$ (B-ratio from 365 nm excitation pupil part of the eye)]. On the other hand, three variables contributed negatively to the model, and they include $R_{365\text{-ratio}}$ (R-ratio from 365 nm excitation images of iris part of the eye), $G_{w\text{-ratio}}$ and $G_{365\text{-ratio}}$ (G-ratio from white light and 365 nm excitation of pupil part respectively). From these loadings, 365 nm excitation light is still powerful in tracking fish freshness changes during storage.

5.5 Conclusions

These results demonstrate that multispectral imaging can successfully evaluate fish freshness non-destructively by just capturing fish images with various excitation wavelengths. From all the image data sets: (i) RGB values only; (ii) RGB values with contrast variation and grey values; (ii) RGB-ratios only; (ii) RGB-ration with contrast variation and grey values, it is evident that this technique can accurately reveal the freshness changes of fish during storage with R^2 of 0.94 and RMSE of 2.42%. With these findings, freshness of an intact fish could be monitored non-destructively by purely relying on the surface changes of fluorescence and color images. For industrial application, refrigeration companies will utilize this technology by designing fish storage compartments with small UV LEDs and cameras to monitor the fish's surface changes. In the near future, this technique could easily be integrated with smartphone technology to achieve smart refrigeration systems for food monitoring. Thus, this technique can offer a basis for developing a nondestructive technique for grading of fish online by tracking the changes of the eye during storage, and subsequently lead to development of automatic fish grading systems.

REFERENCES

Abbas, K. A., Saleh, A. M., Mohamed, A., & Lasekan, O. (2009). The relationship between water activity and fish spoilage during cold storage: A review. *Journal of Food, Agriculture and Environment*, *7*(3–4), 86–90.

Alishahi, A., & Aïder, M. (2012). Applications of Chitosan in the Seafood Industry and Aquaculture: A Review. *Food and Bioprocess Technology*, *5*(3), 817–830. https://doi.org/10.1007/s11947-011-0664-x

Ángeles Esteban, M. (2012). An Overview of the Immunological Defenses in Fish Skin. *ISRN Immunology*, *2012*, 1–29. https://doi.org/10.5402/2012/853470

Castro, P., Padrón, J. C. P., Cansino, M. J. C., Velázquez, E. S., & Larriva, R. M. De. (2006). Total volatile base nitrogen and its use to assess freshness in European sea bass stored in ice. *Food Control*, *17*(4), 245–248. https://doi.org/10.1016/j.foodcont.2004.10.015

Chen, Y. R., Chao, K., & Kim, M. S. (2002). Machine vision technology for agricultural applications. *Computers and Electronics in Agriculture*, *36*(2–3), 173–191. https://doi.org/10.1016/S0168-1699(02)00100-X

Cheng, J. H., Dai, Q., Sun, D. W., Zeng, X. A., Liu, D., & Pu, H. Bin. (2013, November). Applications of non-destructive spectroscopic techniques for fish quality and safety evaluation and inspection. *Trends in Food Science and Technology*, Vol. 34, pp. 18–31. https://doi.org/10.1016/j.tifs.2013.08.005

Cheng, J. H., & Sun, D. W. (2014). Hyperspectral imaging as an effective tool for quality analysis and control of fish and other seafoods: Current research and potential applications. *Trends in Food Science and Technology*, *37*(2), 78–91. https://doi.org/10.1016/j.tifs.2014.03.006

Cheng, J. H., Sun, D. W., Qu, J. H., Pu, H. Bin, Zhang, X. C., Song, Z., … Zhang, H. (2016). Developing a multispectral imaging for simultaneous prediction of freshness indicators during chemical spoilage of grass carp fish fillet. *Journal of Food Engineering*, *182*, 9–17. https://doi.org/10.1016/j.jfoodeng.2016.02.004

Chong, K., Tham, S. Y., Foo, J., Lam, T. J., & Chong, A. (2005). Characterisation of proteins in epidermal mucus of discus fish (Symphysodon spp.) during parental phase. *Aquaculture*, *249*(1–4), 469–476. https://doi.org/10.1016/j.aquaculture.2005.02.045

Dale, N. (1994). National research council nutrient requirements of poultry — ninth revised edition (1994). In *Journal of Applied Poultry Research* (Vol. 3). https://doi.org/10.1093/japr/3.1.101

Fraser, O. P., & Sumar, S. (1998). Compositional changes and spoilage in fish (part II) - microbiological induced deterioration. *Nutrition & Food Science*, *98*(6), 325–329. https://doi.org/10.1108/00346659810235242

Georgakoudi, I., Jacobson, B. C., Müller, M. G., Sheets, E. E., Badizadegan, K., Carr-Locke, D. L., … Feld, M. S. (2002). NAD(P)H and collagen as in vivo quantitative fluorescent biomarkers of epithelial precancerous changes. *Cancer Research*, *62*(3), 682–687.

Ghaly, a E., Dave, D., Budge, S., & Brooks, M. S. (2010). Fish Spoilage Mechanisms and Preservation Techniques : Review Department of Process Engineering and Applied Science , Dalhousie University Halifax , Nova Scotia , Canada. *American Journal of Applied Sciences*, *7*(7), 859–877.

Gram, L., & Huss, H. H. (1996). Microbiological spoilage of fish and fish products. *International Journal of Food Microbiology*, *33*(96), 121–137. Retrieved from http://www.ncbi.nlm.nih.gov/pubmed/8913813

Guardiola, F. A., Cuesta, A., Arizcun, M., Meseguer, J., & Esteban, M. A. (2014). Comparative skin mucus and serum humoral defence mechanisms in the teleost gilthead seabream (Sparus aurata). *Fish and Shellfish Immunology*, *36*(2), 545–551. https://doi.org/10.1016/j.fsi.2014.01.001

Ikoma, T., Kobayashi, H., Tanaka, J., Walsh, D., & Mann, S. (2003). Microstructure, mechanical, and biomimetic properties of fish scales from Pagrus major. *Journal of Structural Biology*, *142*(3), 327–333. https://doi.org/10.1016/S1047-8477(03)00053-4

Jackman, P., Sun, D. W., & Allen, P. (2009). Automatic segmentation of beef longissimus dorsi muscle and marbling by an adaptable algorithm. *Meat Science*, *83*(2), 187–194. https://doi.org/10.1016/j.meatsci.2009.03.010

Jackman, P., Sun, D. W., Du, C. J., & Allen, P. (2009). Prediction of beef eating qualities from colour, marbling and wavelet surface texture features using homogenous carcass treatment. *Pattern Recognition*, *42*(5), 751–763. https://doi.org/10.1016/j.patcog.2008.09.009

Kato, N., Kunimoto, M., Koseki, S., Kitakami, S., & Arai, K. (2009). Freshness and Quality of Fish and Shellfish (Supplementary Edition). *Journal of The School of Marine Science and Technology*, *7*(2), 87–99. Retrieved from http://www2.scc.u-tokai.ac.jp/www3/kiyou/pdf/2009vol7_2/kato.pdf

Lakowicz, J. R. (2006). Principles of fluorescence spectroscopy. *Principles of Fluorescence*

Spectroscopy, (June), 1–954. https://doi.org/10.1007/978-0-387-46312-4

Lamkin, W. M., Unruh, N. C., & Pomerranz, Y. (1991). Use of Fluorometry for the determination of uric Acid in Grain. Elimination of Interfering Fluorescence. *Cereal Chemistry*, *68*(1), 81–86. Retrieved from https://www.cerealsgrains.org/publications/cc/backissues/1991/Documents/68_81.pdf

Lawaetz, A. J., & Stedmon, C. A. (2009). Fluorescence intensity calibration using the Raman scatter peak of water. *Applied Spectroscopy*, *63*(8), 936–940. https://doi.org/10.1366/000370209788964548

Liao, Q., Suzuki, T., Shirataki, Y., Kuramoto, M., & Kondo, N. (2018). Freshness related fluorescent compound changes in Japanese dace fish (Tribolodon hakonensis) eye fluid during storage. *Engineering in Agriculture, Environment and Food*, *11*(3), 95–100. https://doi.org/10.1016/j.eaef.2018.01.001

Liao, Q., Suzuki, T., Yasushi, K., Al Riza, D., Kuramoto, M., & Kondo, N. (2017). Monitoring Red Sea Bream Scale Fluorescence as a Freshness Indicator. *Fishes*, *2*(3), 10. https://doi.org/10.3390/fishes2030010

Liu, D., Sun, D. W., & Zeng, X. A. (2014). Recent advances in wavelength selection techniques for hyperspectral image processing in the food industry. *Food and Bioprocess Technology*, *7*(2), 307–323. https://doi.org/10.1007/s11947-013-1193-6

Lowe, T. E., Ryder, J. M., Carragher, J. F., & Wells, R. M. G. (1993). Flesh Quality in Snapper, Pagrcrs auratus, Affected by Capture Stress. *Journal of Food Science*, *58*(4), 770–773. https://doi.org/10.1111/j.1365-2621.1993.tb09355.x

Masniyom, P. (2011). Deterioration and shelf-life extension of fish and fishery products by modified atmosphere packaging. In *Songklanakarin Journal of Science and Technology* (Vol. 33). https://doi.org/rdo.psu.ac.th/sjstweb/journal/33-2/0125-3395-33-2-181-192.pdf

Masood, Z., Yasmeen, R., Haider, M. S., Tarar, O. M., Lakht-e-Zehra, & Hossain, M. Y. (2015). Evaluations of crude protein and amino acid contents from the scales of four mullet species (Mugilidae) collected from Karachi fish harbour, Pakistan. *Indian Journal of Geo-Marine Sciences*, *44*(5), 724–731.

Menesatti, P., Costa, C., & Aguzzi, J. (2010). Quality Evaluation of Fish by Hyperspectral Imaging. *Hyperspectral Imaging for Food Quality Analysis and Control*, 273–294. https://doi.org/10.1016/B978-0-12-374753-2.10008-5

Ocaño-Higuera, V. M., Marquez-Ríos, E., Canizales-Dávila, M., Castillo-Yáñez, F. J., Pacheco-Aguilar, R., Lugo-Sánchez, M. E., … Graciano-Verdugo, A. Z. (2009). Postmortem changes in cazon fish muscle stored on ice. *Food Chemistry*, Vol. 116, pp. 933–938. https://doi.org/10.1016/j.foodchem.2009.03.049

Oda, Y., Ichida, S., Mimura, T., Maeda, K., Tsujikawa, K., & Aonuma, S. (1984). Purification and characterization of a fish lectin from the external mucous of ophidiidae, genypterus blacodes. *Journal of Pharmacobio-Dynamics*, *7*(43), 614–623. Retrieved from http://www.mendeley.com/research/geology-volcanic-history-eruptive-style-yakedake-volcano-group-central-japan/

Omwange, K. A., Al Riza, D. F., Sen, N., Shiigi, T., Kuramoto, M., Ogawa, Y., … Suzuki, T. (2020). Fish freshness monitoring using UV-fluorescence imaging on Japanese dace (Tribolodon hakonensis) fisheye. *Journal of Food Engineering*, *287*(May), 110111. https://doi.org/10.1016/j.jfoodeng.2020.110111

Park, S. Bin, Jang, H. Bin, Fagutao, F. F., Kim, Y. K., Nho, S. W., Cha, I. S., … Jung, T. S. (2014). Combination treatment against scuticociliatosis by reducing the inhibitor effect of mucus in olive flounder, Paralichthys olivaceus. *Fish and Shellfish Immunology*, *38*(2), 282–286. https://doi.org/10.1016/j.fsi.2014.03.023

Pu, H., Kamruzzaman, M., & Sun, D. W. (2015). Selection of feature wavelengths for developing multispectral imaging systems for quality, safety and authenticity of muscle foods-a review. *Trends in Food Science and Technology*, *45*(1), 86–104. https://doi.org/10.1016/j.tifs.2015.05.006

Ringvold, A., Anderssen, E., Jellum, E., Bjerkås, E., Sonerud, G. A., Haaland, P. J., … Kjønniksen, I. (2003). UV-absorbing compounds in the aqueous humor from aquatic mammals and various non-mammalian vertebrates. *Ophthalmic Research*, *35*(4), 208–216. https://doi.org/10.1159/000071172

Rodionov, V. I., Lim, S. S., Gelfand, V. I., & Borisy, G. G. (1994). Microtubule dynamics in fish melanophores. *Journal of Cell Biology*, *126*(6), 1455–1464. https://doi.org/10.1083/jcb.126.6.1455

Stoknes, I. S., Økland, H. M. W., Falch, E., & Synnes, M. (2004). Fatty acid and lipid class composition in eyes and brain from teleosts and elasmobranchs. *Comparative Biochemistry and Physiology - B Biochemistry and Molecular Biology*, *138*(2), 183–191.

https://doi.org/10.1016/j.cbpc.2004.03.009

Villette, S., Pigaglio-Deshayes, S., Vever-Bizet, C., Validire, P., & Bourg-Heckly, G. (2006). Ultraviolet-induced autofluorescence characterization of normal and tumoralesophageal epithelium cells with quantitation of NAD(P)H. *Photochemical & Photobiological Sciences*, *5*, 483–492. https://doi.org/10.1039/b514801d

Wang, H. H., & Sun, D. W. (2002). Melting characteristics of cheese: Analysis of effect of cheese dimensions using computer vision techniques. *Journal of Food Engineering*, *52*(3), 279–284. https://doi.org/10.1016/S0260-8774(01)00116-9

Wu, D., & Sun, D. W. (2013). Colour measurements by computer vision for food quality control - A review. *Trends in Food Science and Technology*, *29*(1), 5–20. https://doi.org/10.1016/j.tifs.2012.08.004

CHAPTER VI: CONCLUSIONS AND RECOMMENDATIONS

6.1 Conclusions

Based on the research described in this study, we can draw the following conclusions:

Chapter III tries to identify sensitive excitation wavelengths for fish eyeballs and scales related with fish freshness changes during storage. Fourteen excitations (8 for eyeball and 6 for surface containing scales were heighted as important excitations with significant relationship with fish freshness deterioration. The excitations included: 230, 245, 275, 280, 295, 310, 330 & 355 nm for the eyeball and 230, 275, 280, 295, 340 & 350 nm for surface containing scales. For cheaper technologies with fewer sensors, four excitations: 275 and 355 nm for eyeball and 280 and 355 nm for the scales emerged as the most significant wavelengths. If we rely on one part of the body for freshness evaluation, 230 and 355 nm excitations eyeball are sufficient to act as freshness indicators with a performance of 2.9% and 0.96, for RMSE and R^2 respectively. On the other hand, the scales demonstrated that three excitations (275, 295 and 340 nm) could track the fish freshness deterioration with a performance of 1.57% and 0.96 respectively. Since these body parts (eyeball and scales) lie on the fish's surface, combining their results will achieve a more robust approach for monitoring the freshness of intact whole fish. A combination of eyeball and scale data showed that 280 and 350 nm excitation were the most sensitive for freshness evaluation with a performance of 2.8% and 0.95 respectively. This research therefore creates a foundation for establishing simple portable device(s) for non-destructively assessing fish freshness throughout the fish supply chain.

Chapter IV adopts one of the important highlighted wavelengths (excitation: 350 nm) tom establish a simple imaging system for tracking the opacity changes of fisheyes. The fluorescence witnessed on the eyeball is originating from the surface (skin and cornea) of the eye or combination of surface and inside (eye fluid). The fluorescence color changes of the fisheye (iris and pupil) clearly showed a clear distinction of intact fish freshness evaluation at different storage times. A prediction performance of 3.5% and 0.92 as RMSE and R^2 was realized. The results demonstrate great potential of shortening freshness estimation time frame through real-time and in the field by just observing the fluorescence color of fisheyes.

Chapter V employs multiwavelength imaging from visible to UV regions (White, 365, 395, and 280 nm) on the whole fish can allow the development of online monitoring systems with a possibility of promoting automatic grading in the fish industry. From the regression results, the model produced a more improved performance of 2.4% and 0.94 compared to eyeball alone, as seen from figure two above. This research clearly shows that several potentially active areas on the surface of fish can be used for monitoring freshness non-destructively. With this information in place, refrigeration companies can use this technology to design new generation refrigeration systems with monitoring systems (UV LEDs and cameras) to monitor the fish's surface changes. With this technique in place, smartphone technology could easily be synchronized with these smart refrigerators, thus, realizing innovative refrigeration of food monitoring without opening fridges.

In general, this research demonstrates great potential in applying imaging from visible to UV excited fluorescence in evaluating the quality of fish. Through this research, we can realize quick freshness evaluation, guaranteeing food safety and reliability for providing fresh fish products to the consumers. Additionally, developing simple sensors will likely help consumers make informed decisions, thus avoiding food wastage. This approach can help achieve online monitoring systems and even contribute to future innovations like the use of smart refrigerators installed with small cameras and UV LEDs for online monitoring.

6.2 Recommendations

The exposure time of 4 s for acquiring fluorescence images may be too long for handheld devices or automatic grading systems and making it too short may produce noisier images. For future research, a highly powered light source should be used to address this problem.

In the multispectral imaging experiment, two imaging systems were established (UV camera and common digital camera) for monitoring surface changes. The time spent between changing the sample from one imaging system to another and setting up parameters was about 2 minutes for every sample. These 2 minutes is too long for exposure to the open environment, and it may have some effects on the samples. Since the maximum emission of the targeted peaks is about 530 nm, which is less than 600 nm. Instead of two imaging systems, a single camera with a wider sensitivity range in the Ultraviolet and Visible (UV-Vis) range can be used with band pass filters. This will reduce the exposure time for samples and integrating these two imaging systems will generate a more robust system.

The illumination of the sample was done by placing LEDs above the sample. This is called direct lighting, which has a challenge with non-uniform distribution since the fish's surface is not flat or even. In the future, a more uniform lighting could be achieved through indirect lighting where light is first shone on a diffuser before it is reflected on the sample to achieve uniform illumination. Additionally, changing of sample position (from storage and measurement) can affect the results. Adopting intact sampling might be more realistic, towards establishing a tracking system that represents the actual storage condition and state of fish without disturbing it from the resting position.

Water affects the fluorescence intensity of compounds; that is to say, wet samples will show more fluorescence intensity than their dry counterparts. Since there are so many molecules and functional groups in the near infrared (NIR) region, NIR spectroscopy can help to real the most significant compounds in fish related with freshness with their associated wavelengths changes. As a result, an NIR imaging system can be proposed for non-destructive evaluation in the NIR region. This will reveal the moisture content estimation of fish and rate of water loss during storage. Since we have already proposed a fluorescence-based imaging technique, soon, NIR and Fluorescence imaging techniques can be integrated for greater good of monitoring fish freshness.

APPENDIX

a. List of publications

1. Yoshito Saito, Kazumasa Iwasaki, Mai Miyazaki, **Ken Abamba Omwange**, Zichen Huang, Kento Matsuura, Yuki Kitao, Tetsuhito Suzuki, Naoshi Kondo. Estimation of chemical components in Matcha using fluorescence spectroscopy (*Short report*). Journal of the Japanese Society of Agricultural Machinery and Food Engineers. 84 (2) 2022.

2. Hiroki Tamura, Tomoo Shiigi, Takahisa Nishizu, Hitoshi Yoshitomi, Stephen. Njehia Njane, Kohei Ogata, **Ken Abamba Omwange,** Keiichiro Shiraga, Tetsuhito Suzuki, Yuichi Ogawa, Naoshi Kondo. Fish volume estimation and accuracy of multiple-neck underwater Helmholtz resonators. Japanese Society of Agricultural Machinery. March 2022 (*Accepted for publication*)

3. **Ken Abamba Omwange,** Yoshito Saito, Kenta Itakura, Dimas Firmanda Al Riza, Ferruccio Giametta, Naoshi Kondo. Estimation of *K* value and free fatty acids of adulterated olive oil using fluorescence spectroscopy coupled with multivariate analysis and convolutional neural network models. EAEF March 2022 (Accepted for publication).

4. **Ken Abamba Omwange,** Yoshito Saito, Dimas Firmanda Al Riza, Huang Zichen, Makoto Kuramoto, Keiichiro Shiraga, Yuichi Ogawa, Naoshi Kondo, Tetsuhito Suzuki. Japanese dace (*Tribolodon hakonensis*) fish freshness estimation using front-face fluorescence spectroscopy coupled with chemometric analysis. Spectrochimica Acta Part A: Molecular and Biomolecular Spectroscopy. 276 (2022) 121209.

5. Alin Khaliduzzaman, **Omwange Ken Abamba**, Riza Dimas Firmanda Al, Konagaya Keiji, Kamruzzaman Mohammed, Alom Md Siddik, Gao Tianqi, Saito Yoshito, Kondo Naoshi. Antioxidant assessment of agricultural produce using fluorescence techniques_ a review. Critical reviews in Food Science and Nutrition 2021.

6. Zichen Huang, **Ken Abamba Omwange**, Lok Wai Jacky Tsay, Yoshito Saito, Eri Maai, Akira Yamazaki, Ryohei Nakano, Tetsuya Nakazaki, Makoto Kuramoto, Tetsuhito Suzuki, Yuichi Ogawa, Naoshi Kondo. UV excited fluorescence image-based non-destructive method for early detection of strawberry (*Fragaria × ananassa*) spoilage. Food Chemistry. 2021, 130776

7. **Ken Abamba Omwange,** Yoshito Saito, Huang Zichen, Alin Khaliduzzaman, Makoto Kuramoto, Yuichi Ogawa, Naoshi Kondo, Tetsuhito Suzuki. Evaluating Japanese dace

(*Tribolodon hakonensis*) fish freshness during storage using multispectral images from visible and UV excited fluorescence. LWT - Food Science and Technology 151 (2021) 112207

8. **Ken Abamba Omwange,** Dimas Firmanda Al Riza, Yoshito Saito, Tetsuhito Suzuki, Yuichi Ogawa, Keiichiro Shiraga, Ferruccio Giametta, Naoshi Kondo. Potential of front face fluorescence spectroscopy and fluorescence imaging in discriminating adulterated extra-virgin olive oil with virgin olive oil. Food Control Journal 124 2021 107906

9. Keiji Konagaya, Dimas Firmanda Al Riza, **Ken Abamba Omwange,** Noriko Takahashi, Makoto Kuramoto, Yuichi Ogawa, Tetsuhito Suzuki, Naoshi Kondo. Fluorescence intensity ratio of tomato as an index of over-ripeness: An index regardless of maturity at harvest. Journal of the Faculty of Collaborative Regional Innovation, Ehime University 5(1) 25 - 28 Mar 2021.

10. Keiji Konagaya, **Ken Abamba Omwange**, Dimas Firmanda Al Riza, Alin Khaliduzzaman, Andrea Martínez Oliver, Francisco Rovira-Más, Hiroki Nagasato, Kazunori Ninomiya and Naoshi Kondo. Association of fruit, pericarp, and epidermis traits with surface autofluorescence in green peppers. Journal of Photochemical & Photobiological Sciences.

11. **Ken Abamba Omwange**, Dimas Firmanda Al Riza, Nie Sen, Tomoo Shiigi, Makoto Kuramoto, Yuichi Ogawa, Naoshi Kondo, Tetsuhito Suzuki. Fish freshness monitoring using UV fluorescence imaging on Japanese dace (*Tribolodon hakonensis*) fisheye. Journal of Food Engineering 287 2020 110111

b. Conference proceedings

1. **Ken Abamba Omwange**, Naoshi Kondo, Kazuhiko Namba, Mitsuji Monta Assessing acidity of grape berry bunches with anthocyanin using front face fluorescence spectroscopy Comparison of fluorescence properties between the intact eyeball and eye-fluid for fisheye. 79th Annual Meeting of the Japanese Society of Agricultural and Food Engineering (online) 2021, Kyushu University

2. **Ken Abamba Omwange**, N. Kondo, Tomoo Shiigi, Makoto Kuramoto, Tetsuhito Suzuki, Yuichi Ogawa. Comparison of fluorescence properties between the intact eyeball and eye-fluid for fisheye. 79th Annual Meeting of the Japanese Society of Agricultural and Food Engineering (online) 2021, Kyushu University.

3. **Ken Abamba Omwange,** D. F. Al Riza, N. Sen, T. Shiigi, M. Kuramoto, T. Suzuki, Y. Ogawa, N. Kondo Fish freshness estimation during storage using UV fluorescence imaging of the fish's eye International Joint Conference on JSAM, SASJ and 13th CIGR VI [JSAM Hokkaido University, September 2019. (Oral, no review).

4. 椎木 友朗 **Ken Abamba Omwange,** 近藤 直 倉本 誠. 柑橘成分を含んだ飼料を与えたブリ ミカンブリの蛍光特性について International Joint Conference on JSAM, SASJ and 13th CIGR VI [JSAM part], Hokkaido University, September 2019. (Oral presentation)

5. **Ken Abamba Omwange,** D. F. Al Riza, S. Njane, T. Shiigi, M. Kuramoto, T. Suzuki, Y. Ogawa, N. Kondo. Potential of fluorescence spectroscopy for fish freshness monitoring during storage JSAM Conference Ehime University, September 2018 (Oral, no review)

ACKNOWLEDGMENT

126

My special regards to MEXT Council for the opportunity to come and study Japan. Coming to Japan; especially, Kyoto University was dream come true. To Toyota Tsusho Scholarship, I am so grateful for the support you gave me during my Ph.D. course.

I am so grateful to Mr. Ogata Kohei and Ms. Rie Nomura for the time you took to find nursery school for my daughter. And am so happy you finally got married and I wish you the very best in the future. Mr. Chen Siyao, Mr. Hiroki Tamura and Yamashige Yoshihisa for always finding time to translate my daughter's school documents. Mr. Li Nandin, Dr. Huang, and Mr. Jacky, thank you for always standing with me whenever I was in need.

To my late parents (Francis Nyamweno Omwange and Gladys Kerubo Orenge), it is so sad that you never lived to witness this journey; may you rest in eternal peace dad and mom. My relatives; brothers (Michael Owen) and sisters, grandmother (Nyaboke); Uncles (Josiah Momanyi, Willis Onchiri, Araka Josephat), thank you for your prayers and moral support.

Finally, I would like to thank my family; my dear wife Mary Mapenzi Chai and our lovely daughters Sharyl Kerubo Abamba and Shanaya Kaidza Abamba; thank you for your patience, encouragement, and support. This is for you all. This dissertation might not be so perfect same as me as a human being.

Ken Abamba OMWANGE